AN ABSTRACT OF THE THESIS OF

MICHAEL GERHARD SCHULZ for the degree of MASTER OF SCIENCE in GEOLOGY presented on June 5, 1980

Title: THE QUANTIFICATION OF SOIL MASS MOVEMENTS AND THEIR RELATIONSHIP TO BEDROCK GEOLOGY IN THE BULL RUN WATERSHED, MULTNOMAH AND CLACKAMAS COUNTIES, OREGON

Redacted for Privacy

Abstract approved: Frederick J. Swanson

Mass movements are dominant erosional processes in the western Cascades of Oregon. Recent mass movements have degraded water quality and disrupted roads and conduits in the Bull Run Watershed, which is the primary source of drinking water for the City of Portland. The morphology and distribution of mass movements is quantifiably related to lithological, structural, and stratigraphic variations in bedrock.

The base of the stratigraphic section in the Bull Run Watershed consists of 900 feet of middle Miocene, tholeiitic basalt flows of the Grande Ronde and Wanapum Basalt Formations of the Columbia River Basalt Group. These are overlain, with local unconformity, by 600 feet of epiclastic and pyroclastic deposits of the Rhododendron Formation. The Rhododendron Formation is overlain, in the west, by an

eastward thinning wedge of fluvial siltstone, sandstone, and conglomerate of the Troutdale Formation. Greater than 2, 000 feet of basaltic andesite and less abundant basalt and pyroclastics overlie all older units with local unconformity. In the east, Pliocene volcanic rocks are overlain, locally, by Quaternary basalt, andesite, and hornblende andesite flows. Surficial deposits include extensive talus in the east, thick landslide debris in the west, widespread colluvial forest soils, and scattered glacial outwash and moraine. Glaciation did not extend below 2, 200 feet. Bedding of all geologic units is nearly horizontal. The Columbia River Basalt Group, and possibly the Rhododendron Formation, were deformed by gentle N60E-trending folds and a southeastward-dipping thrust fault. All bedrock units and older structures are cut by near vertical, northwest-trending shear faults and tectonic joints.

Chi-square goodness of fit tests indicate that mass movement distribution and morphology are strongly correlated to the distribution of geologic units and to site location with respect to geologic contacts. The highest number of slump-earthflow failures per unit area occur on the Rhododendron Formation and older landslide debris, whereas the density of debris avalanches is greatest on flows of the Columbia River Basalt Group, which form the steep-walled canyons of the Bull Run River. Prehistoric, complex-massive failures have occurred where soft pyroclastics of the Rhododendron Formation are

intercalated with more competent flow rock units. Smaller, recent mass movements have occurred along the contact between the pyroclastics and the overlying, older landslide debris in the North Fork and South Fork drainages, which are the most active drainages in the watershed in terms of recent mass movements. Contacts between pyroclastics and underlying or overlying flow rocks and between flow rocks and overlying Quaternary landslide debris are also associated with a high density of recent mass movements. The density of springs and seeps follows a similar distribution with respect to geologic contacts, and the effluence of groundwater on slopes is related to mass movement occurrence, particularly by debris avalanche.

Mass movement occurrence is favored by high clay content in soils and by abundance of smectite, and possibly hydrated halloysite, in the clay fraction. Soils of this type weather from pyroclastics of the Rhododendron Formation, Quaternary landslide debris, and interflow breccias and interbeds.

Jointing attitudes have only a minor effect on mass movement occurrence in the watershed. Failures are more likely where the attitude of joints dips steeply with the slope. Average slope gradients at mass movement sites vary between 58 and 85 percent with debris avalanches occurring on steeper slopes than slump-earthflows.

A stepwise multiple regression analysis indicates that the occurrence of mass movements is most strongly correlated with the

inverse of distance between a site and a geologic contact, moderately correlated with slope gradient, and weakly correlated with soil texture.

Data generated by statistical tests are used to weight geologic factors in terms of mass movement hazard levels. Stratification of the weighted values produced a mass movement hazard map for the Bull Run Watershed.

The Quantification of Soil Mass Movements and Their Relationship to Bedrock Geology in the Bull Run Watershed, Multnomah and Clackamas Counties, Oregon

by

Michael Gerhard Schulz

A THESIS

submitted to

Oregon State University

in partial fulfillment of
the requirements for the
degree of

Master of Science

Completed June 5, 1980

Commencement June 1981

APPROVED:

Redacted for Privacy

Adjunct Assistant Professor of Geology
in charge of major

Redacted for Privacy

Head of Department of Geology

Redacted for Privacy

Dean of Graduate School

Date thesis is presented June 5, 1980

Typed by Opal Grossnicklaus for Michael Gerhard Schulz

ACKNOWLEDGEMENTS

This work was supported by funds made available through the United States Department of Agriculture Forest Service, Research Work Unit 1653, Forestry Science Laboratory, Corvallis, Oregon. Personnel of the Columbia River Gorge Ranger Station, particularly Fred Heisler, Charles Caughlan, Glenn McDonald, and Terry Brown, provided friendship and logistical support during the field work phases of the project. I am indebted to the City of Portland Bureau of Water Works for the provision of accommodations in the field and for access to their files.

I would like to extend special appreciation to Kathy Manning of the Mount Hood National Forest, Douglas N. Swanston, Moyle E. Harward, Richard L. Fredriksen, Donald L. Henshaw, John Hazard, and my committee members Harold E. Enlows and Robert D. Lawrence for numerous discussions pertaining to interpretations of the data.

Last, but certainly not least, I wish to express my sincerest thanks to my advisor, Frederick J. Swanson for the boundless patience and conscientious guidance that shaped this thesis, and to my parents and future wife Diane for their unfaltering support.

TABLE OF CONTENTS

LIST OF ILLUSTRATIONS

LIST OF TABLES

LIST OF PLATES

THE QUANTIFICATION OF SOIL MASS MOVEMENTS AND THEIR RELATIONSHIP TO BEDROCK GEOLOGY IN THE BULL RUN WATERSHED, MULTNOMAH AND CLACKAMAS COUNTIES, OREGON

INTRODUCTION

Purpose

Mass movements are the dominant erosional processes in mountainous regions of the Pacific Northwest, where characteristically steep slope gradients, thick surficial deposits, and high annual precipitation rates provide an environment conducive to mass wasting. The consequences of massive slope failures are of great economic importance in resource planning and management. In the Bull Run Watershed, recent landslides have degraded water quality and disrupted conduits and roads. Activities such as road construction and logging may seriously decrease natural slope stability, and it is necessary to assess the magnitude of mass movement hazards that may be associated with these activities before they are undertaken.

Geologic, vegetative, and hydrologic factors determine the occurrence, distribution, and type of slope failures (Swanston and Swanson, 1976; Swanson and Swanston, 1977). These controlling factors are fairly well understood in a general, qualitative way, however research has only recently begun to quantify these factors in attempts

to organize them into widely applicable, predictive models of mass movement hazards.

The specific problems with which this study is concerned are to quantify occurrence frequencies, distribution patterns, and failure characteristics of soil mass movements in the Bull Run Watershed as they relate to variations in bedrock lithology, geologic structure, and stratigraphic sequence. The ultimate goal is to understand relationships between geologic factors and mass movement occurrence which can be used to predict failure hazard in the Bull Run Watershed and in similar geologic terrane.

Previous Work

The literature contains a number of assessments of basic geologic factors related to mass movement processes. The tendency of landslides to occur within certain types of bedrock, notoriously volcaniclastics, shales, mudstones, and serpentine-rich rocks, has long been recognized intuitively and by general observation (Varnes, 1978; Pope and Anderson, 1960; Zaruba and Mencl, 1969; and others). Dyrness (1967) discovered that 94 percent of the mass movement events mapped in the H. J. Andrews Experimental Forest occurred in areas underlain by pyroclastic bedrock, even though only 34 percent of the total study area surface was made up of these rocks.

The presence of bedrock materials which weather to thick, cohesive, clay-rich soils is a major factor in the occurrence and distribution of deep-seated mass movements (Swanston and Swanson, 1976; Swanson and Swanston, 1977). Soils developed from highly altered pyroclastic parent materials tend to be unstable due to high concentrations of expandable clay (Paeth and others, 1971; Taskey, 1978). Soils developed from lava flow rock have coarser texture and are better drained and therefore tend to be more stable than those derived from pyroclastic rocks. Based on data from the H. J. Andrews Experimental Forest, Swanson and James (1975) determined that more than 25 percent of the area underlain by pyroclastic rock is covered by earthflow landforms, whereas less than 1 percent of the area underlain by flow rock exhibits earthflow activity. Slump-earthflow failure is particularly likely to occur where pyroclastic rocks underlie a capping of hard, competent rock (Wilson, 1970; Swanson and James, 1975). From data collected in the Redwood Creek Basin of northern California, Colman (1973) observed a very high percentage of unstable areas located in sheared, clay-rich sedimentary rocks.

The Bull Run Watershed has been the subject of numerous engineering studies related to dam construction (Ruff, 1957; Stevens and Thompson, 1957; Shannon and Wilson, 1958a, 1958b, 1963, 1973,

1978; Schlicker, 1961, Geo-Recon. Inc., 1962). A few major slides have been studied within and near the boundaries of the watershed. Shannon and Wilson (1965) and Stevens and Thompson (1965) investigated the Ditch Camp slide, located near the community of Bull Run, and found that failure was in part due to the nature of the contact between an upper conglomeratic sandstone unit and a lower mudstone unit contained within the Troutdale Formation. Dames and Moore (1972a, 1972b, 1973) and Patterson (1973) studied the very damaging North Fork slide. Failure occurred in older, more extensive landslide material, which contained blocks of deeply weathered pyroclastics of the Rhododendron Formation.

The geology of the Bull Run Lake area was described in reports by Williams (1920) and Shannon and Wilson (1961). Vogt (1979) has studied the structure and stratigraphy of the Columbia River Basalt Group exposures within the Bull Run Watershed. Complete soil survey reports, which include the watershed, were compiled by Stephens (1964) and Howes (1979). The most inclusive geologic study of the Bull Run Watershed (Beaulieu, 1974) contains maps of the bedrock geology and a number of slides. Beaulieu's study reveals a correlation between mass movement and the distribution of the Rhododendron Formation and, to a lesser extent, the Troutdale Formation.

GEOGRAPHY

Location

The Bull Run Watershed lies within the Mount Hood National Forest, and is located between Mount Hood and Portland, in the northern part of the western Cascade Range of Oregon (Figure 1). The study area encloses approximately 134 square miles and occupies the intersection of the Cherryville, Bonneville Dam, Mount Hood No. 2, and Bridal Veil 15 minute quadrangles. Primary access to the area is provided by U.S. Highway 26 from the south, and by Interstate 80N from the northeast. Secondary access is provided by numerous county roads, and within the watershed, by a network of Forest Service roads, which are generally passable with two-wheel drive vehicles. Admittance to the watershed is restricted by the Exclusion Act of 1904.

Climate

The Bull Run Watershed experiences wet winters, due to cyclonic storms moving eastward from the Pacific Ocean, and dry summers. As the winter storms rise to cross the Cascade Range, intensification of rainfall occurs on the western flanks of the range due to orographic effects.

Average annual precipitation varies from 85.71 inches at the Headworks to 141.22 inches at the North Fork dam (Stevens,

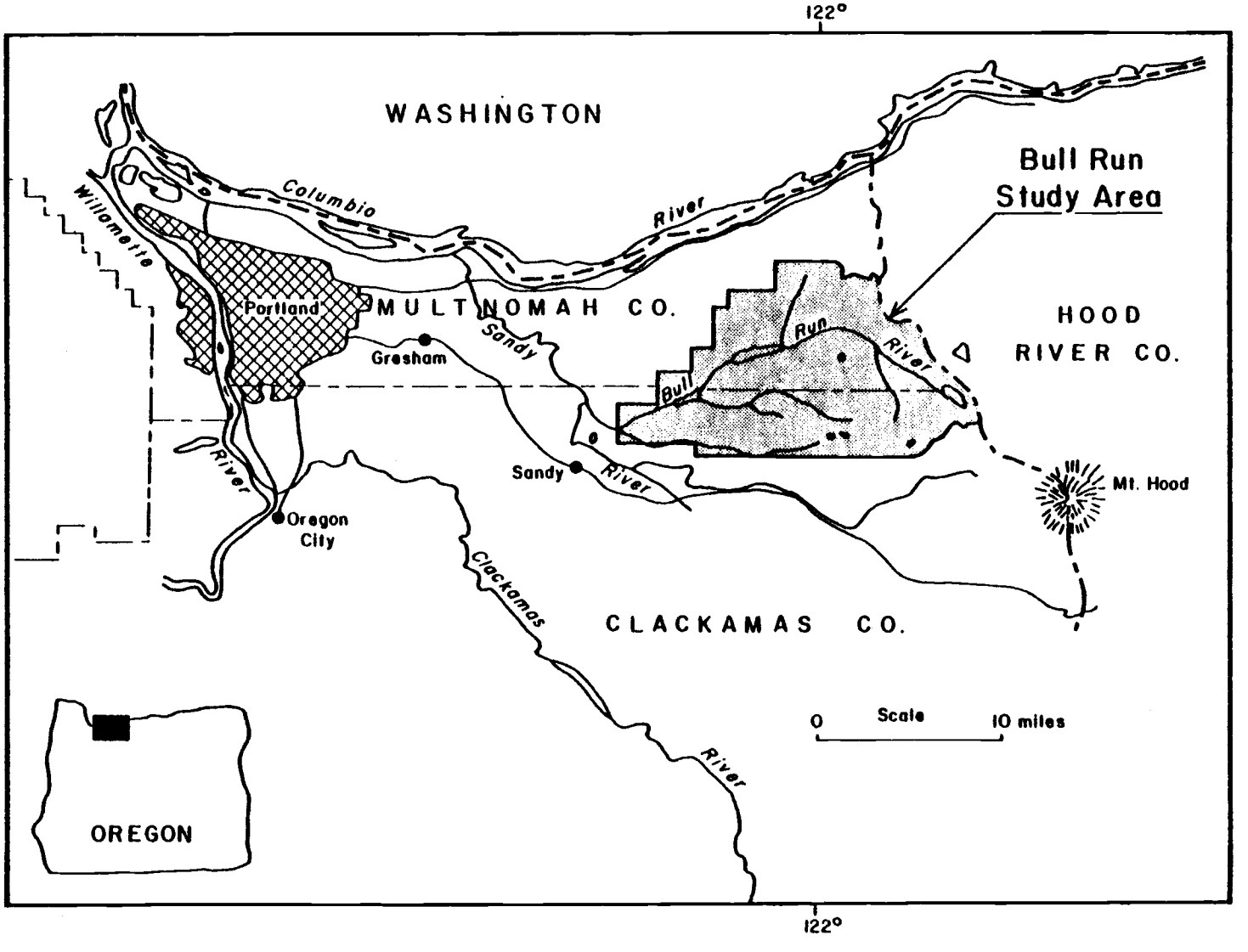

Figure 1. Location map of the Bull Run Watershed study area.

Thompson, and Runyan, Inc., 1974). Over 70 percent of this precipitation falls during the period from October through March.

The mean annual temperature, taken from data recorded at the Headworks over a 32 year period through 1962, is 51°F (Stephens, 1964), and daily temperatures rarely exceed 90°F in summer or drop below 32°F in winter. Snowfall at the Headworks averages 21.6 inches per year, but persistent snowpack is limited to higher elevations, where it often remains until late spring.

Vegetation

The lower elevations of the Bull Run Watershed, generally below 3,000 feet, are characterized by Humid Transition life zone vegetative species (Stephens, 1964). Conifers typically found in the Humid Transition zone are Douglas-fir (Pseudotsuga menziesii), which is the dominant overstory species, western hemlock (Tsuga heterophylla), western redcedar (Thuja plicata), and grand fir (Abies grandis). Red alder (Alnus rubra) and big leaf maple (Acer macrophyllum) are the most common hardwood species, and dominant shrubs include vine maple (Acer circinatum), salal (Gaultheria shallon), red huckleberry (Vaccinium parvifolium), and dull Oregon grape (Mahonia nervosa). Herbaceous understory includes swordfern (Polystichum munitum), and oxallis (Oxallis oregona).

In the eastern part of the watershed, the Canadian life zone extends above the Humid Transition zone. There, typical conifers are Douglas-fir, silver fir (Abies amabilis), noble fir (Abies procera), western hemlock, western redcedar, western white pine (Pinus monticola), Engelman spruce (Picea engelmanni), and lodgepole pine (Pinus contorta latifolia). Shrub species include blue huckleberry (Vaccinium ovalifolium), rhododendron (Rhododendron macrophyllum), and vine maple. Herbaceous vegetation includes beargrass (Xerophyllum tenax), vanilla leaf (Achlys triphylla), and devil's club (Oplapanax horridum).

Topography

Topography in the Bull Run Watershed is varied. Broad, flat or gently west-dipping lava plains are the result of Pliocene volcanism. In the eastern part of the watershed, alpine features are present as evidence of Pleistocene glaciation. Cirque basins now hold alpine lakes such as Hickman Lake, Blue Lake, and Bull Run Lake. Quaternary fluvial erosion has incised steep canyons in the younger flow rocks. Downcutting, however, has been effectively retarded by the resistant flows of the Columbia River Basalt Group, which forms the lowest stratigraphic unit exposed in streambeds of the watershed. In the western half of the watershed, mass wasting of pyroclastics of

the Rhododendron Formation has produced concave bench slopes on both sides of the Bull Run River and along portions of its western tributaries.

Primary drainage of the watershed is provided by the Bull Run River mainstem, which extends approximately 30 miles from its origin at Bull Run Lake to its confluence with the Sandy River. In its course through the watershed, the Bull Run River flows first northwest and then abruptly changes direction to flow southwest towards the Headworks. The overall drainage pattern is dendritic, with short, steep-gradient northern tributaries and longer, lower-gradient southern tributaries.

Elevations in the Bull Run Watershed range from a maximum atop Hiyu Mountain (4, 600 ft) in the southeast corner to 748 ft at the Headworks. Prominent peaks, all located in the eastern portion of the area, are Burnt Peak (4, 419 ft), Hickman Butte (4, 385 ft), Blazed Alder Butte (4, 258 ft), and Big Bend Mountain (4, 017 ft).

Land Use

The entire Bull Run Watershed is located within the Bull Run Forest Reserve, which was incorporated into the National Forest Area by the Federal Government in 1892. On January 1st, 1895 Bull Run water first flowed into the city of Portland. Presently, the Bull Run Watershed serves the water needs of the entire city of Portland and

also supplies 42 water districts outside of the city proper.

Most of the Bull Run Watershed is publicly owned and lies within the boundaries of the Mount Hood National Forest. The system of waterways and lakes making up the physical watershed is administered by the City of Portland Bureau of Water Works, whose primary directive is to maintain or improve the high quality and yield of water. All other management activities are administered by the Forest Service of the U.S. Department of Agriculture. The management objectives of the Forest Service are to define the capabilities and limitations of the area to sustain multiple use without adverse effects to the present or future quality of the water, land, and wildlife. Timber harvesting in the Bull Run Watershed began in 1956 and timber sales have been regularly conducted by the Forest Service since. The Bull Run Watershed is closed to public access and has sustained no recreational use since its incorporation.

METHODS

Field Methods

Field work was conducted from June 22, 1978 to November 13, 1978. Field checks were made from April 28, 1979 to May 13, 1979. Regional geology was mapped on USGS 15-minute quadrangle base maps, and detailed traverses were done on low altitude (1:15, 840), 1977, infrared air photos. High altitude (1:70, 000), black and white air photos proved useful in the recognition of large geologic and topographic features.

Dimensions of mass movement features were measured with a tape and rangefinder, or estimated by sight and pace, depending on the size of the feature and the terrain. Estimates were spot checked with a tape for accuracy and found to be within reasonable error limits (less than 10%). Mass movements less than 100 ft^3 in volume were not included in the inventory. Slope gradients were measured with the Brunton compass inclinometer. Stream profiles and detailed maps were made with a Brunton compass, tape, and rangefinder.

Soil samples of mass movements were taken from the center of the exposed failure surface, at a depth of 8-12 inches below the failure surface. When the failure surface consisted of bedrock, samples were taken from the scarp near the soil-bedrock interface. Soil

samples from stable sites were taken at a depth of 12 inches in flat-lying areas, where the soil profile appeared to be residual. All samples were double bagged in plastic to prevent drying. While in the field, soil samples were kept as cool as possible; and pending analysis, they were stored at 5 °C. All soil samples were approximately 100 grams in weight.

In situ soil shear tests were performed with the Iowa bore-hole shear device. Procedures outlined in the instruction manual were followed. Using the shear device, repeated shearing on the walls of an open bore-hole may be conducted at varying degrees of normal pressure, exerted hydraulically by the shear head against the bore-hole walls. Plots of shear strength versus normal pressure produce a Mohr failure envelope, from which the angle of internal friction and the cohesion intercept can be derived.

Laboratory Methods

Infrared, 1977, air photos (1:15, 840) were used to map topographic, vegetative, and hydrologic features prior to work in the field. Features indicative of mass movements were then checked in the field. Only mass movements larger than about 25,000 yd^2 in area were visible on this scale.

Soil samples were analyzed for particle size distribution by the Bouyoucos hydrometer method (Bouyoucos, 1962). Clay fractions were

separated and treated for X-ray diffraction (XRD) by the method of Taskey (1978). XRD determinations of clay mineralogy were made on a Phillips Norelco diffractometer, set at 35kv and 25ma. The diffractometer was equipped with a Cu Kα source and graphite filters.

Petrographic determinations of bedrock samples were made with a standard petrographic microscope. Plagioclase mineralogy was determined by the Michel-Levy method. Computer analyses, using SPSS programs, were done by the Pacific Northwest Forest and Range Experiment Station, Portland, Oregon.

GEOLOGY

Regional Aspects

The Bull Run Watershed is located in the Cascade Range of Oregon in a zone of transition between the northernmost extent of the western Cascade physiographic province and the High Cascade province (Figure 2). The western Cascade Range is maturely dissected and descends westward, relatively gently, to the Willamette Valley and several other smaller valleys further south near Medford and Roseburg. The High Cascades form the crest of the range and descend relatively steeply eastward to the Deschutes Plateau, the Klamath Basin, and the intervening high lava plains.

The western Cascade Range consists predominantly of early to middle Tertiary volcanic flows, tuffs, and small intrusive bodies. The late Eocene Colestin Formation (Wells, 1956) contains the oldest rocks exposed in the range. These are andesitic tuffs, conglomerates, volcanic-wacke sandstones, and minor flows and breccias of basaltic andesite and pyroxene andesite. The Colestin Formation averages 1,500 feet in thickness and is in part equivalent to the Calapooya Formation of Wells and Waters (1935) and the Fisher Formation of Hoover (1963). In the foothills of the western Cascade and Coast Ranges, the Colestin Formation overlies Eocene marine sedimentary rocks of the Spencer, Tyee, and Umpqua Formations;

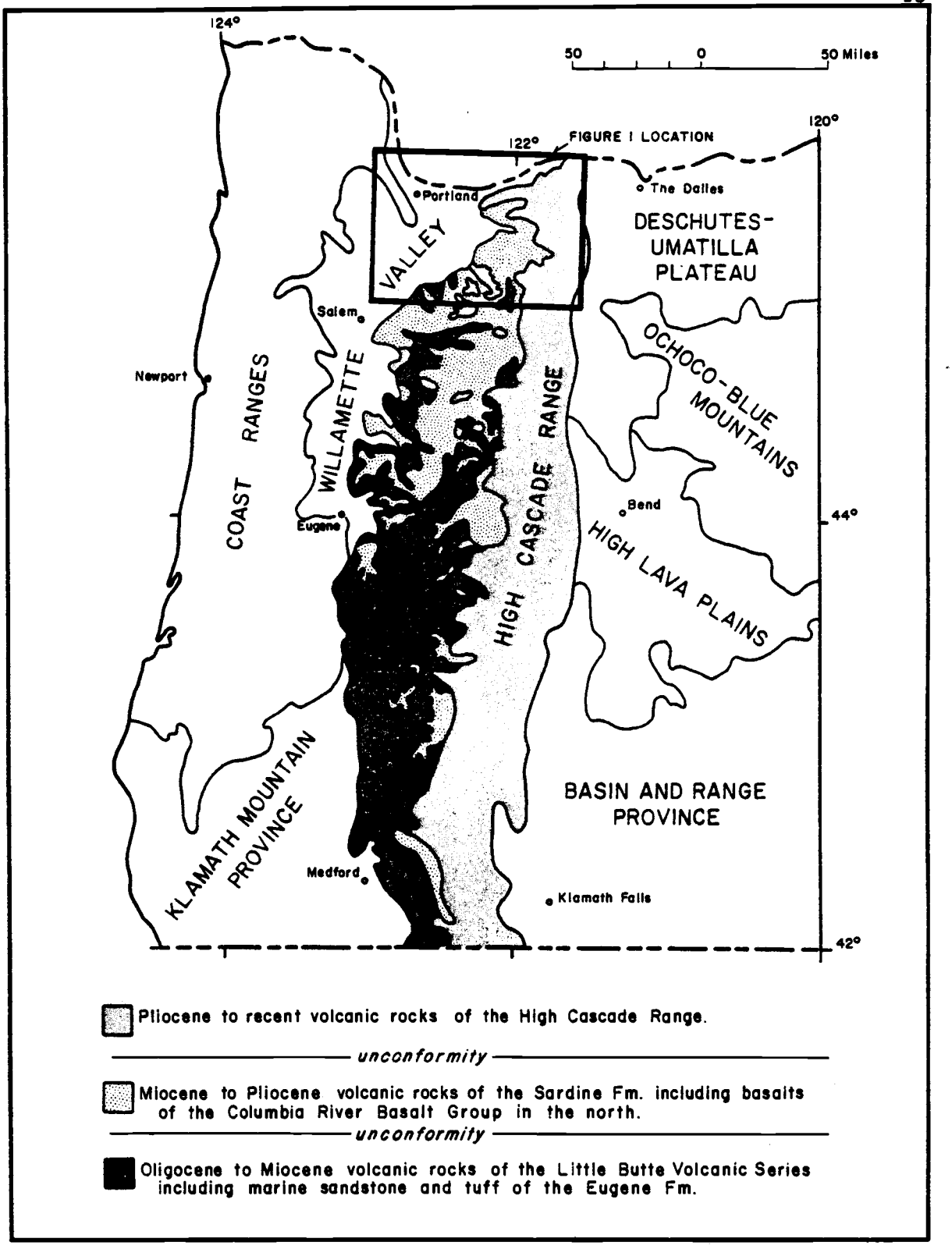

Figure 2. Regional geologic map of the western Cascade Range, showing the physiographic provinces of western Oregon and the location of Figure 1.

and in the southern extent of the western Cascades, it overlies pre-Tertiary metamorphic and plutonic rocks of the Klamath Mountains (Peck and others, 1964).

The Colestin Formation is overlain with local unconformity by the Little Butte Volcanic Series (Wells, 1956), which averages 5, 000 to 10, 000 feet in thickness and consists of Oligocene and early Miocene dacitic and andesitic tuff and less abundant olivine basalt, basaltic andesite, pyroxene andesite flows and breccias, dacitic and rhyolitic flows and domes, and rhyodacitic tuff. The Little Butte Volcanic Series, as mapped by Peck and others (1964), includes the Mehama Volcanics and Breitenbush Series of Thayer (1939), the Mollala Formation and pre-Butte Creek Lavas of Harper (1946), and the Eagle Creek Formation and Bull Creek Beds of Barnes and Butler (1930). Middle Oligocene to early Miocene marine tuff and sandstone, in part equivalent to the Eugene Formation (Vokes and others, 1951) and the Butte Creek Beds (Harper, 1946), interfinger with the Little Butte Volcanic Series in the central foothills of the western Cascade Range.

In the northern part of the western Cascades, the Little Butte Volcanic Series and time equivalent marine tuff and sandstone are unconformably overlain by thick, middle Miocene, tholeiitic basalt flows of the Columbia River Basalt Group (Russel, 1893; Merriam, 1901). Unlike the older flows of the range, the Columbia River

Basalts are not indigenous, but have been traced eastward to a source area in eastern Oregon and Washington by Peck and others (1964), who have included the Stayton Lavas of Thayer (1936) in the Columbia River Basalt Group.

The Sardine Formation (Thayer, 1936) averages 3, 000 feet in thickness and consists of indigenous flows, lapilli tuff, and tuff of hypersthene andesite, and less abundant basaltic andesite, augite andesite, aphyric silicic andesite, dacite, and olivine basalt. The Sardine Formation, as mapped by Peck and others (1964), includes the Rhododendron Formation (Hodge, 1933), the Boring Agglomerate (Treasher, 1942), and the Fern Ridge Tuffs and parts of the Breitenbush Series (Thayer, 1936). It overlies the Little Butte Volcanic Series with angular unconformity in the southern portion of the western Cascade Range and overlies the Columbia River Basalt Group with local unconformity in the northern part of the range (Wise, 1969; Beaulieu, 1974).

Early Pliocene conglomerate, sandstone, and micaceous siltstone of the Troutdale Formation (Hodge, 1933) average approximately 400 feet in thickness and unconformably overlie the Sardine Formation and older units in the northern extent of the western Cascade Range (Peck and others, 1964). According to Trimble (1957) the Troutdale Formation is divided into an upper sandstone and conglomerate member and a lower mudstone member (the Sandy River Mudstone). In

most localities the Troutdale Formation consists of detritus derived from Pliocene volcanic Cascade Range rocks. Locally present are quartzite pebbles, whose source area was a terrane of Paleozoic and older rocks located to the east in the ancestral Columbia River drainage (Baldwin, 1964).

The High Cascade Range of Oregon consists of generally greater than 3,000 feet of Pliocene and Quaternary flows and minor pyroclastic rocks of basaltic andesite and olivine basalt, and less abundant pyroxene andesite and dacite. As mapped by Peck and others (1964), these rocks include the Boring Lavas of Treasher (1942). The Pliocene and Quaternary volcanics interfinger with the Troutdale Formation and unconformably overlie the Sardine Formation, the Columbia River Basalt Group, and the Little Butte Volcanic Series. Pliocene-Quaternary volcanic flows are commonly present in the western Cascade Range as intracanyon flows.

Intrusive rocks of the western Cascade Range vary in composition from rhyodacitic to basaltic equivalents and occur as stocks, plugs, dikes, sills, and domes. Propylitic alteration halos commonly accompany the intrusives (Callaghan and Buddington, 1938). Intrusive plugs and dikes in the High Cascade Range are compositionally similar to their extrusive equivalents and are commonly only slightly coarser in texture.

In a gross structural sense, the Cascade Range of Oregon is a northerly-trending, downwarped volcanic pile, which has been deformed by broad, northeast trending folds and steep, northwest-trending faults (Peck and others, 1964). Most of the folding and intrusion occurred during the middle of the Miocene Epoch, and thus was limited to rocks of the western Cascade Range. Late Miocene erosion smoothed the topography created by the earlier orogeny. Intense periods of volcanism and uplift characterized the late Tertiary and Quaternary of the Cascade Range (McKee, 1972).

Stratigraphy

General Statement

Bedrock units mapped in the study area include 900 feet of middle Miocene Columbia River Basalt Group flows, 600 feet of late Miocene to early Pliocene tuff, lapilli tuff, pyroclastic breccia, and laharic breccia of the Rhododendron Formation, an eastward thinning wedge of early to middle Pliocene fluvial siltstone, sandstone, and conglomerate of the Troutdale Formation, and greater than 2, 000 feet of middle Pliocene to Quaternary basaltic andesites, hornblende andesites, olivine basalts, and minor pyroclastic equivalents (Figure 3).

These rocks are mantled with surficial deposits, which include thick landslide debris, scattered glacial moraine and outwash deposits,

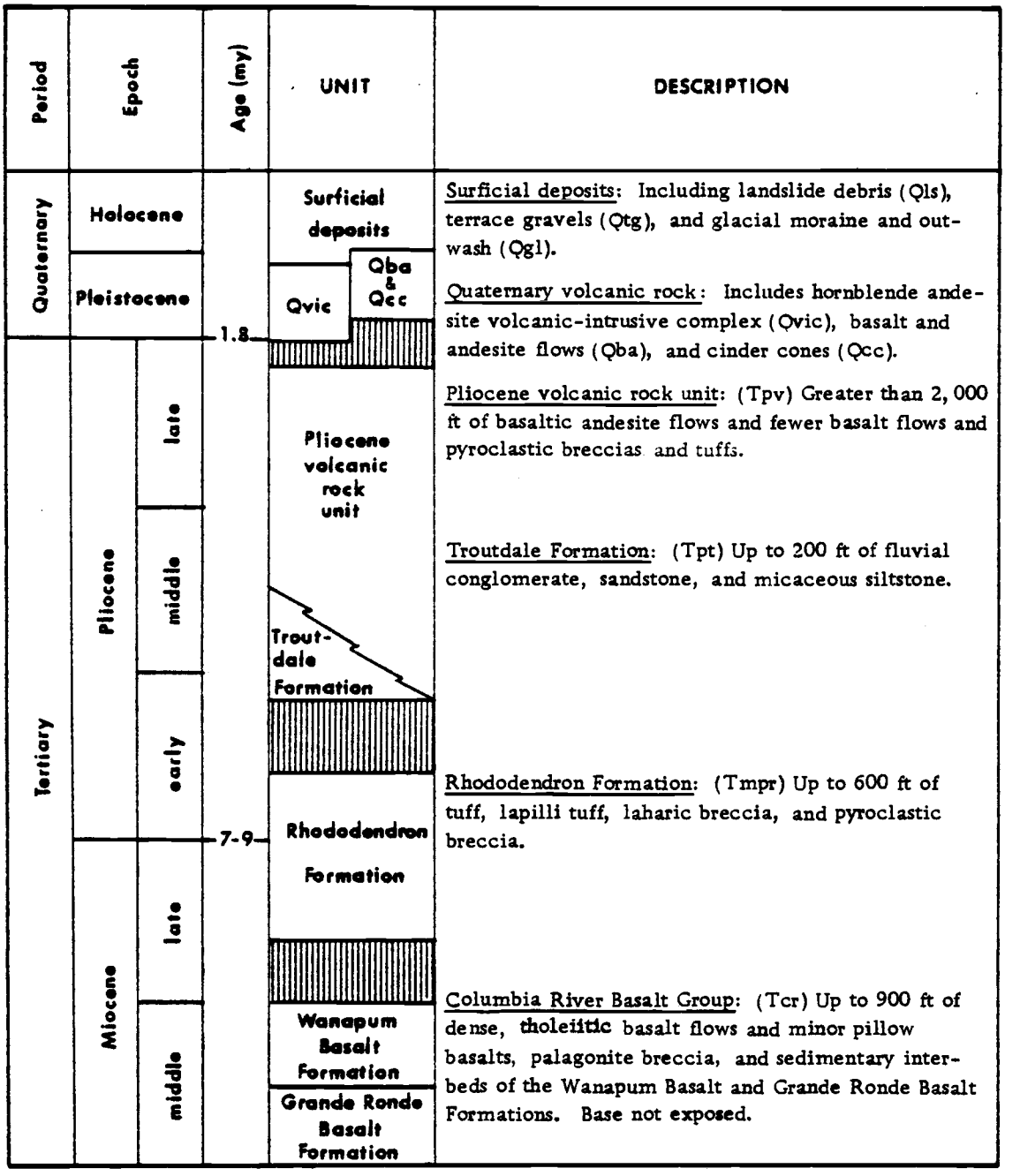

Figure 3. Stratigraphic chart for geologic units exposed in the Bull Run Watershed.

terrace gravels and other alluvium, talus and felsenmeer, and colluvial and lesser residual forest soils.

Columbia River Basalt Group

The oldest unit mapped in the Bull Run Watershed is a sequence of dense, tholeiitic basalts of the Yakima Basalt Subgroup (Waters, 1961) of the Columbia River Basalt Group. Columbia River Basalts are exposed in the deep canyons of the Bull Run River and proximal parts of its tributaries, at elevations ranging from 480 feet near the confluence of the Bull Run and Little Sandy rivers, to 3,000 feet in the eastern extents of the Bull Run River and Bedrock Creek. The base of the Columbia River Basalt Group is not exposed in the study area.

B. F. Vogt (1979) has determined the stratigraphic sequence of the flows present in the watershed. The following discussions concerning the structure and stratigraphy of the Columbia River Basalt Group are based, in large part, on her data. The nomenclature used is that of Swanson and others (1979).

Grande Ronde Basalt Formation

In the Bull Run Watershed the lowest part of the Columbia River Basalt Group section consists of low-Mg, paleomagnetically reversed flows of the Grande Ronde Basalt Formation. These flows are exposed

in Blazed Alder Creek and are overlain by four or more normal flows of low-Mg Grande Ronde Basalt. The normal flows total 310 feet in thickness. In hand specimen, all low-Mg flows are finely crystalline with small, clear plagioclase phenocrysts present locally.

Overlying the low-Mg flows are two high-Mg Grande Ronde flows, averaging 140 feet in total thickness. Sedimentary interbeds, to 30 feet in thickness (Figure 4), and local pillow basalts (Figure 5) separate these flows. The tops of each flow show soil development, indicating a period of weathering between successive flows. The high-Mg flows are somewhat coarser than the low-Mg flows beneath them.

The Vantage Horizon, a major interbed in the Columbia River Basalt Group, occurs locally above the Grande Ronde flows. It consists of cream colored to light yellow, silty sand and organic matter (Figure 6). Pillow basalt is locally present in the Vantage Horizon.

Wanapum Basalt Formation

Overlying the Vantage Horizon are six flows of the Frenchman Springs Member of the Wanapum Basalt Formation. The Frenchman Springs flows are coarse textured and commonly contain large, glassy plagioclase phenocrysts. The two upper flows, however, are aphyric. These are separated by a red paleosol horizon.

Figure 4. Sedimentary interbed between high-Mg Grande Ronde Basalt flows (S-10 north of Reservoir no. 1).

Figure 5. Pillow basalts at the base of the Wanapum Basalt Fm. (S-10 near Falls Ck.)

Figure 6. Vantage Horizon of the Columbia River Basalt Group (below dam no. 1). Note thin, upper carbonaceous layer.

One or two Priest Rapids Member flows of the Wanapum Basalt Formation, which consist of very well indurated, bedded palagonite, are present in the Bull Run Watershed as intracanyon flows. Exposures of Preist Rapids flows suggest that they coursed through a channel roughly coincident with the present day Bull Run River channel between Log Creek and North Fork, and then flowed northward toward the Columbia River Gorge.

Age

Radiometric age dates for the Columbia River Basalt Group flows range from 16 to 6 my (Watkins and Bakshi, 1974; McKee and others, 1977). The flows exposed in the Bull Run Watershed are probably middle Miocene in age.

Rhododendron Formation

General Statement

The Rhododendron Formation unconformably overlies the Columbia River Basalt Group in the Bull Run Watershed. Mapping relationships suggest that the pyroclastic rocks of the Rhododendron Formation accumulated discontinuously, in topographic depressions, on the middle Miocene surface of the Columbia River Basalt Group; and thus a period of erosion, and probably some broad folding,

intervened between the deposition of the last Columbia River Basalt flows and the first Rhododendron pyroclastic flows. Relief on the basalt exceeded several hundred feet.

Exposures of the Rhododendron Formation occur in the steep canyon walls of the Bull Run River, in the western-most extent of the study area, and in scattered outcrops between the Headworks and Falls Creek. Other than a local occurrence in Log Creek, no rocks assigned to the Rhododendron Formation were observed between Falls Creek and Otter Creek, either due to non-deposition or erosion of the unit in this area. A fairly continuous sequence of the Rhododendron Formation is exposed in the southeastern part of the watershed.

The Rhododendron Formation is 1,400 feet thick at its type section near Zig Zag Mountain, south of the Bull Run Watershed (Wise, 1969). There, it consists of a lower 300 feet of laharic breccias and conglomerates, a central 900 feet of tuffs and lapilli tuffs, and a 200 foot capping of interbedded tuff and olivine andesite.

Laharic Breccias and Conglomerates

In the western part of the study area, below the Headworks, the Rhododendron Formation consists predominantly of laharic breccias (Figure 7), which typically contain large, unsorted, generally rounded blocks of heterolithologic andesite in a clay-rich matrix, which commonly shows flow laminae. Included in the matrix are 0.5 to 1.3

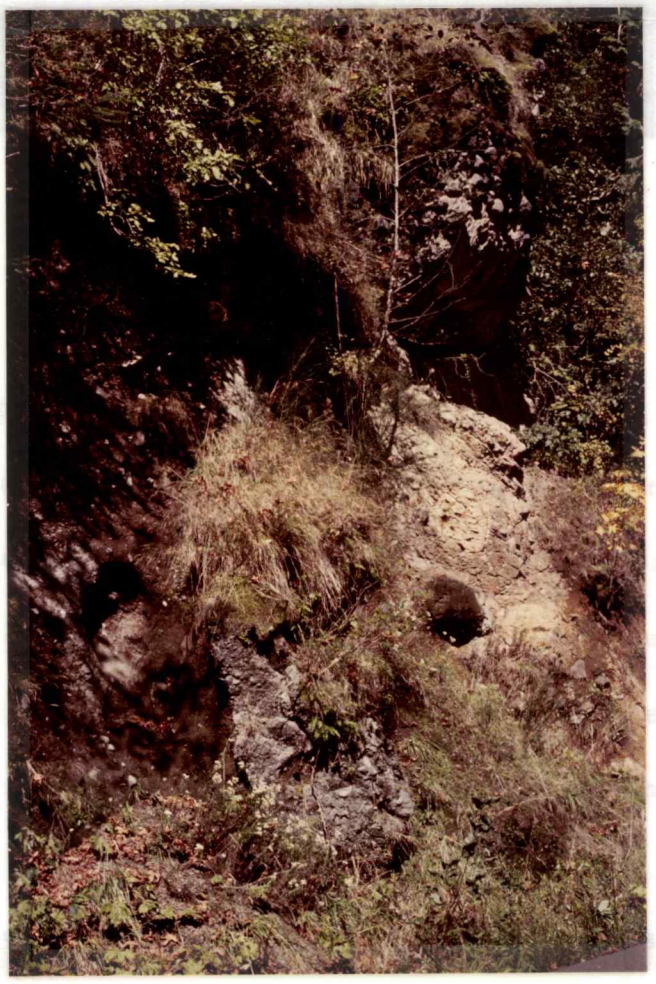

Figure 7. Laharic breccias of the Rhododendron Fm. (S-10 near main access gate). Note contact between two laharic deposits (center) and weathered, red-gray laminated clay pods (lower center and lower left).

meter wide pods of convoluted and thinly laminated, red and gray bentonitic clay. The pods may have originated as fragments of a widespread ash layer that was ripped up and incorporated by the flowing lahars. Similar pods of laminated clay were found in the Fir Creek area, on S-10 west of Falls Creek, and in the channel of Bedrock Creek. At least two laharic pulses deposited material in the western part of the watershed.

Laharic breccias are also present low in the section of exposed Rhododendron Formation in the drainage of Clear Creek, on the southeast margin of the study area. Here, they contain boulders of gray and maroon, porphyritic andesites (to 1 m in diameter) in a green, well-indurated matrix, which is apparently propylitically altered.

Laharic breccias or epiclastic conglomerates occur high in the Rhododendron Formation section in the channel of South Fork. Conglomerates, with andesitic boulders ranging to 1 meter in diameter, are present as capping layers above pyroclastic units on S-111 east of Fir Creek, on S-10 west of Falls Creek, and on S-127 east of Hickman Creek. These conglomerates probably resulted from reworking of Rhododendron Formation rocks shortly after their deposition. Alternatively, where field relationships are not clear, some of these conglomerates may be Quaternary glaciofluvial deposits.

In general, the laharic breccias predominate lower in the Rhododendron Formation section exposed in the Bull Run Watershed. Their

total thickness is no more than 200 feet, and they compose approximately one third of the unit.

Tuffs

Tuffs make up a minor part of the Rhododendron Formation in the study area. They generally occur in the middle of the stratigraphic section as local interbeds (30-60 ft thick) between coarser pyroclastic units. The thickest sequence of tuffs is exposed in the South Fork drainage (Figure 8). These rocks are medium to coarse grained and consist of plagioclase crystals, multi-colored, aphanitic, volcanic-lithic fragments, and occasional inflated pumice fragments (0.5-3.0 mm) in a gray ash matrix. The tuffs are poorly indurated to moderately well indurated, but never welded. They generally show sedimentary structures, including crude bedding and small amplitude cross-bedding; and thus were waterlaid in part.

Another distinctive tuff is located in the Hickman Creek drainage It is rich in cream colored, uncollapsed pumice fragments, a few as large as 70 mm in diameter. The pumice fragments are contained in a dark-gray, very poorly indurated matrix. No sedimentary features were noticed in this tuff.

Figure 8. Well-indurated tuff of the Rhododendron Fm. (South Fork drainage).

Pyroclastic Breccias and Lapilli Tuffs

In the Bull Run Watershed, the most common rock types of the Rhododendron Formation are an assortment of lapilli tuffs and breccias of ashflow origin (Figure 9). These rocks compose roughly two thirds of the Rhododendron Formation and have a maximum total thickness of approximately 500 feet. They occur predominantly higher in the section than the laharic breccias and fine-grained tuffs.

Lithic fragments in the breccias and lapilli tuffs are poorly sorted and consist of multi-colored, multi-textured, sub-rounded to sub-angular andesite (to 0.6 m), fewer rounded, inflated, cream-colored pumice fragments (8-10 mm), and sparse red cinder fragments (5-10 mm). Among andesite fragments, porphyritic textures predominate.

The matrix of the lapilli tuffs and breccias is usually drab, greenish-gray or light gray and consists of ash-sized lithic fragments, visible angular plagioclase and fewer mafic crystals, and glass. Large pieces of charred organic debris are included in the pyroclastic breccia located on S-111, east of Fir Creek.

Lithification of the breccias varies from very poorly to moderately well indurated, but no truly welded units were observed. In general, the least competent rocks were found in the western part of the watershed, however local exceptions to this observation exist.

Figure 9. Pyroclastic breccia of the Rhododendron Fm. (South Fork drainage). Notice that jointing breaks around fragments, indicating poor lithification of the matrix.

Red clay pods of possible fumarolic origin are locally present in the lapilli tuffs and breccias. These pods, though usually less than one or two meters in length, are capable of creating serious turbidity problems when they enter the streams of the watershed. Red clay pods were observed in the central South Fork and North Fork drainages in recent landslide scarps, on S-123 north of Reservoir 1, and on S-10 west of Falls Creek.

Platy Andesite

Wise (1969) reports 200 feet of interbedded tuffs and microporphyritic olivine andesite at the top of the Rhododendron Formation type section; and several hundred feet of platy andesite, located above the Columbia River Basalt Group in the North Fork drainage, were mapped as equivalent Rhododendron Formation flows by Beaulieu (1974). However, a sample of the flows in question, taken from the quarry on S-10M, is a finely crystalline, equigranular hypersthene andesite with no olivine. Furthermore, megascopically similar flows occur stratigraphically higher, well into the overlying Pliocene volcanic rock unit. Mapping relationships do not preclude interbedding of the andesites with Rhododendron Formation pyroclastics, however, since these flows are present only in this localized area of the watershed and occur at elevations below the generally flat lying pyroclastic

layer here, their presence is perhaps best explained as intracanyon flows of the Pliocene volcanic rock unit. They are mapped as such in this report.

Petrography

Thin sections were prepared from six samples of lapilli tuff and pyroclastic breccia. Petrographic examination indicates that the pyroclastic rocks of the Rhododendron Formation are rich in essential crystals and lithic fragments. Porphyritic hypersthene andesite with hyalopilitic groundmass is the most common lithology of the fragments. Virtually all fragments are andesitic. Augite is often present as sparse phenocrysts in the fragments and as interstitial crystals in the fragment groundmass. Hornblende is an accessory mineral in some of the lithic fragments. Pumice fragments are completely inflated and may contain minor plagioclase microlites. Pumice is devitrified to various extents.

Crystals present in the matrix include ubiquitous fragmental andesine and lesser labradorite, minor hypersthene and augite, and accessory magnetite and hornblende. The rest of the matrix is glass in various stages of devitrification.

Alteration in the pyroclastic rocks is usually extensive. Plagioclase may be fresh or altered to clay or sericite. Pyroxenes are

altered to smectite, hornblende is rimmed with magnetite and hematite, and glass in the matrix is altered primarily to smectite. Much of the alteration material is too finely or poorly crystallized to be identified with the petrographic microscope.

Age

By K-Ar analysis of a hornblende separate from an andesite boulder, Wise (1969) was able to determine an age of 7±2 my for the lower part of the Rhododendron Formation and considered the unit late Miocene (Clarendonian) in age. Beaulieu (1974) cites evidence for Hemphilian age and concludes that the Rhododendron Formation is best considered late Miocene to Pliocene.

Troutdale Formation

Field Relations

The Troutdale Formation overlies the Rhododendron Formation in the western-most part of the watershed. It is exposed on S-10 near the main access gate. The nature of the contact between the Troutdale Formation and the underlying Rhododendron Formation is not clear in the limited exposure in the study area. Peck and others (1964), however, report that the Troutdale Formation unconformably overlies the Rhododendron Formation between Molalla and Troutdale.

Maximum thickness of the Troutdale Formation is probably less than 200 feet, at the main access gate, and thins to nothing beneath extensive landslide debris to the east. On the basis of exposures farther west, outside the study area, it is assumed that the lower 25 feet of the Troutdale Formation, in the watershed, consists of siltstone and the remainder consists of coarser sandstone and conglomerate.

The siltstone is light gray to buff weathering, micaceous, massively bedded, and poorly to moderately well indurated (Figure 10). The sandstones and conglomerates contain rounded quartzite clasts, derived from metamorphic sources east of the Cascade Range, and volcanic flow rock fragments, derived from contemporaneous Pliocene volcanic rock unit flows.

Petrography

One thin section was prepared from a volcanic-wacke siltstone of the Troutdale Formation. Most grains are subangular, less than 0.1 mm in diameter, and consist of andesine and labradorite and lesser andesitic lithic fragments, biotite, muscovite, chlorite, and quartz. The matrix consists of clays, now predominantly smectite. Platy minerals show bedding alignment.

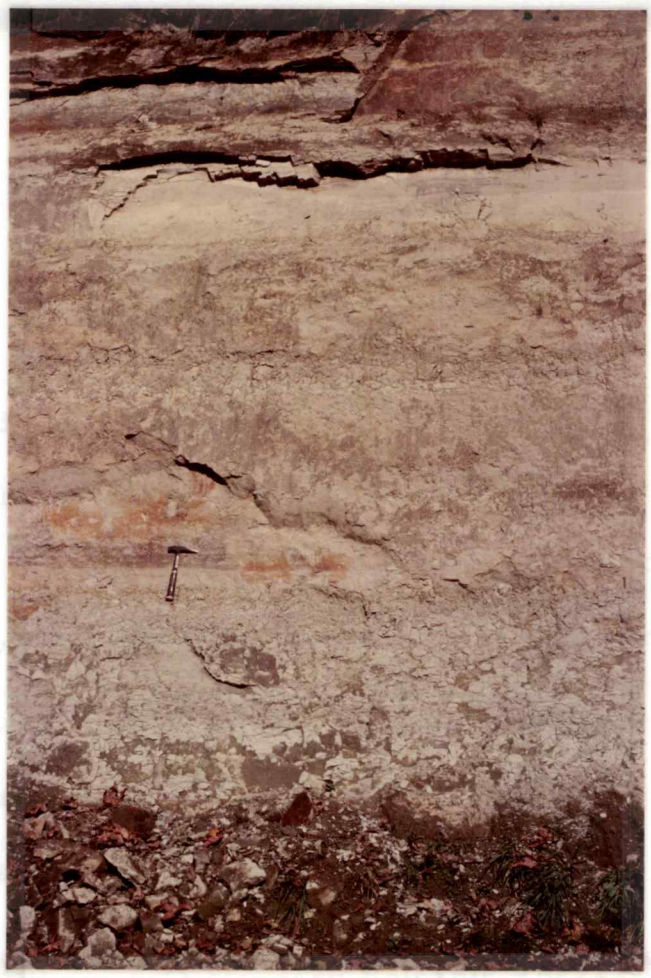

Figure 10. Massively bedded siltstone of the Sandy River Mudstone member of the Troutdale Fm. (S-10 near main access gate). Note moisture at base of outcrop, indicating high groundwater retention.

Age

The Troutdale Formation contains early Pliocene leaves (Hodge, 1938; Trimble, 1963). Troutdale Formation clasts are in part derived from the earlier flows of the Pliocene volcanic rock unit. Later Pliocene flows were deposited above the Troutdale Formation, indicating partial age equivalence between the two formations. Beaulieu (1974) reports an early to possibly middle Pliocene age for Troutdale Formation rocks exposed in the watershed.

Pliocene-Quaternary Volcanic Rocks

General Statement

Greater than 2, 000 feet of basaltic andesite and lesser olivine basalt, hornblende andesite, and equivalent pyroclastics overlie the Columbia River Basalt Group, the Rhododendron Formation, and the Troutdale Formation with local unconformity. Pliocene-Quaternary volcanic rocks cover 80 percent of the study area. The sequence is thickest in the eastern portion of the watershed, where a porphyritic pyroxene andesite flow caps Hiyu Mountain, the highest point in the Bull Run. The Pliocene-Quaternary volcanic rocks are divided into three sub-units following the descriptions of Wise (1969) and Beaulieu (1974); Pliocene volcanic rock unit, Quaternary volcanic-intrusive complex, and Quaternary basalt and andesite.

Pliocene Volcanic Rock Unit

Flows of the Pliocene volcanic rock unit are widespread in the Bull Run Watershed. They form lava plains in the west and glaciated peaks in the east. Basaltic andesites predominate among these flows and vary in texture from dense to porous, aphanitic to coarsely porphyritic varie ties, which contain megascopically visible plagioclase, olivine and/or pyroxene. Subordinate olivine basalts are intercalated with the andesites.

The basal flow in the western portion of the study area is a dark to medium-gray, porous, crudely diktytaxitic andesite with small (< 2 mm) subhedral plagioclase phenocrysts in a finely crystalline to aphanitic matrix. Many of the higher flows in this area contain small (1 mm) pyroxene or olivine phenocrysts in addition to plagioclase.

Flows in the eastern part of the study area are generally coarsely crystalline and porphyritic. A thick flow exposed in the channel of Log Creek near Blue Lake contains distinctive, glassy plagioclase phenocrysts (to 4 mm) and fewer black, subhedral pyroxene phenocrysts (to 4 mm) in a dense, finely crystalline groundmass. Similar, but coarser, basaltic andesite is exposed on the slopes northwest of Bull Run Lake.

A very thick basal sequence of massive porphyritic andesite is present in the drainage of Bedrock Creek. Phenocrysts are white,

subhedral plagioclase (5-10 mm in length). The groundmass is finely crystalline and dense. Stratigraphically above these flows is an 800 foot thick sequence of olivine basalt, olivine andesite, and pyroxene andesite, which forms Hiyu Mountain and the ridge to the northwest. Wise (1969) reports a 300-foot thick flow in this sequence, which cooled slowly enough to allow olivine phenocryst accumulation by gravitational sinking.

A dark, porphyritic olivine basalt is exposed on the eastern ridge at the head of Hickman Creek. A 15-foot thick, well-indurated, reddish-orange, monolithologic, scoriaceous breccia, overlain by dense aphanitic andesite, is exposed near Big Bend Mountain. A minor, well-indurated, light-gray, pyroclastic breccia, containing clinkery andesite fragments (to 80 mm), occurs on the ridge north of Thimble Mountain. Twenty-five feet of tuffaceous sandstone, in part a reworking of Troutdale sediments, is interbedded with two basal Pliocene volcanic rock unit flows, in the Cedar Creek drainage.

Several flow breccia horizons were mapped between flows of the Pliocene volcanic rock unit. These flow breccias are from 5 to 50 feet thick and are fairly persistent laterally, however limited exposure precluded determination of the exact number of flow breccia horizons. It is estimated that at least six separate horizons are present in the watershed. They consist of blocky to rounded, very vesicular andesite fragments (to 0.3 m) in a matrix composed of

andesitic, gravel-sized fragments and bentonitic clay. Clay fills vesicles in the fragments and blocks and tends to bind them together as a moderately well indurated unit when dry. The presence of groundwater decreases the induration. Flow breccia units weather buff to maroon and can often be identified as the autobrecciated top or bottom of a specific flow (Figure 11).

Petrography

Thin sections were prepared from three of the lower flows exposed in the South Fork and North Fork drainages. These rocks are all basaltic andesites. Textures are granular to microporphyritic, and the groundmass is diabasic or intersertal to sub-ophitic. Voids make up as much as 10 modal percent of the rock, but glass content is low. Plagioclase (andesine-labradorite) has oscillatory or normal zoning and occasional crude diktytaxitic or pilotaxitic orientation in the groundmass. Augite is the dominant pyroxene, sometimes accompanied by hypersthene. Olivine is present occasionally as microphenocrysts with iddingsite rims and rarely in the groundmass. Opaques (magnetite and lesser illmenite) are ubiquitous in the groundmass.

One thin section was prepared from a tuffaceous sandstone interbed in the Cedar Creek drainage. Aphanitic andesite, pumice, and occasional quartzite, are present as lithic fragments.

Figure 11. Flow breccia overlain by massive andesite flow of the Pliocene volcanic rock unit (N-130 A).

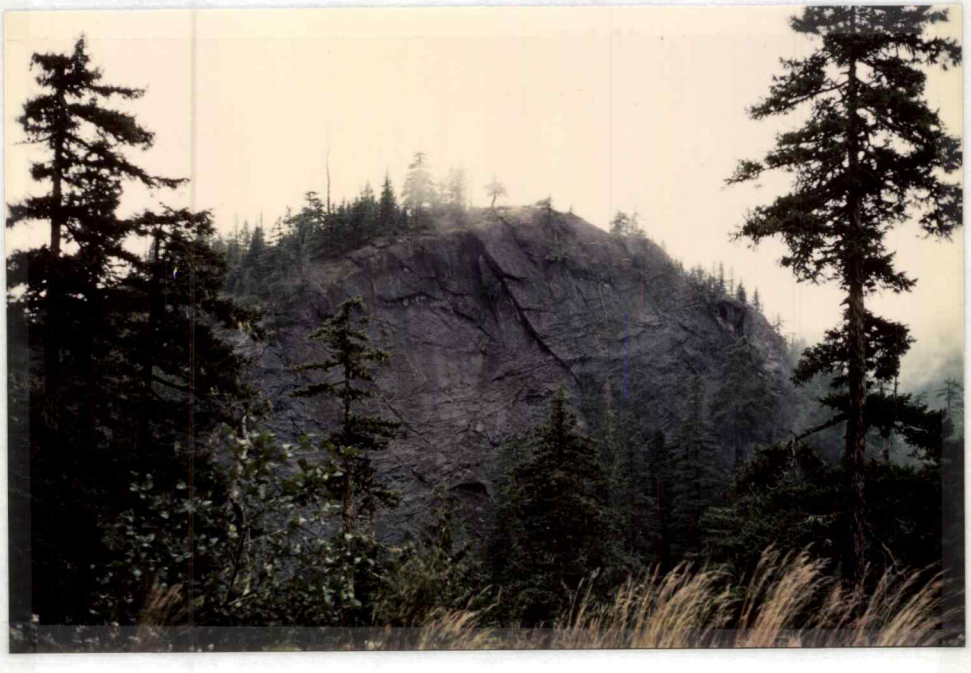

Figure 12. Thunder Rock. Composed of coarsely-crystalline, massive andesite porphyry, possibly an intrusive plug of the Quaternary volcanic-intrusive complex.

Crystals are abundant and consist of shattered andesine laths, lesser clinopyroxene, hypersthene, and magnetite, and accessory biotite and hornblende. The rest of the matrix consists of devitrified glass and ash-sized fragments, both heavily altered to smectite. Biotite is altered to chlorite, and feldspar in the lithic fragments is altered to sericite and clay. Limonite staining is concentrated along crude bedding planes.

Thin sections were prepared from the coarsely porphyritic basaltic andesites of the Log Creek drainage and the ridge northwest of Bull Run Lake. Plagioclase phenocrysts (calcic labradorite) occur as large, well-formed, nearly equidimensional crystals (4-5 mm) with normal zoning. The sample from the Bull Run Lake area has hypersthene and fewer augite phenocrysts, in addition to plagioclase, in a diabasic to intersertal groundmass of sodic labradorite (less than 0.05 mm), augite, cryptocrystalline material, and magnetite. The sample from Log Creek has augite and minor hypersthene and olivine phenocrysts in addition to minor plagioclase. The plagioclase and pyroxene phenocrysts are resorbed and embayed by the groundmass assemblage. The groundmass is diabasic with crudely pilotaxitic plagioclase laths (0-5 mm) and interstitial augite and lesser olivine and magnetite. The Bull Run Lake sample has olivine rimmed with iddingsite and unusually heavy alteration of plagioclase to clays, cryptocrystalline material to smectite, and magnetite to hematite. The extensive

alteration seen in the Bull Run Lake sample may be related to its proximity to a plug at Preachers Peak (Williams, 1920).

Two porphyritic basaltic andesite flows, located in the Hiyu Mountain-Lolo Pass area, were thin sectioned. The flow atop Hiyu Mountain contains 1-2 mm, subhedral, normally zoned, sodic labradorite phenocrysts, and lesser subhedral augite and hypersthene phenocrysts (0.5-1.5 mm) in a diabasic to intersertal groundmass of calcic andesine laths (less than 0.1 mm) and interstitial clinopyroxene and cryptocrystalline material. The stratigraphically lower flow, exposed on S-10 near Lolo Pass, is petrographically very similar to the flow atop Hiyu Mountain and is distinguished only by the presence of olivine phenocrysts, which are rimmed with iddingsite and altered to serpentine along fractures.

Age

Wise (1969) obtained a 5.8 my age date for the rocks exposed at Lolo Pass. Stratigraphically lower flows in the Bull Run Watershed are older but probably all Pliocene in age (Beaulieu, 1974).

Quaternary Volcanic-Intrusive Complex

Wise (1969) mapped two plugs of hornblende andesite, outside of the study area, in a tributary of Clear Fork two miles west of Lolo Pass. Two and one half square miles of flows extruded from these

plugs are present as an erosional remnant in the southeast corner of the watershed. The Quaternary hornblende andesites overlie the Pliocene volcanic rocks and the Rhododendron Formation with local unconformity. They form young, constructive landforms at Blazed Alder Butte, Burnt Peak, and Halfway Hill. The Quaternary flows are coarsely porphyritic and probably cooled under their own cogenetic pyroclastic cover. Remnants of hornblende andesite breccia are present along S-127.

Megascopically, the hornblende andesite contains prominent, zoned plagioclase phenocrysts (3-10 mm) and fewer euhedral hornblende phenocrysts (to 9 mm) in a dense, finely crystalline, dark olive-gray to medium-gray groundmass. The associated breccias are composed of monolithologic, sub-angular fragments of hornblende andesite in a compositionally similar matrix. The breccias are well indurated.

Thunder Rock is a massive cylindrical outcropping of andesite porphyry, which is probably a Quaternary plug related to those exposed in Clear Fork (Figure 12); however it is not associated with much alteration of country rock or much volume of extrusive material.

Apparent propylitic alteration was noticed in Rhododendron Formation pyroclastics in the Clear Fork drainage, and some minor alteration was observed along fractures in Pliocene volcanic rock unit andesites near Clear Fork Butte. Epidote, probably a product of

propylitic alteration, is present in a thin section prepared from a Rhododendron Formation lapilli tuff located in upper Hickman Creek. Alteration in these areas was most likely related to the Quaternary intrusions.

Petrography

Hornblende andesites of the Quaternary volcanic-intrusive complex are porphyritic with subhedral, calcic, oscillatory-zoned andesine phenocrysts and lesser augite and hypersthene phenocrysts (0.6-0.8 mm) in an intersertal to diabasic groundmass. Hornblende is distinctive in these flows, occurring as large, originally euhedral phenocrysts (to 9 mm). In its present state, hornblende has been altered to a granular assemblage of plagioclase, hypersthene, augite, and magnetite in order of decreasing abundance. The alteration of hornblende may proceed to total replacement, leaving only the pseudomorphic outline of the amphibole as proof of its original existence. Similar textures were reported by Wise (1969), who interpreted them as the result of an anhydrous reaction caused by a decrease in the partial pressure of H_2O during extrusion.

One hornblende andesite breccia was sampled for petrographic analysis. Fragments are rounded to sub-rounded, generally larger than 2 mm, monolithologic hornblende andesites, with 4-5 mm hornblende phenocrysts, 1-2 mm hypersthene phenocrysts, and

oscillatory-zoned, severely shattered plagioclase (andesine-labradorite) phenocrysts, in a pilotaxic groundmass. The composition and texture of the matrix is strikingly similar to that of the fragments. The matrix microlites show flow alignment around fragment boundaries. The texture in this thin section suggests possible autoclastic brecciation, either within a flow or around the margin of an intrusive plug, possibly Thunder Rock. Hornblende in the breccia is altered to the plagioclase+pyroxene+magnetite assemblage, locally, but is more commonly altered to a thick rind of hematite.

Age

Wise (1969) assigns a Quaternary age to the hornblende andesite plugs and equivalent flows. They intrude Pliocene volcanic rocks and form constructional landforms but are glacially dissected.

Quaternary Basalt and Andesite

Minor basaltic and andesitic flows and cinder cones are exposed, locally, in the Bull Run Watershed. These units were assigned a Quaternary age by Wise (1969). Bedded cinders compose the Aschoff Buttes and a topographic high in Walker Prairie. A blue-gray vesicular basalt or basaltic andesite flow is exposed on S-10 near the Bull Run Lake access road. A porphyritic, medium to dark-gray basalt is exposed on the ridge north of the Bull Run Lake spillway. A

distinctive, dark-brown, badly weathered, micro-porphyritic olivine basalt is present in the spillway excavation. The brown basalt is typically very vesicular and locally broken into slickensided fragments. Glacial moraine is present above this flow. These features suggest that the Quaternary basalt and andesite unit was partially extruded beneath glacial ice and extensively sheared at the snout of the glacier.

Three thin sections were prepared from samples of the Quaternary flows at Bull Run Lake. Two samples were badly weathered, one of them brecciated. In thin section, the badly weathered flows consist of palagonitized tachylite with occasional micro-phenocrysts of olivine and pyroxene. Plagioclase is present as microlites in the tachylite. Fractures are filled with amorphous silica. The presence of abundant magnetite in the tachylite indicates rapid quenching of the rock, which is consistent with sub-glacial extrusion.

A fresher sample, taken from the ridge north of the Bull Run Lake spillway, is a porphyritic olivine basalt, with olivine phenocrysts (to 2.5 mm) and occasional large bytownite laths (to 1 mm) in a pilotaxitic groundmass of plagioclase and interstitial olivine and pyroxene. This sample was extruded subaerially.

Surficial Deposits

General Statement

Unconsolidated surficial deposits, overlying bedrock units in the Bull Run Watershed, include thick, mappable landslide deposits, mappable terrace gravels, scattered glacial deposits, talus, and a variety of soils. All surficial deposits are Quaternary in age.

Landslide Debris

Large, 50-100 foot thick deposits of landslide debris obscure bedrock geology in the lower reaches of the Bull Run River and along Reservoir 2 (Figure 13). Similar, but less extensive, deposits are present in the drainages of North Fork and South Fork. Landslide debris of this type is discussed in further detail in following sections.

Terrace Gravels

Quaternary terrace gravel and sand were formed by down-cutting of the Bull Run and Little Sandy rivers in the western extent of the study area, perhaps by glaciofluvial processes. The terrace gravels are very porous. They are located at elevations as high as 500 feet above the present-day channels.

Figure 13. Thick deposit of Quaternary landslide debris (quarry on S-10 north of Reservoir no. 2). Note the disoriented blocks of platy andesite derived from the Pliocene volcanic rock unit located upslope.

Figure 14. Bull Run Lake from Hiyu Mt. Note cirque-shaped headwalls and the lateral barrier at the mouth of the lake (left center) which is composed of Quaternary basalt and andesite flows overlain by terminal moraine.

Talus

Talus is widespread on the glacially scoured, high elevation slopes of the eastern part of the Bull Run Watershed. Most of these talus deposits were probably formed in the Pleistocene by glacial plucking and freeze-thaw erosional processes. Talus is still being formed at the present, but at a slower rate due to the current milder climate. Individual blocks of talus are derived from underlying bedrock or from bedrock located immediately upslope from the talus deposit. The shape and size of the blocks are dictated, in part, by the jointing geometry of the parent bedrock. Some talus slopes, occurring on closely jointed Pliocene volcanic rock unit flows, are so extensive as to be properly called felsenmeer. In general, talus slopes remain stable at their natural angle of repose (30-40°), however, when these slopes are undercut by road construction or stream bank erosion, downslope movement of the talus deposit can occur.

Glacial Deposits

Glacial deposits in the Bull Run Watershed are not extensive. They consist of scattered moraine, outwash, and glaciofluvial cut and fill. Terminal moraines were mapped at the head of Log Creek and the outlet of Bull Run Lake. They consist of unsorted, heterogenous cobbles and boulders of andesites and basalts in a

matrix of light-yellow silty sand. The source rocks for moraine material are present in the cirque walls of Bull Run Lake and Blue Lake. Lateral moraines are present at Bull Run Lake and were noticed at elevations up to 200 feet above lake level by Williams (1920). Maximum thickness of moraines at Bull Run Lake is roughly 100 feet. A blanket of impermeable till lines the bottom of the lake (Shannon and Wilson, 1961).

In the area east of North Fork and Fir Creek, topographic evidence of alpine glaciation is abundant. Numerous cirques form the headwater regions of North Fork, Falls Creek, Log Creek, Bull Run Lake, Hickman Creek, Nanny Creek, Cedar Creek, Fir Creek, and the drainages of Big Bend Mountain. Hickman Lake, Bull Run Lake, and Blue Lake are high elevation alpine lakes (Figure 14). Glacial scouring and cirque formation did not proceed below an elevation of 2,200 feet, and thus the western half of the watershed shows few signs of past glacial activity other than numerous glaciofluvial cut and fill deposits (Figure 15), and scattered outwash deposits observed on S-156 near Cedar Creek and in the upper Bear Creek area.

Soils

Soils in the Bull Run Watershed vary from thin colluvial soils on the steep high elevation slopes to thick residual soils on the lower elevation plateaus. The colluvium on steep slopes generally contains

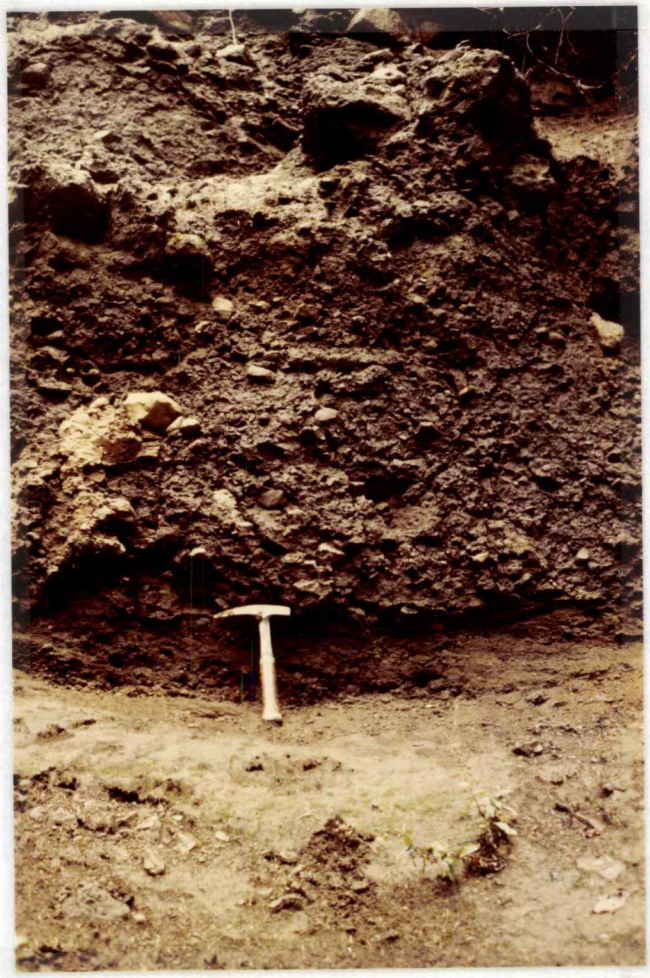

Figure 15. Glaciofluvial cut and fill deposits (exposed in scarp of mass movement no. 26).

angular fragments of bedrock in a silty sand and gravel matrix and averages 0.3-1.0 meter in thickness. Colluvial soils predominate in the study area. Heavy vegetation in the Bull Run Watershed contributes a thick layer of organic litter to most soil profiles.

Complete soil surveys of the watershed have been conducted by Stephens (1964) and Howes (1979). Soils derived from glacial deposits are not as widespread as indicated in these reports. Confusion may result from misinterpretation of residual Rhododendron Formation and Pliocene-Quaternary volcanic breccias, which weather to produce a deposit similar in appearance to glacial till or outwash.

Structure

Bedding and Folds

Bedding in the Bull Run Watershed is everywhere nearly flat (Figures 16 and 17). A slight regional dip to the west is evident in Figure 17.

The Columbia River Basalt Group flows, and possibly younger units, are deformed by broad, gentle folds (Vogt, 1979). Fold axes trend N60E. A synclinal axis roughly parallels the Bull Run River channel from Falls Creek westward, and the synclinal trough must have controlled drainage direction. An anticlinal axis traverses the southeastern section of the watershed. The Bull Run folds are

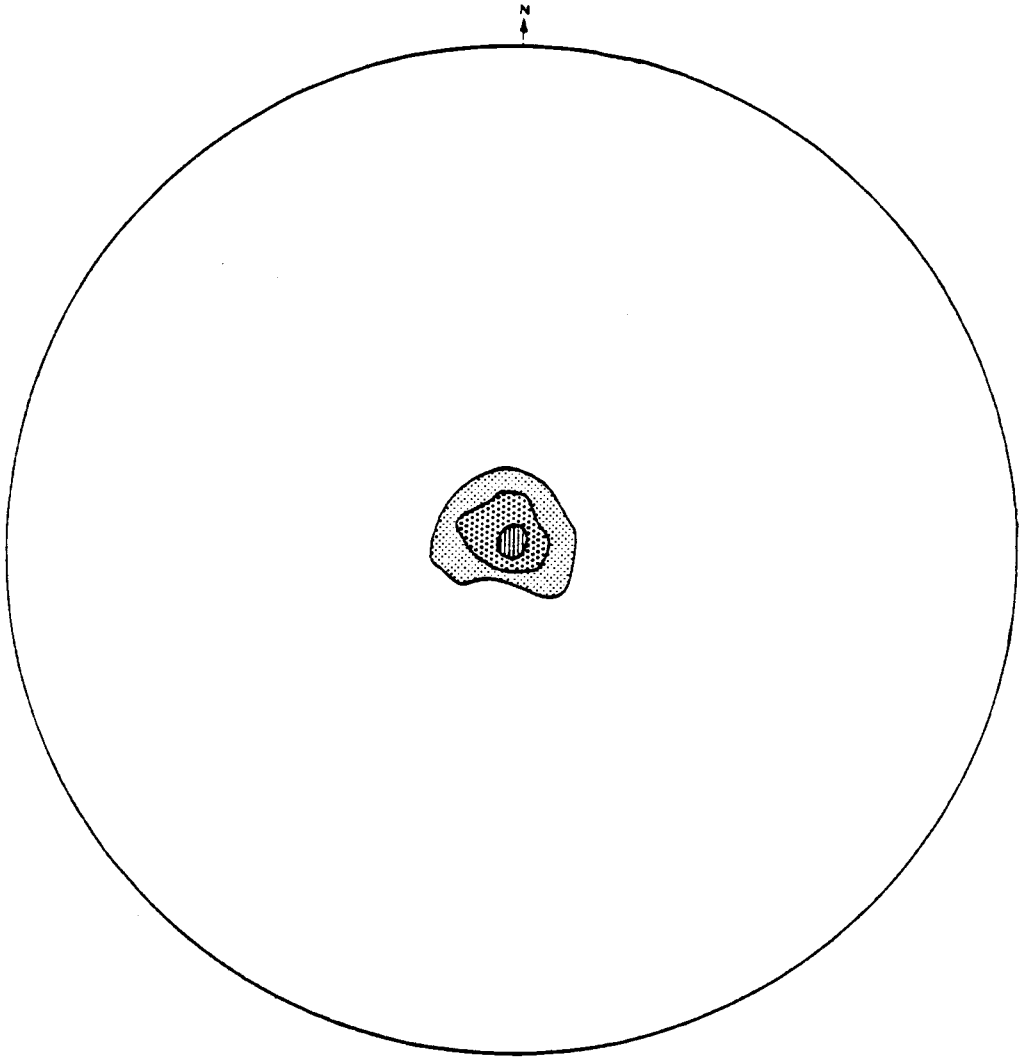

Figure 16. Contoured stereonet diagram of bedding in the Columbia River Basalt Group. Contours 20-40-60% per 1% area, maximum 77%, 18 pts.

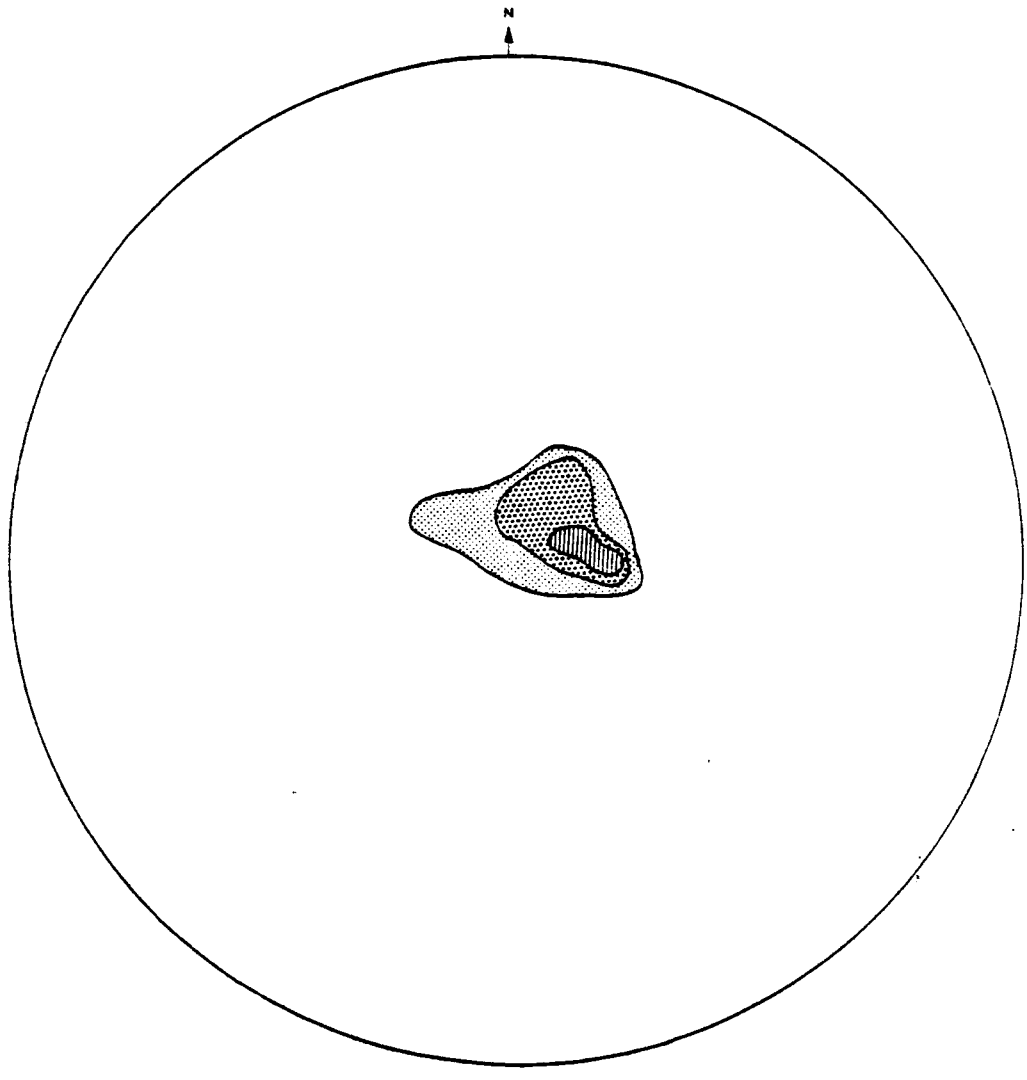

Figure 17. Contoured stereonet diagram of bedding in the Pliocene volcanic rock unit. Contours 10-20-30% per 1% area, maximum 42%, 7 pts.

equivalent to the Mosier Syncline and Ortley Anticline of the Columbia River Gorge region (Beeson and others, 1979).

The folding is very gentle, with a 2-3°dip on the northwestern limb and a 3-4°dip on the southeastern limb. The entire structure has a regional plunge of about 2° to the west-southwest.

Folding was active during early Columbia River Basalt (Pre-high-Mg Grande Ronde) time. Northeast-trending folding continued through Miocene time and probably deformed Rhododendron Formation rocks to some extent; but folding of the Rhododendron Formation cannot be established with certainty due to the subtle dips of the folds, limited exposures, and the discontinuous nature of Rhododendron deposition.

Superimposed on the northeast-trending folds, in the Bull Run area, is a gentle west-southwest regional dip, which affects all exposed units. The regional structure is a result of post-Miocene, north-trending uplift of the Cascade arch (McKee, 1972).

Faults

Two types of faults are present in the Bull Run Watershed; a low angle, northeast-trending thrust fault and northwest-trending high angle faults. Vogt (1979) mapped a thrust fault on the northwest limb of the Bull Run anticline. The thrust fault trends N60E, parallel to the trend of the anticlinal fold axis, and dips 12° to the southeast. It

probably reflects brittle release of the same N-NW to S-SE compressive forces that caused the folding. The thrust plane is exposed in rocks of the Columbia River Basalt Group in Blazed Alder Creek (Figure 18) and on S-10. A massive, well-indurated zone of tectonic breccia (30-40 feet thick) is present at the base of the hanging wall. Net slip along the fault is approximately 3,000 feet, and vertical separation of Columbia River Basalt flows is 600 feet.

Thrusting apparently did not offset the Rhododendron Formation or the Pliocene-Quaternary volcanic rocks. No brecciation or other expression of faulting was noticed in outcrops of pyroclastic rocks and andesites of these formations. Where contact relations are fairly clear, along S-10, there is only 200 feet of maximum change in the elevation of the base of the Rhododendron Formation, as it crosses the fault trace. The difference in elevation is probably an expression of topographic relief existing prior to Rhododendron Formation deposition in this area, or conversely it is possible that minor readjustment or continued movement on the thrust fault did disrupt these Rhododendron Formation units. However, Vogt (1979) dates the period of active thrusting as pre-Priest Rapids.

A high angle fault, trending N25W, is exposed in a quarry on S-10 near North Fork (Figure 19). Three feet of fault gouge are associated with this fault, and slickensides indicate that latest movement

Figure 18. Exposure of the Bull Run thrust fault offsetting flows of the Columbia River Basalt Group (Blazed Alder Ck.). Brecciated thrust plane dips 12° SE (right to left above geologists for scale).

Figure 19. Sinistral strike slip fault offsetting a high-Mg Grande Ronde Basalt flow (quarry on S-10 near North Fork). Note thick gouge zone and cut and fill deposit to the right of the fault.

Figure 20. "Bisquit structure" jointing in the Pliocene volcanic rock unit, produced by a combination of platy and columnar jointing in a basaltic andesite (S-10 near Otter Ck.).

was sinistral, strike slip. A N60W trending fault, with 1 1/2 feet of down-to-the-south displacement, cuts Quaternary rocks at Bull Run Lake (Shannon and Wilson, 1961). High altitude air photos reveal a topographic lineation trending N10-15W, which is defined, in the study area, by Blazed Alder Creek, the upper section of Falls Creek, and a saddle leading from Falls Creek to Tanner Creek. Severely fractured rocks were noticed at these locations, suggesting that the lineation defines a shear zone or fault. The northwest-trending structures cut all rock units in the watershed, and therefore they are produced by a young stress field which may still be active.

Joints

Joints in the rocks of the Bull Run Watershed may be separated into two genetic classes; joints caused by cooling contraction and joints caused by tectonic stresses. The distribution pattern of joint attitudes is different for each class. Cooling joints are tight and often have curvilinear surfaces. In basalts they display the typical geometric patterns of columnar jointing. Tectonic joints tend to be more open fissures, are planar and persistent, and often crosscut cooling joints.

Cooling Joints

The geometric pattern and spacing of cooling joints are variable, determined in part by the cooling gradients that were present in the solidifying flow and the chemical composition of the flow. Cooling joints in basalts are typically columnar, sometimes with well-developed entablature and collonade. Blocky and occasional platy jointing are also present in basalts. The spacing between cooling joints in basalts ranges from 30 mm to nearly 2 m. Generally cooling joints in basalts are either roughly horizontal or nearly vertical; oblique attitudes are rare. Trends of vertical cooling joints in basalts of the Bull Run Watershed are random when entire formations or large geographical areas are considered. Although six-sided columns are typical, the attitude of individual sides varies over short distances.

Andesites show great variance in cooling joint orientation and spacing. Columnar jointing may be present but is less frequent in andesites than in basalts. Platy jointing is common as is massive blocky jointing. A style of jointing intermediate between platy and columnar produces a biscuit or cup and socket type structure (Figure 20). Attitudes of cooling joints in andesites of the Bull Run are random, and in some outcrops, the attitudes of platy joints can be seen to change orientation 180° over a few tens of feet. Platy jointing in the andesites may be a product of cooling contraction or ramping in

an advancing aa aa flow.

Cooling joints in pyroclastic units of the Bull Run Watershed are typically poorly developed. In the better indurated breccias and tuffs, widely spaced joints do develop. Jointing in breccias usually breaks around fragments. Most of the pyroclastic units are so badly weathered that any original jointing has now been obscured.

Tectonic Joints

Joints caused by active or residual tectonic stresses have a number of preferred orientations in the Bull Run Watershed. Figure 21 illustrates the orientation of tectonic joints measured in the Columbia River Basalt Group; and we see that most joints are nearly vertical and exhibit several preferred trends. Analysis of the measurements by division of the watershed into geographic quadrants reveals no major change in the orientation pattern from area to area. The pattern of tectonic joint orientation in the Pliocene-Quaternary volcanic rocks (Figure 22) is crudely similar to that of Columbia River Basalt Group rocks (Figure 21) and reveals no difference in tectonic joint orientation for different quadrants of the study area. These observations suggest that a regional tectonic stress regime, resulting in preferred orientation of near vertical joints, has affected the Columbia River Basalt Group and Pliocene-Quaternary volcanic rocks, with little apparent change. This stress regime is younger than the

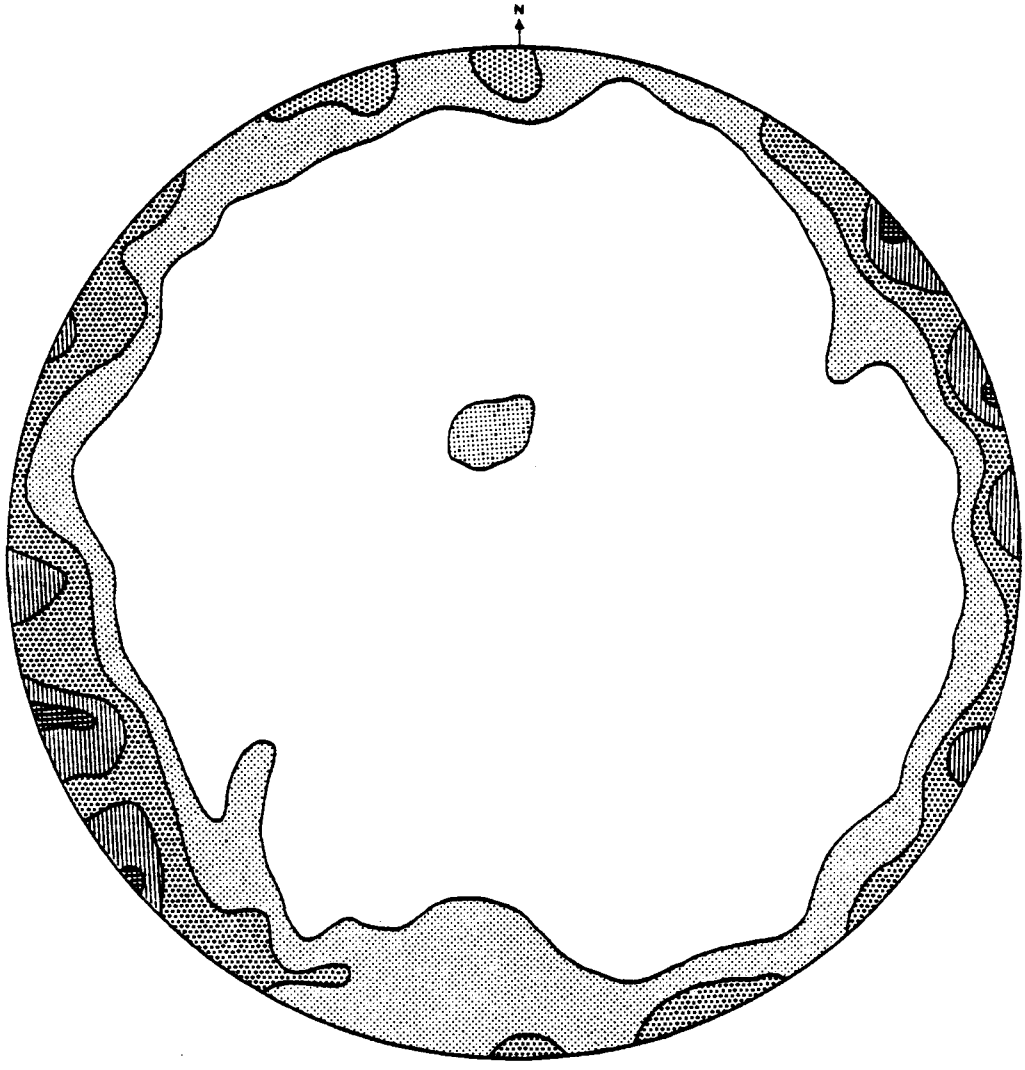

Figure 21. Contoured stereonet diagram of tectonic joints in the Columbia River Basalt Group. Contours 2-4-6-8% per 1% area, maximum 9%, 57 pts.

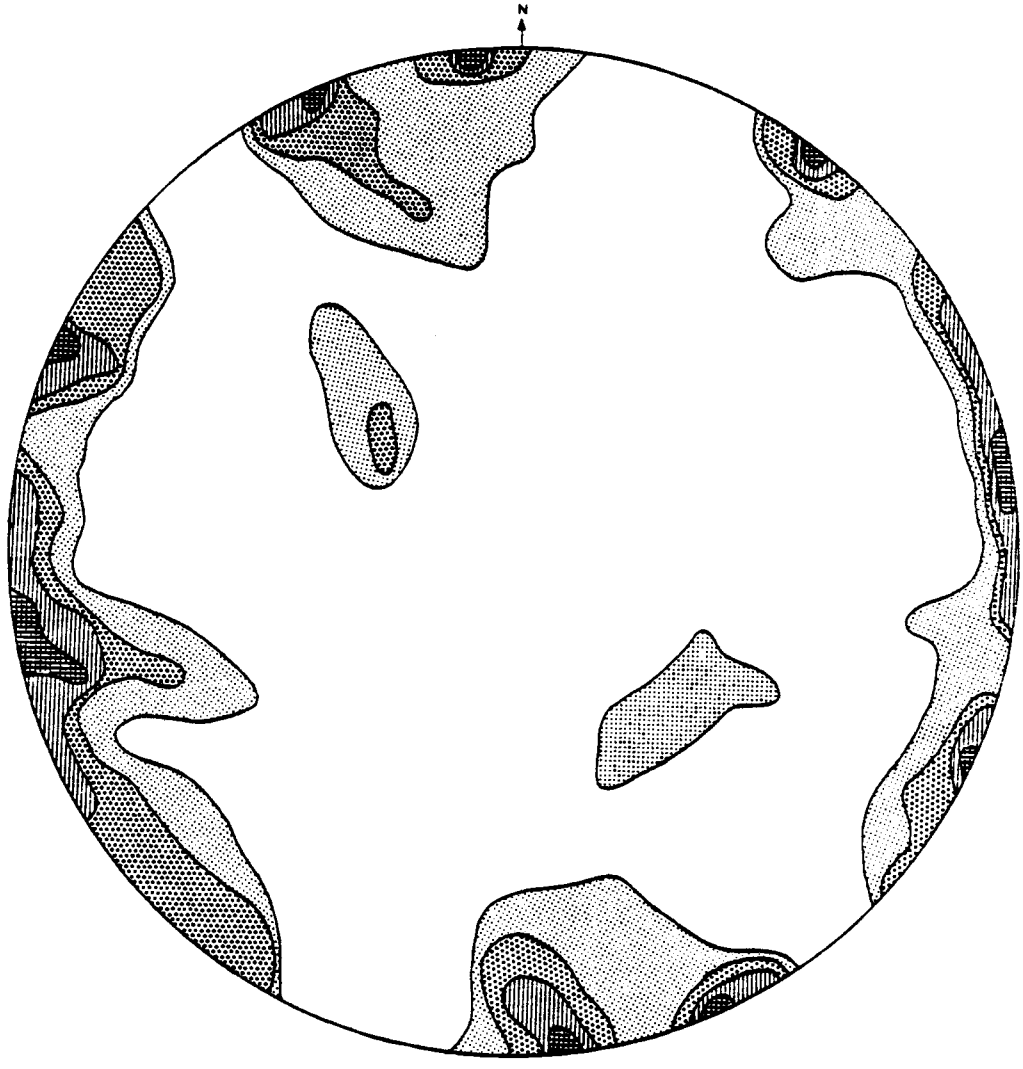

Figure 22. Contoured stereonet diagram of tectonic joints in Pliocene-Quaternary volcanic rocks. Contours 1-4-8-12% per 1% area, maximum 13%, 84 pts.

late Pliocene rocks it affects.

Tectonic joints measured in both Columbia River Basalt Group flows and the Pliocene-Quaternary volcanic rocks are near vertical. These data are plotted on the same diagram, since trends were found to be similar in both formations (Figure 23). The strongest trends are north-northwest, with N10-20W and N40-50W predominating. A scattering of east-northeast trends are slightly preferred.

These preferred trends are reported in other works as well. Buddington and Callaghan (1938) mapped mineralized veins in the Cascade Range, which were probably deposited along fault planes. The dominant trend in their study was N50-60W. Vogt (1979) reported a dominant N10-20W trend and other strong trends of N55W, N-S, N20E, and N80E, for fractures measured in Columbia River Basalt Group flows. These results agree very closely with the findings of this study.

Beeson and others (1979) present a tectonic model to explain the structural trends observed in the Columbia River Basalt Group of the western Cascade Range. They cite evidence for a N45W dextral wrench zone, which cuts across the Cascade Range and is the result of north-south compression and east-west extension. According to this model, N30W fractures are arranged en echelon to the trend of the wrench zone itself. N10-20W fractures, which frequently host Plio-Plesistocene Boring Lava dikes, are extensional. The northeast

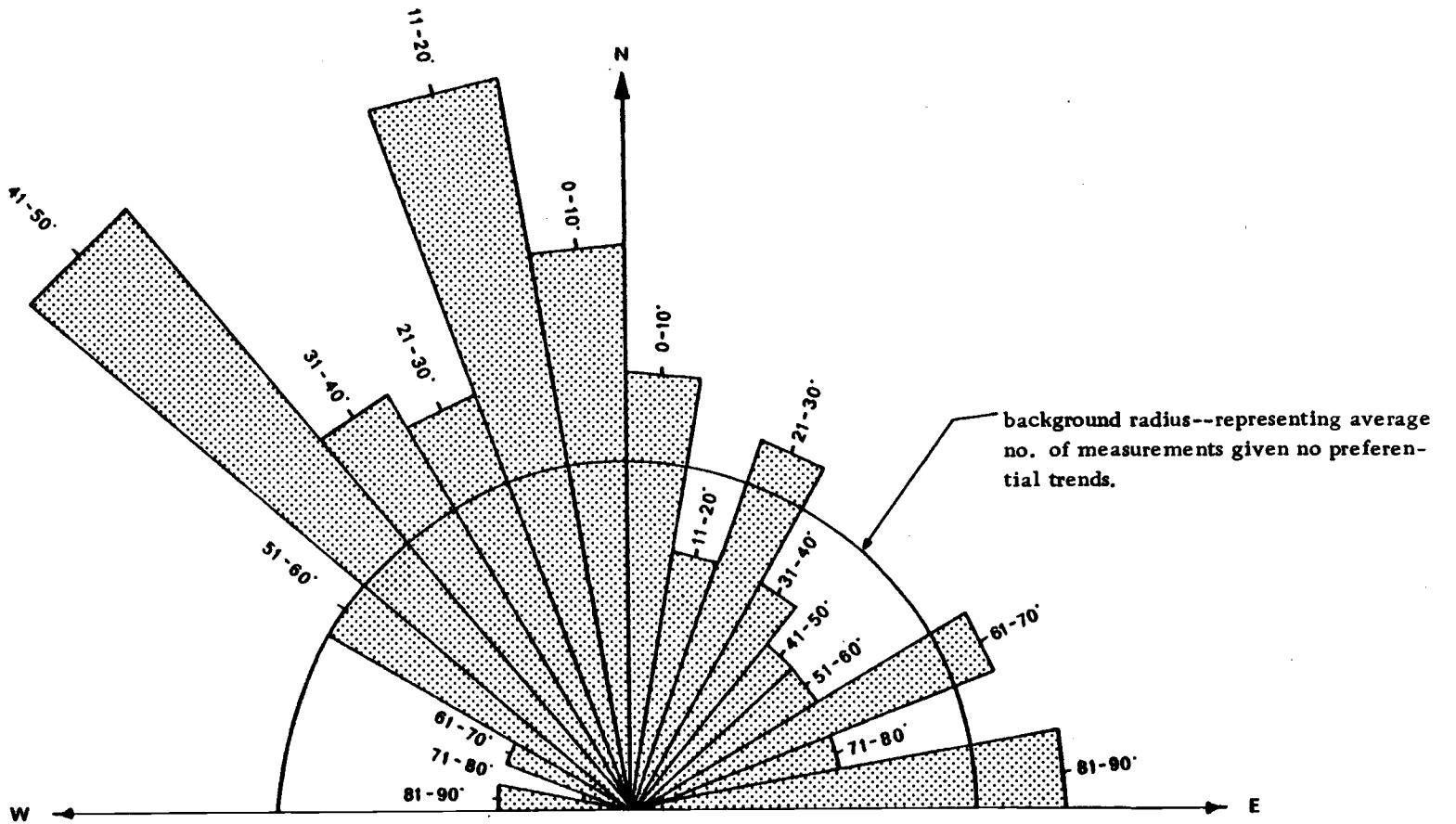

Figure 23. Rose diagram of trends of tectonic joints in Columbia River Basalt Group and Pliocene-Quaternary volcanic rocks, 147 measurements.

trending fractures and joints may represent a weaker conjugate set of the strong, northwest trending joint set.

MASS MOVEMENTS

Classification

Certain types of mass movements, each with unique implications for management, consistently occur in specific climatic and geologic environments. An adequate classification of mass movements is essential in order to distinguish and define these types and to provide for common terminology for discussing them. Several classification schemes have been devised to describe mass movements (Savarenski, 1935; Sharpe, 1938; Skempton, 1953; Zaruba and Mencl, 1969). The system of Varnes (1978) is frequently used by geologists working in the Cascade and Coast Ranges of northwestern North America; and it has been adopted, with some modification, in the following discussions. The basis of Varnes' classification is a grouping of mass movement types by their geometric form, nature of material, and rate of movement. Thus it is a descriptive, morphological system rather than a genetic one. The reasons for this are apparent when one considers the complexity of interactions among the numerous factors which contribute to the occurrence of most mass movements. A singular event may trigger a landslide, however a combination of geologic, vegetative, and climatic factors set the stage for failure long in advance. Mass movements occurring in the western Cascades

generally fall into the categories of creep, slump-earthflow, debris avalanche, rockfall-rockslide, and debris torrent.

Creep

Creep is the most widespread type of mass movement in the western Cascades (Swanson and Swanston, 1977). It is defined as a very slow, quasi-viscous movement of a volume of soil mantle in response to the long-term application of gravitational stress. Mobilization of the soil mass results from intergranular rotational and translational movements and from deformation within the clay mineral structure. Creep is distinguished from other mass movements by the lack of a discrete failure plane. Maximum rate of movement of the soil mass undergoing creep occurs near the surface and diminishes with depth to the stationary material below.

Slopes undergoing movement by creep are in a dynamic state, and the balance of forces acting on the slope changes with time. When shear stress becomes great enough, or shear resistance in the soil mass decreases below a critical point, portions of the slope may develop tension cracks (Figure 24), pressure ridges, and other features characteristic of movement by slump-earthflow. The transition from creep to slump-earthflow, or other types of mass movement, is

Figure 24. Tension cracks developing around a potential slump-earthflow scarp in roadfill overlying Quaternary landslide debris (mass movement no. 86). Cracks are also present near the vehicle, 150 ft from those in the foreground.

complete when a discrete failure surface develops.

Slump-earthflow

Although Varnes (1978) defined slump and earthflow as separate mass movement types, studies in the western Cascades often refer to these two types of failure as a single process. Commonly a failure will begin as a slump, characterized by concave-up rotation of a homogenous, cohesive soil mass. Subsequently, the mobilized material at the toe of the slump becomes broken and is transported as earthflow; a complex, but generally translational, flowage of viscous debris. Various degrees of dominance of motion type form a transitional series between the end-members of slump and earthflow, but generally both processes are present to some extent in a single failure of this type.

Mappable slump-earthflows in the Bull Run Watershed range from 5 to 20 feet in depth and from 100 square yards to about 15 acres in area. Small slump-earthflows in the watershed tend to be roughly equidimensional (Figure 25). Indicative of slump-earthflow terrain are steep headwall scarps, arcuate tension cracks, "jackstrawed" trees, disrupted drainage, hummocky topography, and sag ponds formed by the backward rotation of large blocks.

A separate category, streamside slump-earthflow, is used in the following factor analyses. This category distinguishes

Figure 25. Small, slump-earthflow developed in weathered pyroclastic breccia of the Rhododendron Fm. overlain by 3 feet of glacial outwash (mass movement no. 2). Note roughly equidimensional failure surface. Hammer on head-scarp for scale.

slump-earthflow mass movements that were probably triggered by stream bank erosion from those occurring higher on the hillslope, due to other processes. Criteria for classification of a mass movement as a streamside failure include location of the toe within floodwater stages, evidence of streambank erosion in the vicinity of the slide, and location on the outside of stream meander bends (Figure 26).

Debris Avalanche

Varnes (1978) has defined a gradational series of rapid translational slides, with individual members varying from debris slide through debris avalanche to debris flow. Distinctions are based on increasing water content. In practice, however, it is often difficult to distinguish the individual types of this series unless a well preserved depositional mass remains on the hillslope for observation. Blong (1973) has shown that the distinction between debris slide, debris avalanche, and debris flow, as defined by Varnes, does not hold up under close morphological scrutiny by numerical taxonomy. In addition, the land management impact of all three types is similar (Swanston and Swanson, 1976). Therefore, the term debris avalanche is used herein, in accordance with the recently established custom, to include debris flows and debris slides as well.

Debris avalanches are the most frequently occurring type of mass movement in the Pacific Northwest (Dyrness, 1967; Swanston,

Figure 26. Streamside slump-earthflow developed in weathered pyroclastic breccia of the Rhododendron Fm. (mass movement no. 14). Log jam in foreground deflected the stream against its south bank, undercutting the slope.

1969). These are shallow, rapid translational failures of cohesionless soil, bedrock, and organic debris (Figure 27). In the Bull Run Watershed, depths of debris avalanche failure are generally less than 5 feet. The failure plane essentially parallels the topography and usually coincides with joint or bedding planes, the soil-bedrock interface, or a hydraulic discontinuity in the soil mass. Field evidence of debris avalanche failure includes spoon-shaped depressions at the head of the slide, V-shaped troughs or chutes below the head, and disoriented, heterogenous debris piles at the toe.

As with slump-earthflows, streamside debris avalanches are distinguished from debris avalanches occurring higher on the hillslope. Again the distinction is based on the likelihood of stream erosion as a triggering mechanism of the failure.

Rockfall-Rockslide

Rockfall and rockslide are considered jointly in this discussion, since they are often transitional, they involve similar management implications, and they bear similar relationships to geologic factors. This class of failure is defined as the movement of blocks of bedrock either by free fall through the air or by sliding along one or more finite, translational shear planes. Unlike debris avalanche, rockfall-rockslide involves little or no soil or organic debris. Dimensions are highly variable, in some cases reaching catastrophic proportions.

Figure 27. Debris avalanche developed on the contact between pyroclastics of the Rhododendron Fm. and overlying Quaternary landslide debris (mass movement no. 35). Note planar failure surface. Length of failure from head scarp to depositional mass is 250 ft.

Hazards, however, are generally limited to road and quarry safety and maintenance problems (Figure 28).

Complex Mass Movements

One major drawback of a morphological system of mass movement classification is that many transitional forms exist between groups. Commonly more than one type of mass movement results from a single event, and a single landslide may show features of two or more classification types. Rockfall-rockslide may overlap with debris avalanche, depending on the nature of the material. Slump-earthflow may result in rockfall-rockslide by undermining of cap rock. Large slump-earthflows or creep masses may locally oversteepen hillslope areas which later result in debris avalanches. Although complex forms of mass movement are common, in the majority of these cases it is possible to assign a predominant type of morphology to the mass movement.

Very large, prehistoric mass movements were mapped in the western portion of the Bull Run Watershed. These are treated separately as complex-massive failures. Most likely these failures were predominantly rotational, however, due to their age direct evidence of the nature of the shear plane has been obscured by vegetation and erosion. The average size of the complex-massive failures is

Figure 28. Rockfall-rockslide, developed in bedded sandstone of the Troutdale Fm., poses road maintenance problems (between the communities of Bull Run and Aims, west of the study area).

Figure 29. Debris torrent related streambank scour and channel deposition (mass movement no. 16 in center of photo). Note streamside debris avalanche on outside stream meander, in center of photo, and deposition of channel debris against roadbed in foreground.

more than an order of magnitude larger than the recent slump-earthflows mapped in the study area (greater than 1×10^6 yd^3). Estimations of the depth to failure for this class of mass movements range from 25 to more than 100 feet, based on the present relief of scarps. Blocks of andesitic debris littering the scarps and included in the toes indicate that substantial undercutting of the capping flow rock occurred during and after the main mass movement event.

Field features associated with complex-massive failures are similar to those of the slump-earthflows, including sag ponds, hummocky topography, and disrupted drainage. Generally, the mature forest canopy covering these old slide terrains is undisturbed by more recent mass movement other than small failures and locally accelerated creep. This suggests that the complex-massive failures in the watershed have been stable for at least several hundred years.

Debris Torrents

Debris torrents are rapid mass movements of water-charged soil, rock, and organic debris down steep-gradient stream channels. These events may be triggered by failure of man-made or natural dams, pre-existing in the stream channel; or they may originate as debris avalanches or slump-earthflows on hillslopes adjacent to first or second order streams if the debris from these failures enters the streams, increasing bedload and possibly creating a temporary dam.

Huge quantities of debris, up to about 10,000 yd^3, may be entrained and flushed down stream channels (Figure 29), completely scouring stream banks and endangering life and property enroute (Swanston and Swanson, 1976). Descriptions of debris torrents are given by Morrison (1975), and Swanson andLienkaemper (1978).

Effects of Lithology

General Statement

The association of certain mass movement types with underlying bedrock lithology is well documented for the western Cascade Range (Pope and Anderson, 1960; Dyrness, 1967; Paeth and others, 1971; Swanson and James, 1975; Burroughs and others, 1976). The major link in this association is the transformation of bedrock into soil by mechanical and chemical weathering. Most rocks are unstable at the conditions present at the surface of the earth; and reactions between primary minerals and H_2O (meteoric or hydrothermal), CO_2, and O_2 result in the formation of hydrous secondary minerals, which become the clay fraction of soils. Early in the process of chemical weathering, soil variability is primarily determined by the lithology of the parent material. As soils mature, however, continual leaching and redistribution of ions throughout the soil by solution and precipitation tends to lessen the influence of parent lithology, and the nature of the soil is

dictated more by climate. Soils in the Bull Run Watershed have formed from relatively young rocks and have high erosion rates where they occur on steepland, and therefore they still show much variability attributable to the distribution of parent bedrock.

Basalts and andesites, which predominate in the watershed, can be expected to form smectites, kaolin minerals, amorphous alumino-silicates, and amorphous hydrous oxides, with moderate leaching. Generally the smectites are found deeper in the soil profile, closer to the bedrock, than are the kaolin minerals (Loughnan, 1969). Pyroclastic rocks usually contain significant quantities of glass, which is highly unstable and alters rapidly to hydrated halloysite and lesser smectite (Loughnan, 1969; Taskey, 1978).

Bedrock lithology influences mass movement distribution in other indirect ways. The competence of geologic units, a function of their mineralogical composition, determines their resistance to weathering, which in turn influences topography and in particular slope gradients. The texture of bedrock units dictates their porosity and permeability in large part. Permeability of rock units is extremely important in analysis of mass movement hazards because of the controls of permeability on groundwater flow.

Clay Content

The clay content of soils has a direct bearing on the stability of

slopes. Soils consisting predominantly of silt, sand, and gravel, with very little clay, derive shear strength primarily from internal friction. Internal friction opposes shear forces acting on the soil, in part by friction between the surfaces of individual soil particles, but predominantly by the interlocking of angular grains within the soil mass. The degree of shear resistance due to these factors is measured by the angle of internal friction, which is a quantitative soil property. Generally, coarse-textured soils do not fail on slopes with gradients less than the angle of internal friction of the soil (Swanston, 1969).

Soils with a high clay content derive shear strength from cohesion. Cohesion in soils is a result of cementation, capillary tension, and electrical bonding between clay particles (Terzaghi and Peck, 1967). Clay-rich soils may derive some of their shear strength from internal friction between clay aggregate structures, especially when the soil is dry.

Table 1 illustrates the relationship among clay percentage (soil fraction less than 2 μm), mass movement type, and underlying geologic units. With a few exceptions, clay content of soils sampled in the Bull Run Watershed rarely exceeds 15 percent. Samples with clay percentages greater than 25 percent were taken from a slump-earthflow occurring on Rhododendron Formation breccia and from a tuffaceous sandstone interbed in the Pliocene volcanic rock unit. The red clay pods in the South Fork drainage have clay contents greater than 60 percent.

The average clay content in failure sites is higher than in stable sites (Table 1), indicating a positive correlation between clay content of soils and mass movement occurrence. Streamside events occurred in soils with lower clay contents (approximately equal to stable soils) than did the hillslope events. The distribution of streamside events apparently is not strongly related to the clay content of soils, because the occurrence of these failures is determined by stream bank erosion, as well as soil saturation. Another possibility is that the low hillslope position of streamside failure sites results in these sites being more readily saturated, and therefore failure can occur at lower clay contents.

Slump-earthflow and debris avalanche in the Bull Run Watershed do not seem to be distinguishable on the basis of soil clay content. Contrary to what might be expected, the average clay content of debris avalanche soils is slightly higher than that of slump-earthflow soils. This is largely due to the effect of one anomalous sample taken from a local clay-rich (35.8%) tuffaceous interbed, which was not representative of the soil profile in the vicinity of the associated debris avalanche. In addition, a number of mass movements occurring on the South Fork were classified as debris avalanches, but possessed many features of slump-earthflow and were actually transitional between the two types. These South Fork slides occur in clay-rich (about 15%) soils, which leads to overestimatation of the average clay

Table 1 . Clay percentage in relation to mass movement types and in relation to geologic units at failure sites and stable sites
[number of samples in parentheses]

Mass movement type	Ave clay %		Low	High
Slump - earthflow	12.5	(10)	7.6	26.8
Streamside slump - earthflow	6.2	(2)	4.6	7.8
Debris avalanche	14.5	(11)	5.8	35.8
Streamside debris avalanche	9.3	(7)	5.8	17.8
Stable	8.1	(8)	5.6	12.6

Geologic unit	Average percent clay			
	Failure sites		Stable sites	
Columbia River Basalt Group flow	10.5	(5)	6.6	(3)
Rhododendron Formation breccia	14.0	(8)	12.6	(1)
Pliocene-Quaternary volcanic rocks				
flow	7.8	(4)	6.8	(1)
flow breccia	14.2	(5)	9.8	(2)
intrusive complex	10.6	(1)	5.6	(1)
Quaternary landslide debris	12.1	(7)	--	
Quaternary glacial moraine	--		6.6	(1)
Red clay pod	62.0	(1)	--	
Vantage Horizon	--		11.8	(1)

content of debris avalanche soils. Some of these clay-rich soils may fail by debris avalanche because of the limiting effect of soil depth on mass movement morphology. Cohesive soils may develop translational failure planes if the soil mantle is too thin to develop the rotational, more equidimensional failure plane of a slump-earthflow. The debris avalanches occurring in cohesive soils are located on steep slopes, which do not develop thick soils because of high erosion rates.

The most clay-rich soils develop on the pyroclastic rocks of the Rhododendron Formation, Quaternary landslide debris, and interbeds in the Columbia River Basalt Group and Pliocene volcanic rock unit. The flow rocks generally weather to stonier, less-cohesive soils, and on the basis of clay content should be considered more stable than soils developed from pyroclastic rocks, older landslide deposits, and sedimentary interbeds. Flow breccias apparently weather rapidly to clay because of their vesicular and fragmental texture, which presents greater surface area for weathering. Also the original glassy texture of the tops and bottoms of flows results in rapid alteration to clay. Likewise, pyroclastics weather to secondary minerals rapidly because of high original glass contents. The development of clay in pyroclastics may be compounded by the effects of hydrothermal alteration of primary minerals, during and shortly after deposition of the pyroclastic unit. Quaternary landslides occurred predominantly in pyroclastic rocks of the Rhododendron Formation, and thus soils developed on

their debris are also clay-rich.

Values of C (cohesion) and ϕ (angle of internal friction) were determined from six in situ shear tests with the Iowa bore-hole shear device (Table 2). Most soils in the Bull Run Watershed are far too gravelly to allow for uniform shearing in the bore-hole; and consequently the data points plotted for shear failures often yielded ambiguous Mohr envelopes. Nonetheless, the best interpretations of the data suggest that soils developed on the Rhododendron Formation are the most cohesive and have the lowest angle of internal friction, whereas the soil tested above a flow of the Pliocene volcanic rock unit has a lower cohesion intercept and a higher angle of internal friction. The highest value of C is found in a smectite-bearing soil of the Rhododendron Formation. Residual soil overlying a Columbia River Basalt Group flow is relatively clay-rich and cohesive but has a high angle of internal friction, perhaps a result of compaction during road construction. Quaternary landslide debris is also cohesive relative to the other samples. With the exception of the two compacted sites, the more cohesive soils failed by slump-earthflow, whereas the least cohesive soil failed by debris avalanche.

Clay Mineralogy

The mineralogy of the soil clay fraction is a contributing factor to the distribution and morphology of mass movements in the western

Table 2. Values for cohesion (C) and angle of internal friction (ϕ) determined in situ with the Iowa bore hole shear device

C (psi)	ϕ (degrees)	% Clay	Parent lithology	Mass movement type
4.5	28	18.8	Columbia River Basalt Group flow	debris avalanche[1]
5.5	17	26.8	Rhododendron Formation pyroclastic breccia	slump-earthflow
4.0	22	14.8	Rhododendron Formation laharic breccia	slump-earthflow
2.5	29	9.8	Pliocene volcanic rock unit flow	debris avalanche
4.5	28	13.8	Quaternary landslide debris	slump-earthflow
3.0	26	--	Quaternary glacial outwash	slump-earthflow[2]

[1] Sample site compacted during road construction.

[2] Glacial outwash underlain by Rhododendron Formation pyroclastic breccia, sample site compacted during logging.

Cascades (Taskey, 1978). Certain clay minerals absorb water molecules and dissociated ions into lattice positions between clay structural layers. Water absorbtion and adsorption results in expansion, or swelling, of the layered structure and reduced bonding within and between clay particles, hence reduced shear strength. Different degrees of expansion characterize different clay minerals.

Smectites have a large water-holding capacity, and the association of soils rich in smectite with high frequency of mass movement occurrence is widely reported. Water absorbtion by smectites can mobilize the soil mass, and alternate shrinking and swelling mechanically disrupts the soil structure, decreasing its shear strength. On the other hand, soils containing significant amounts of smectite have greater cohesive strength than soils lacking smectite. The high cohesion generally dictates rotational motion when failure occurs in smectite-rich soils.

Saprolite layers containing abundant smectite are common in the western Cascades. These layers are impermeable and may support perched water tables, creating high pore pressures and resulting in debris avalanche failure in overlying soils (Taskey, 1978).

According to Taskey (1978), halloysite, a common component of western Cascade soils, is found in abundance on both stable and unstable sites. The importance of halloysite to mass movement occurrence depends on water availability. Where soils are wet

year-round, halloysite exists in a hydrated state and is associated with mass movement occurrence. If the soil undergoes a drying period, hydrated halloysite is irreversibly transformed into a dehydrated state, which is more likely to be associated with stable sites.

Table 3 lists the various clay minerals present in 40 soil samples taken from different types of mass movements and from soil overlying various geologic units in the Bull Run Watershed. Halloysite is the most common mineral in the clay fraction of both stable and unstable soils. It occurs predominantly in the hydrated state, indicating that soils in the Bull Run Watershed seldom dry thoroughly. Chloritic intergrades and smectites are also common. Most of the smectites are actually hydroxy-interlayered smectites which show some expansion after saturation with ethylene glycol and glycerol, but do not show complete collapse with heating. Mica and kaolinite are present but are less abundant.

The distinction between slide sites and stable sites on the basis of clay mineralogy is clear. Mass movement occurrence is favored by abundant smectite. Stable sites are favored by high chloritic intergrade and kaolinite contents. The distinction between hydrated halloysite and dehydrated halloysite, in terms of mass movement occurrence, is not clear on the basis of Table 3. However, the only stable soils sampled that were found to contain hydrated halloysite were either Rhododendron Formation soils, which are slide prone, or

Table 3. Distribution of clay minerals contained in soil as related to mass movement class and to underlying geologic units
[Data presented is the percent of the number samples in each class showing stong XRD peaks for the mineral listed]

Mass movement type	Mica	Kaolinite	Chloritic intergrade	Dehydrated halloysite	Hydrated halloysite	Smectite	Number of samples
Slump-earthflow	--	--	30	30	60	40	10
Debris avalanche	6	11	28	22	50	33	18
Stable	--	38	63	13	75	25	8
Geologic unit							
Columbia River Basalt Group	--	57	57	--	14	14	7
Rhododendron Formation	--	10	10	30	50	60	10
Pliocene-Quaternary volcanic rocks							
flow	--	--	100	--	100	--	2
flow breccia	--	--	13	13	75	38	8
intrusive complex	33	33	67	33	--	--	3
Quaternary landslide debris	--	--	29	43	86	29	7
Glacial moraine	amorphous	--	--	--	--	--	1
Vantage Horizon	--	--	--	--	100	100	1
Red clay pods	--	100	--	--	--	(minor)	1

flow breccia soils, which tend to remain saturated because they are impermeable. It appears, therefore, that mass movement occurrence may be favored by abundant hydrated halloysite as well as smectite. Slump-earthflows contain higher hydrated halloysite, slightly higher smectite, and lower kaolinite contents than debris avalanches. Diffractograms of typical slump-earthflow, debris avalanche, and stable soils are contained in the appendix.

Clay mineralogy of soils varies distinctly between different geologic units. This indicates that most soils in the watershed developed in situ or from colluvial deposits which were not transported far from the source bedrock. They were not weathered from extensive glacial deposits, which would result in soils that were more homogenous and less related to the underlying bedrock. The flow rocks of the Columbia River Basalt Group and the Pliocene-Quaternary volcanic rocks tend to have high chloritic intergrade and kaolinite contents and low smectite contents. These soils, especially those developed on Quaternary volcanic-intrusive complex rocks, display the clay mineralogy of stable sites and to a lesser extent debris avalanche sites. Slump-earthflow would not be expected in soils overlying flow rocks on the basis of clay mineralogy.

Soils overlying the Rhododendron Formation, flow breccias of the Pliocene volcanic rock unit, Quaternary landslide debris, and the Vantage Horizon have clay mineral abundances resembling

slump-earthflow sites; and on the basis of clay mineralogy, these parent materials are expected to produce soils prone to mass movement occurrence, particularly by slump-earthflow. Soils overlying pyroclastics of the Rhododendron Formation are high in smectite, but Quaternary landslide debris, which is largely derived from the Rhododendron Formation, develops soils containing less smectite. The reason for this might be a dilution in smectite content due to the observed mixing of boulders of Pliocene volcanic rock unit flows in with Rhododendron Formation pyroclastic debris by undercutting of the capping flow rock during Quaternary landsliding.

Permeability and Groundwater Flow

Bedrock lithology influences mass movement distribution in other less direct ways. The permeability of a rock, which dictates the movement of groundwater, is in part dependent upon the original texture of the rock and its weathering capabilities. Nearly all rocks have interconnecting pore spaces and are thus permeable, however different rates of permeability prevail for different lithologies. Some rocks have such low rates of groundwater transmission as to be effectively impermeable.

When geologic units are impermeable, they may support perched water tables or they may channel groundwater out to the surface, saturating the soil mass at the intersection between the impermeable unit

and the slope. Saturation of the soil mass decreases cohesion and intergranular friction, hence the soil shear strength is decreased. Perched water tables may maintain positive pore pressures in the soil mass, decreasing the effective weight of soil particles and the internal friction of the soil mass.

Chi-square Test of Mass Movement--Bedrock Distribution

The overall significance of bedrock distribution to mass movement type and distribution was analyzed by a chi-square (X^2) goodness of fit test. The null hypothesis (H_o) is that the distribution of failures for each mass movement class corresponds to the areal distribution of each geologic unit. In other words, if H_o is accepted, we assume that bedrock has no control on the occurrence of mass movements, and the number of mass movements occurring on a certain rock type is simply a function of the areal opportunity for those mass movements to occur. For each mass movement class, the number of events occurring on each geologic unit were counted (Table 4a). These observed values were compared to expected values, which represent the area of each geologic unit. Table 4b is the same test, however volumes of soil moved by mass movements are considered rather than the number of occurrences. Positive numbers in the observed-expected column indictate a higher occurrence of mass movements on a geologic unit than is expected on the basis of its area of outcrop,

Table 4. X^2 test for bedrock control on mass movement type and distribution (a) by number of events (b) by volume of soil moved
[Abbreviations of geologic units is the same as for Figure 3. Degrees of freedom = 6, X^2 at 0.05 level of significance = 12.59]

(a) Number of events Mass movement type	X^2 Calculated	Geologic unit	Observed	Expected	Obser. -Expect.
Slump-earthflow	183.707	Qls	5	0.24	+ 4.76
		Tmpr	5	0.99	+ 4.01
		Tpt	1	0.015	+ 0.985
		Tcr	2	1.68	+ 0.32
		Qtg	0	0.075	- 0.075
		Qvic	0	0.3	- 0.3
		Tpv	2	11.595	- 9.595
Complex-massive	99.012	Tmpr	7	0.462	+ 6.538
		Tpt	0	0.007	- 0.007
		Qtg	0	0.035	- 0.035
		Qvic	0	0.140	- 0.140
		Tcr	0	0.784	- 0.784
		Tpv	0	5.411	- 5.411
Streamside debris avalanche	76.081	Tcr	9	2.128	+ 6.872
		Qls	4	0.304	+ 3.696
		Qvic	1	0.38	+ 0.62
		Tpt	0	0.019	- 0.019
		Qtg	0	0.095	- 0.095
		Tmpr	1	1.254	- 0.254
		Tpv	4	14.687	-10.687
Debris avalanche	69.235	Tcr	11	1.904	+ 9.096
		Tmpr	3	1.122	+ 1.878
		Tpt	0	0.017	- 0.017
		Qtg	0	0.085	- 0.085
		Qvic	0	0.34	- 0.34
		Qls	2	0.272	- 1.728
		Tpv	1	13.141	-12.141
Streamside slump-earthflow	57.345	Qls	2	0.08	+ 1.92
		Tmpr	2	0.33	+ 1.67
		Tpt	0	0.005	- 0.005
		Qtg	0	0.025	- 0.025
		Qvic	0	0.1	- 0.1
		Tcr	0	0.56	- 0.56
		Tpv	1	3.865	- 2.865
Rockfall-rockslide	37.606	Tcr	5	1.456	+ 3.544
		Qvic	2	0.260	+ 1.74
		Tmpr	1	0.858	+ 0.142
		Qtg	1	0.065	+ 0.035
		Tpt	0	0.013	- 0.013
		Qls	0	0.208	- 0.208
		Tpv	4	10.049	- 6.049

Table 4. (Continued)

(b) Volume of soil moved (yd^3) Mass movement type	X^2 Calculated	Geologic unit	Observed	Expected	Obser. - Expect.
Complex-massive	3,886.182	Tmpr	276,000	18,216	+257,784
		Tpt	0	276	-276
		Qtg	0	1,380	-1,380
		Qls	0	4,416	-4,416
		Qvic	0	5,520	-5,520
		Tcr	0	30,912	-30,912
		Tpv	0	213,348	-213,348
Slump-earthflow	364.781	Tpv	1,400	1,105	+295
		Tpt	5.18	1.430	+3.75
		Qls	17.5	22.888	-5.388
		Qtg	0	7.152	-7.152
		Qvic	0	28.610	-28.610
		Tmpr	7.64	94.412	-86.772
		Tcr	0.17	160.215	-160.045
Debris avalanche	240.100	Tmpr	19.06	1.939	+17.121
		Qls	6.07	0.47	+5.6
		Tcr	3.59	3.291	+0.299
		Tpt	0	0.029	-0.029
		Qtg	0	0.147	-0.147
		Qvic	0	0.588	-0.588
		Tpv	0.66	22.771	-22.051
Streamside debris avalanche	142.267	Qls	6.24	0.256	+5.984
		Tpt	0	0.16	-0.16
		Qtg	0	0.08	-0.08
		Qvic	0.02	0.319	-0.299
		Tcr	1.35	1.789	-0.439
		Tmpr	0.55	1.054	-0.504
		Tpv	7.81	12.345	-4.535
Streamside slump-earthflow	111.187	Qls	3.17	0.087	+3.083
		Tpt	0	0.005	-0.005
		Qtg	0	0.027	-0.027
		Tmpr	0.029	0.360	-0.07
		Qvic	0	0.109	-0.109
		Tcr	0	0.612	-0.612
		Tpv	2.0	4.221	-2.221

that is that the unit is slide prone. Negative numbers indicate that a unit is relatively stable. The larger the magnitude of observed-expected, the stronger the relationship. When observed-expected values approach 0, there is no significant variance from a direct relationship between the area of outcrop and the frequency of mass movement for that respective geologic unit.

For each slide type, calculated X^2 values in Table 4 exceed the critical value, and therefore H_o must be rejected in each case. In other words, the test indicates that bedrock geology is a controlling factor in the distribution of all classes of mass movement in the Bull Run Watershed. The greater the difference between the calculated and critical values of X^2, the more emphatically H_o is rejected and the greater the control of bedrock geology on mass movement distribution.

In terms of the number of mass movements inventoried, the distribution of slump-earthflow and complex-massive types is controlled most by bedrock geology, whereas rockfall-rockslide and streamside slump-earthflow are most randomly distributed with respect to geologic units. The occurrence of slump-earthflow is highly correlated with the distribution of Quaternary landslide debris and the Rhododendron Formation. Likewise, complex-massive mass movements are highly correlated with the Rhododendron Formation. Debris avalanches, both streamside and hillslope, are most highly correlated with rocks of the Columbia River Basalt Group, mainly

because these rocks form the steepest hillslopes adjacent to the major streams in the watershed.

In terms of the volume of soil displaced by mass movement, the complex-massive types are by far the most correlated with bedrock geology. This relationship is a reflection of the great volume of these slides, and they occur almost entirely within the Rhododendron Formation. Slump-earthflow volumes are highly related to bedrock lithology, however the greatest volumes are associated with the Pliocene volcanic rock unit and not the Rhododendron Formation, as might be expected from Table 4a. The discrepancy arises because two very large slump-earthflows were mapped above the Pliocene volcanic rock unit in the eastern part of the watershed. These are distinctive slides and represent a somewhat special subgroup of slump-earthflow, because of their greater size and age than that of the average for this class. Overall, the volume of soil displaced by mass movement is most related to the distribution of Quaternary landslide debris and the Rhododendron Formation.

In general, mass movement occurrence is strongly related to bedrock geology. The volume of mass movements is more significantly controlled by bedrock lithology than is the distribution of their occurrence. In addition, some types of mass movement occur more frequently on one geologic unit, but involve the greatest volumes of soil on another unit (slump-earthflow and debris avalanche). These

observations have implications for land management policies, which should consider the difference between the likelihood of occurrence of a particular mass movement and the volume of soil that will ultimately be disturbed by it.

Effects of Geologic Structure

Joints and Bedding

Bedrock structure is an important factor in the stability of rock and soil slopes (Swanston, 1969; Burroughs and others, 1976; Piteau and Peckover, 1978). Failure surfaces in hard rock masses tend to follow pre-existing discontinuities such as joint and bedding planes. Discontinuities dipping out of the slope may represent a high rockfall-rockslide hazard, especially when the strike of the discontinuities approaches that of the slope. Such is the case on S-10 near Falls Creek, where a large block of basalt was separated from the slope along a fracture parallel to the strike of the slope, and threatens to enter the road by rockfall. Fracture spacing is also important, since a rock mass is mechanically weaker if spacing is close. The asperity of a fracture surface may determine the amount of frictional shear resistance to sliding along it. Groundwater in a fracture may exert hydrostatic pressure

along potential failure surfaces or may promote weathering of the rock along fracture walls, reducing shear resistance and contributing to a high rockfall-rockslide hazard.

Failure of thin soils over bedrock by debris avalanche may be more likely to occur on slopes with principal joint or bedding planes parallel to the slope, because there is a lack of mechanical support for the soil mantle on the structural surface and because the structural planes usually function as an impermeable barrier, above which high pore pressures can exist. Theoretically, structural planes dipping against the slope may promote stability of the overlying soil mass by creating surface irregularities, which act as mechanical supports for the soil mantle.

Fractures often act as avenues for groundwater flow. Flow rocks in the Bull Run Watershed are relatively impermeable where massive, but are good conductors of groundwater where highly fractured. Where groundwater-bearing fracture planes intersect the slope, saturation of the soil mass may result in mass movement, typically as a debris avalanche.

In the Bull Run Watershed, a number of debris avalanches occurred on highly fractured bedrock with joint planes paralleling the slope, and it was apparent in the field that this coincidence of attitudes was the primary reason for failure at these sites (Figure 30). The overall importance of this relationship, however, was difficult to

Figure 30. Debris avalanche related to the coincidence of joint planes with the slope (mass movement no. 42). Joint planes and slope dip from upper right to lower left. Failure occurred on highly fractured flow rock of the Quaternary volcanic-intrusive complex.

determine in the study area, since bedrock generally was poorly exposed in the vicinity of a given mass movement. In order to assess the regional relationship between structural attitudes and mass movement occurrence, rose diagram plots of slope aspects (Figure 31) and failure plane aspect (Figure 32) were compared to a plot of the trends of tectonic joints (Figure 23). Cooling joints in the Bull Run Watershed are far too randomly oriented to have any utility in a regional analysis of mass movement hazards, however project level studies should take the attitudes of all types of joints into consideration.

Slope aspects in the watershed are bimodally distributed and generally face south, southwest, and northwest (Figure 31), mainly because primary drainage is from east to west. However, failure plane aspects face predominantly southeast, suggesting that mass movement distribution is not entirely random in relation to slope aspects (Figure 32). The difference between slope aspect and slide aspect distribution may be due to several factors favoring the occurrence of mass movements on specific slope aspects, especially southeast aspects. The general northwest-southeast trend displayed by failure plane aspects is partially coincident with the northwest-southeast trend of tectonic joints, suggesting a possible relationship between the two. If jointing does control failure plane aspect, it is not in the sense expected, since the dominant trend of the near vertical

Figure 31. Rose diagram of slope aspects. Determined from 232 pts. Selected randomly on USGS 15 minute quadrangle sheets.

Figure 32. Rose diagram of mass movement failure planes, measured in the field. Direction of dip is plotted per unit slope area, 86 pts.

Figure 33. Rose diagram of the aspects of slopes bearing springs and seeps mapped in the field. Plotted per unit slope area, 269 pts.

Figure 34. Rose diagram of the aspects of slopes with gradients greater than 25 percent as shown on slope gradient map (Beaulieu, 1974). Plotted per unit slope area, 210 pts.

Figure 35. Rose diagram of the aspects of slopes underlain by the Rhododendron Fm. or Quaternary landslide debris, as shown on Plate 1. Plotted per unit slope area, 65 pts.

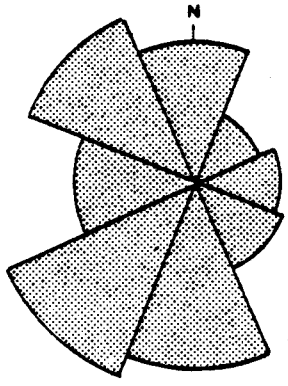

Figure 31

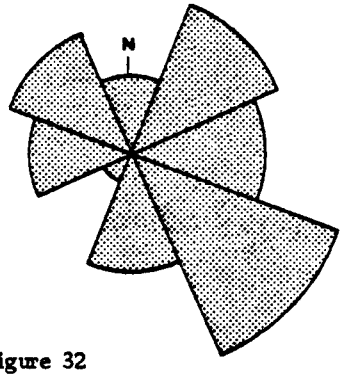

Figure 32

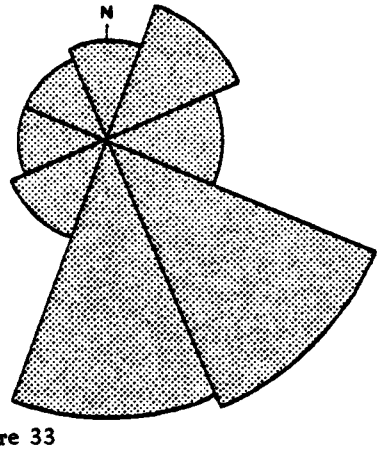

Figure 33

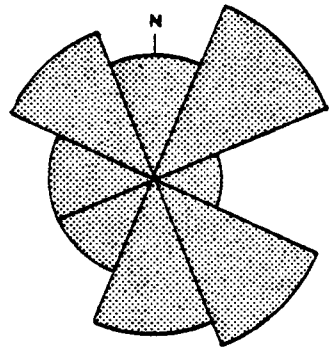

Figure 34

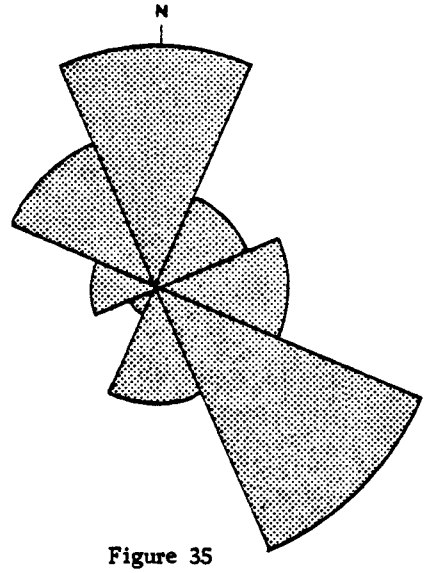

Figure 35

tectonic joints is perpendicular, not parallel, to the dominant strike of the failure planes. It is possible that vertical joints intersecting slopes perpendicularly may contribute to mass movement occurrence by conducting groundwater out to the soil mantle, whereas a vertical joint trending parallel to the strike of the slope would conduct groundwater downward and laterally without intersecting the slope.

In order to test this hypothesis, a rose diagram plot of the aspects, per unit slope area, of slopes with springs and seeps on them was constructed (Figure 33). The dominant south-southeast aspects of spring-bearing slopes and the dominant southeast aspects of failure planes, indicate that groundwater flow is important in mass movement occurrence, and that it is possible that the trend of tectonic joints influences groundwater flow in a regional sense. The distribution, per unit slope area, of the aspects of slopes with gradients greater than 25 percent (Figure 34) closely resembles the distribution of failure plane aspects, indicating that slope gradient is also an important factor in controlling mass movement occurrence. The distribution of the aspects of slopes underlain by slide-prone geologic units such as older landslide debris and pyroclastics (Figure 35) in part explains the abundance of southeast failure plane aspects and the lack of southwest failure plane aspects.

A chi-square test for goodness of fit was used to test the significance of coincidence between slope and joint attitudes measured at

mass movement sites with attitudes measured at randomly selected stable sites (Table 5). Eight classes of slope-joint attitude coincidence were defined, taking into account both strike and dip of the joint plane. The null hypothesis is that the distribution of slope-joint attitude coincidence, among these eight classes, is the same for mass movement sites (observed) as for stable sites (expected) and thus that jointing attitudes in relation to slope attitudes have no control on mass occurrence. The null hopothesis is rejected at the 0.05 level of significance. The test indicates that the degree of coincidence between slope attitudes and joint attitudes does have some control on mass movement occurrence, but the influence is small.

Mass movements are most likely to occur where joint attitudes dip steeply with the slope, especially where the strike of the joints and the strike of the slope are within 45° of one another (Table 5). Overall, where joints dip steeply with the slope mass movements are more likely to occur than where joints dip steeply against the slope. Shallow dips do not appear to be strongly correlated with mass movement occurrence in the Bull Run Watershed. In a general sense, the coincidence between the strike of joint attitudes and the strike of slope attitudes has no strong correlation with mass movement occurrence, when considered independently of dip; and therefore the association between failure plane aspects and tectonic joint trends, discussed previously in relation to groundwater control, may not be a

Table 5. X^2 test of the relationship between mass movement occurrence and the coincidence of joint attitudes with slope attitudes. [Expected values represent slope and joint attitudes measured at randomly selected stable sites. Observed values represent attitudes measured at or within 1000 feet of a mass movement. Degrees of freedom = 7, X^2 at 0.05 level of significance = 14.07, X^2 calculated = 23.364]

Direction of dip	With the slope				Against the slope			
Angle between strike of joints and strike of slope	0-44°		45-90°		0-44°		45-90°	
Dip of joints	0-44°	45-90°	0-44°	45-90°	0-44°	45-90°	0-44°	45-90°
Observed	3.0	18.0	2.0	7.0	2.0	5.0	1.0	9.0
Expected	5.222	9.574	1.741	2.611	0.87	13.056	1.741	12.185
Obser. - expect.	-2.222	+8.426	+0.259	+4.389	+1.13	-8.056	-0.741	-3.185

strong relationship.

Major Faults

Fault zones usually contain fractured, crushed, and partly altered rock; and thus they are major zones of geologic weakness. Fracturing and alteration of wall rocks adjacent to a fault may promote rockfall and rockslide. Fault gouge is usually impermeable because of high clay content, and the fault plane may act as a barrier to groundwater flow, which can affect the stability of overlying materials by increasing pore pressure. High-angle faults tend to develop steep scarp faces, which may be susceptible to rockfall-rockslide or debris avalanche.

The tectonic breccia, developed in the upper plate of the thrust fault exposed in Blazed Alder Creek, is a common source of rockfall-rockslide. Large blocks of breccia have descended from the steep slopes adjacent to Blazed Alder Creek and now litter the stream channel (Figure 36).

The strong N15W topographic lineation defined by Blazed Alder Creek and Tanner Creek, to the north of the study area, probably represents a zone of shearing. Fracture spacing in flows of the Columbia River Basalt Group and the Pliocene volcanic rock unit, located along the lineation, is closer than the average spacing for these units. Small debris avalanche failures are common in Blazed

Figure 36. Rockfall-rockslide of tectonic breccia from the Bull Run thrust fault (mass movement no. 67). Geologist for scale, left center.

Alder Creek, mainly because slope gradients are very steep, probably as a result of the structure in this area.

Folds

Folding has indirectly affected the distribution of many mass movements in the Bull Run Watershed. The Bull Run syncline acted as a topographic trough throughout Miocene time and perhaps later (Beeson and others, 1979). The trough served as a depositional basin between successive influxes of Columbia River Basalt Group flows, and localized the distribution of sedimentary interbeds and pillow basalts along its axis. Interbeds in the Columbia River Basalt Group may be impermeable due to the presence of abundant clay, or they may be relatively permeable if the deposits are coarse. Impermeable interbeds may channel groundwater and lead to saturation of soil and debris avalanche failure where the interbeds intersect steep slopes. The Boathouse Slide of 1973, a debris avalanche of about 700 yd^3, occurred on a sedimentary interbed in the Columbia River Basalt Group. According to Beaulieu (1974), blasting during road construction mobilized the sedimentary layer and caused undercutting of soil and flow rock upslope. Most importantly, the Bull Run syncline seems to have persisted at least throughout Rhododendron Formation time as a topographic low and consequently localized the deposition of mass movement-prone pyroclastics of the Rhododendron Formation.

Effects of Stratigraphic Sequence

General Statement

The stratigraphic sequence of rock units is an essential factor in determining mass movement hazards. In essence, stratigraphy, as it applies to slope stability, is an extension of the previous discussions on lithology and structure; however the focus in this section is on the alternation of different lithologies and how this affects the flow of groundwater and the development of topography. High hazard areas for large slump-earthflows exist where pyroclastic units are intercalated between flow units.

Contacts and Groundwater

Field observations indicate that aquicludes in the Bull Run Watershed include the Sandy River Mudstone member of the Troutdale Formation, pyroclastics and epiclastics of the Rhododendron Formation, especially where badly weathered, most interbeds of the Columbia River Basalt Group, most flow breccias of the Pliocene rock unit, any dense, weakly fractured flow rock, and glacial till. Aquifers in the watershed are fractured flows, especially the platy flows of the Pliocene volcanic rock unit, some Columbia River Basalt Group interbeds and interflow horizons, Quaternary terrace gravels, and some blocky deposits of Quaternary landslide debris.

In the tributary east of Bear Creek and at the head of the Bull Run River, streams abruptly disappear in their channels, then continue by subterranean flow through fractured Pliocene-Quaternary volcanic rocks, and finally re-emerge at the upper contact of the Rhododendron Formation, attesting to the function of pyroclastics as a barrier to groundwater. In the Bear Creek area, a slump-earthflow has occurred on the channel bank at precisely the spot where the stream re-emerges in its channel, indicating a probable perched water table in this area.

In order to evaluate the association of each contact mapped in the watershed to mass movement occurrence, a chi-square test (Table 6) was used to compare the relative area of each contact zone (expected) to the number of mass movements contained in that area (observed). Contact lengths were measured from the geologic map and a width of 200 feet was arbitrarily assigned to each contact in order to establish an area in which mass movements, influenced by contact zones, might be inventoried. The actual zone of influence surrounding a contact may be greater or less than 200 feet. Since it was not always possible to laterally trace interflow contacts in the Columbia River Basalt Group and the Pliocene volcanic rock unit, two estimates of their respective areas were made; a minimum estimate based only on the interflow contacts actually mapped, and a maximum estimate assuming laterally continuous interflow contacts. For the maximum

Table 6. X^2 test of the relationship between geologic contacts and mass movement distribution [Expected values are derived from the area of each contact zone, assuming a 200 ft width. Observed values represent the number of mass movements inventoried within the contact zone. Minimum (a) and maximum (b) estimates of contact areas are shown (see text). Degrees of freedom = 24, X^2 at 0.05 level of significance = 36.42. Abbreviation of geologic units is the same as in Figure 3]

Contact	Observed	(a) X^2 Calculated = 183.834 Expected	Obser.-Expect.	(b) X^2 Calculated = 308.997 Expected	Obser. -Expect.
Tmpr-Tpv	20.0	13.44	+ 6.56	6.468	+13.532
Tmpr-Qls	7.0	1.176	+ 5.824	0.588	+ 6.412
Tcr-Tmpr	14.0	10.5	+ 4.5	5.04	+ 8.96
Tcr-Qls	4.0	0.756	+ 3.244	0.336	+ 3.664
Tmpr-Tpt	2.0	0.084	+ 1.916	0.084	+ 1.916
Qls-Qtg	2.0	0.084	+ 1.916	0.084	+ 1.916
Tpv-Tpt	1.0	0.084	+ 0.916	0.084	+ 0.916
Tmpr-Qgl	1.0	0.084	+ 0.916	0.084	+ 0.916
Tcr-Qgl	1.0	0.084	+ 0.916	0.084	+ 0.916
Tcr-Qtg	1.0	0.168	+ 0.832	0.084	+ 0.916
Tpv-Qls	2.0	1.848	+ 0.152	0.840	+ 1.16
Tmpr-Qba	0	0.084	- 0.084	0.084	- 0.084
Tcr-Qba	0	0.084	- 0.084	0.084	- 0.084
Tpt-Qls	0	0.084	- 0.084	0.084	- 0.084
Qba-Qgl	0	0.168	- 0.168	0.084	- 0.084
Tpv-Qba	0	0.420	- 0.420	0.168	- 0.168
Tpv-Qgl	0	0.504	- 0.504	0.252	- 0.252
Tmpr-Qtg	0	0.504	- 0.504	0.252	- 0.252
Tmpr-Qvic	0	0.588	- 0.588	0.252	- 0.252
Tpv-Qcc	0	1.176	- 1.176	0.588	- 0.588
Tpv-Qvic	0	1.428	- 1.428	0.672	- 0.672
Tpv-Qtg	0	1.680	- 1.680	0.840	- 0.840
Tcr-Tpv	2.0	3.948	- 1.948	1.932	+ 0.068
Tpv interflow	7.0	9.996	- 2.996	15.120	- 8.12
Tcr interflow	20.0	35.28	-15.28	50.232	-30.232

estimates, the Columbia River Basalt Group was assumed to be composed of 16 individual flows (Beeson and others, 1979) and the Pliocene volcanic rock unit was conservatively estimated to be composed of 6 flows. The null hypothesis in this test is that mass movements are randomly distributed with respect to contact areas as defined above.

The null hypothesis is emphatically rejected (Table 6), indicating that mass movements are preferentially distributed with respect to certain contacts. This association is generally more significant for the maximum rather than the minimum estimates of contact area, because the expected values become very high when maximum estimates of the interflow areas are used. Most mass movements are associated with the Tmpr-Tpv contact. Also significantly associated with high mass movement occurrence per unit contact area are the Tmpr-Qls, Tcr-Tmpr, and Tcr-Qls contacts. Mass movements mapped in the Tmpr-Tpv and Tcr-Tmpr contact zones are generally the complex-massive type. More recent failures are associated with the Tmpr-Qls and Tcr-Qls contacts. These are generally smaller reactivations of older landslide deposits in the South Fork and North Fork drainages.

Although large numbers of mass movements were mapped within the Tpv and Tcr interflow contacts (7 and 20 respectively), these contact zones were so large as to render their association with mass

movements insignificant. That is, fewer mass movements were observed than would be expected on the basis of areal opportunity for their occurrence in the interflow zones, using either the maximum or minimum estimates of contact area.

It must be remembered, however, that the ranking of contacts in Table 6 essentially gives an estimate of the likelihood of a mass movement occurrence within a unit area of a given contact zone. This test does not consider the element of time, that is the frequency of mass movement occurrence within different contact areas. For example, the number of mass movements per unit area is far greater on the Tmpr-Tpv contact than on the Tcr interflow contact. However, the number of mass movements inventoried on these contacts is the same (20 each). Assuming that these 20 events occurred over the same time span, the frequency of mass movement occurrence is the same on the Tmpr-Tpv and Tcr interflow contacts. Therefore, the likelihood of a mass movement occurring on either of these contact zones at any given time is the same.

The importance of contacts to mass movement distribution is assumed to lie partly in the controls that the juxtaposition of lithologic units of different permeability has on groundwater flow. In order to examine this hypothesis, a chi-square test (Table 7) was used to compare the number of springs and seeps mapped within each contact zone (observed) to the area of the contact zone (expected).

Table 7. X^2 test of the relationship between groundwater flow as springs and seeps and geologic contact zones. [Observed values are the number of springs mapped within the contact zone. Expected values represent the area of each contact zone. Contact zones and geologic unit abbreviations are the same as for Table 6. Degrees of freedom = 24, X^2 at 0.05 level of significance = 36.42]

		(a) X^2 Calculated = 124.771		(b) X^2 Calculated = 151.771	
Contact	Observed	Expected	Obser. -Expect.	Expected	Obser. - Expect.
Tpv interflow	51.0	16.66	+34.34	25.2	+25.8
Tcr-Tmpr	21.0	17.5	+ 3.5	8.4	+12.6
Tmpr-Qls	5.0	1.96	+ 3.04	0.98	+ 4.02
Tcr-Qls	4.0	1.26	+ 2.74	0.56	+ 3.44
Tmpr-Qba	1.0	0.14	+ 0.86	0.14	+ 0.86
Tmpr-Tpt	1.0	0.14	+ 0.86	0.14	+ 0.86
Qls-Qtg	1.0	0.14	+ 0.86	0.14	+ 0.86
Tcr-Tpv	7.0	6.58	+ 0.42	3.22	+ 3.78
Tpv-Qba	1.0	0.7	+ 0.3	0.28	+ 0.72
Tpv-Tpt	0	0.14	- 0.14	0.14	- 0.14
Tmpr-Qgl	0	0.14	- 0.14	0.14	- 0.14
Tcr-Qgl	0	0.14	- 0.14	0.14	- 0.14
Tpt-Qls	0	0.14	- 0.14	0.14	- 0.14
Tcr-Qba	0	0.14	- 0.14	0.14	- 0.14
Tcr-Qtg	0	0.28	- 0.28	0.14	- 0.14
Qba-Qgl	0	0.28	- 0.28	0.14	- 0.14
Tpv-Qvic	2.0	2.38	- 0.38	1.12	+ 0.88
Tmpr-Qtg	0	0.84	- 0.84	0.42	- 0.42
Tpv-Qgl	0	0.84	- 0.84	0.42	- 0.42
Tpv-Qcc	1.0	1.96	- 0.96	0.98	+ 0.02
Tmpr-Qvic	0	0.98	- 0.98	0.42	- 0.42
Tpv-Qtg	1.0	2.8	- 1.8	1.40	- 0.4
Tpv-Qls	1.0	3.08	- 2.08	1.4	- 0.4
Tmpr-Tpv	17.0	22.4	- 5.4	10.78	+ 6.22
Tcr interflow	26.0	58.8	-32.8	83.72	-57.72

Contact zone areas are defined in the same way as for Table 6, and the null hypothesis is that springs are randomly distributed with respect to contacts. Once again the null hypothesis is rejected, at the 0.05 level of significance.

If the maximum estimates of contact area are used, the Tmpr-Tpv, Tmpr-Qls, Tcr-Tmpr, and Tcr-Qls contacts are highly associated with the presence of springs and thus exert the most control on groundwater movement. These same contacts were found to be most associated with mass movements as well (Table 6), thus there is a good basis for the assumption that the importance of contacts to mass movement distribution lies in their ability to channel groundwater. The major exception to this assumption, in Table 7, is that the Tpv interflow zones, which are impermeable and contain the most springs per unit area, exhibit among the lowest rates of mass movement per unit area. Perhaps this is because the texture of the soil developed on Tpv flow rocks precludes high mass movement occurrence.

Table 8 illustrates the relationship between mass movement type and the presence of springs on the slope. Of all mass movements mapped in the Bull Run Watershed, more debris avalanches (61%) had springs issuing from their failure surfaces than any other class of mass movement. Fewer slump-earthflow sites had springs, even fewer streamside mass movements, and only 15 percent of the rockfall-rockslide events showed signs of groundwater emergence

as springs or seeps. The concentration of springs on failure sites is 39 springs per square mile, whereas the concentration for the Bull Run Watershed overall is only 2 springs per square mile, again an indication of the relative importance of groundwater distribution to mass movement occurrence. The presence of springs on a slope, however, does not always relate directly to increased mass movement hazards. In some cases a steadily flowing system of springs may have a stabilizing effect on the slope, by acting as a release for piezometric pressures in the aquifer (Sowers and Royster, 1978).

Table 8. The relationship between mass movements and groundwater, as represented by distribution of springs flowing from failure surface
[Total no. of springs mapped = 272]

Mass movement type	% Mass movements with springs	No. of events
Slump-earthflow	44	18
Streamside slump-earthflow	40	5
Debris avalanche	61	18
Streamside debris avalanche	35	23
Rockfall-rockslide	15	13

In general, it seems that discharge of water from springs and seeps on slopes increases the hazard of smaller slump-earthflow and debris avalanche failure by soil saturation, but may indicate stability in relation to larger failures, by relieving piezometric pressures.

Topography

Different geologic units, because of different response to weathering and physical erosion processes may be associated with distinctive landforms. Landforms are defined by characteristic topography, and consequently possess characteristic ranges of slope gradient, which directly relate to mass movement hazards.

Flows of the Columbia River Basalt Group, in the western part of the study area, commonly underlie flat areas or gentle slopes bordering the reservoirs. In the east, these flow units form the steep slopes incised by the Bull Run River and its tributaries. The Rhododendron Formation generally forms benches in the Bull Run River valley. Where Rhododendron Formation rocks are well-indurated, they commonly form steep slopes. Where complex-massive landslides have occurred in the Rhododendron Formation, the topography is hummocky and partially outlined by steep headwall and flank scarps. Sedimentary rocks of the Troutdale Formation are associated with steep slopes adjacent to the Bull Run River, in the western-most extent of the watershed. Flows of Pliocene-Quaternary volcanic rocks generally form flat lava plains, but they underlie steep slopes where glacially dissected.

Table 9 illustrates the distribution of each mass movement class with respect to slope gradients measured in the field. Average

Table 9. Slope gradients at mass movement sites
[measured from head to toe]

Mass movement type	Slope gradient (%)			No. of sites
	Average	Highest	Lowest	
Slump-earthflow	66	100	26	17
Streamside slump-earthflow	58	75	50	6
Debris avalanche	83	100+	59	19
Streamside debris avalanche	85	100+	60	22
Rockfall -rockslide	80	100+	40	12

gradients for all classes exceed 50 percent. One slump-earthflow occurred on a 26 percent slope and numerous slides occurred on slopes greater than 100 percent. Debris avalanches generally occur on steeper gradient slopes than do slump-earthflows (both hill-slope and streamside events).

Cap-Rock Situations

The large complex-massive failures occurred in areas where pyroclastics are overlain by a capping of flow rock. The headwall scarps of these mass movements lie along the contact between the Rhododendron Formation and the Pliocene volcanic rock unit. Similar cap-rock situations, that have controlled slump-earthflow distribution, have been reported by Wilson (1970), Taskey (1978), and Swanson and James (1975). Pyroclastic rocks are more erodible than are flow rocks, which hinders establishment of a stable slope profile in these areas.

A generalized cross section of the South Fork drainage (Figure 37, location shown on Plate 1) illustrates the major features of the cap-rock situation and the development of complex-massive failures. In the early stages of drainage development, stream incision was limited to the upper flow rock (Tpv). Eventually downcutting proceeded to the softer, underlying pyroclastics (Tmpr). With further downcutting, a critical height of streambank slopes must have been reached

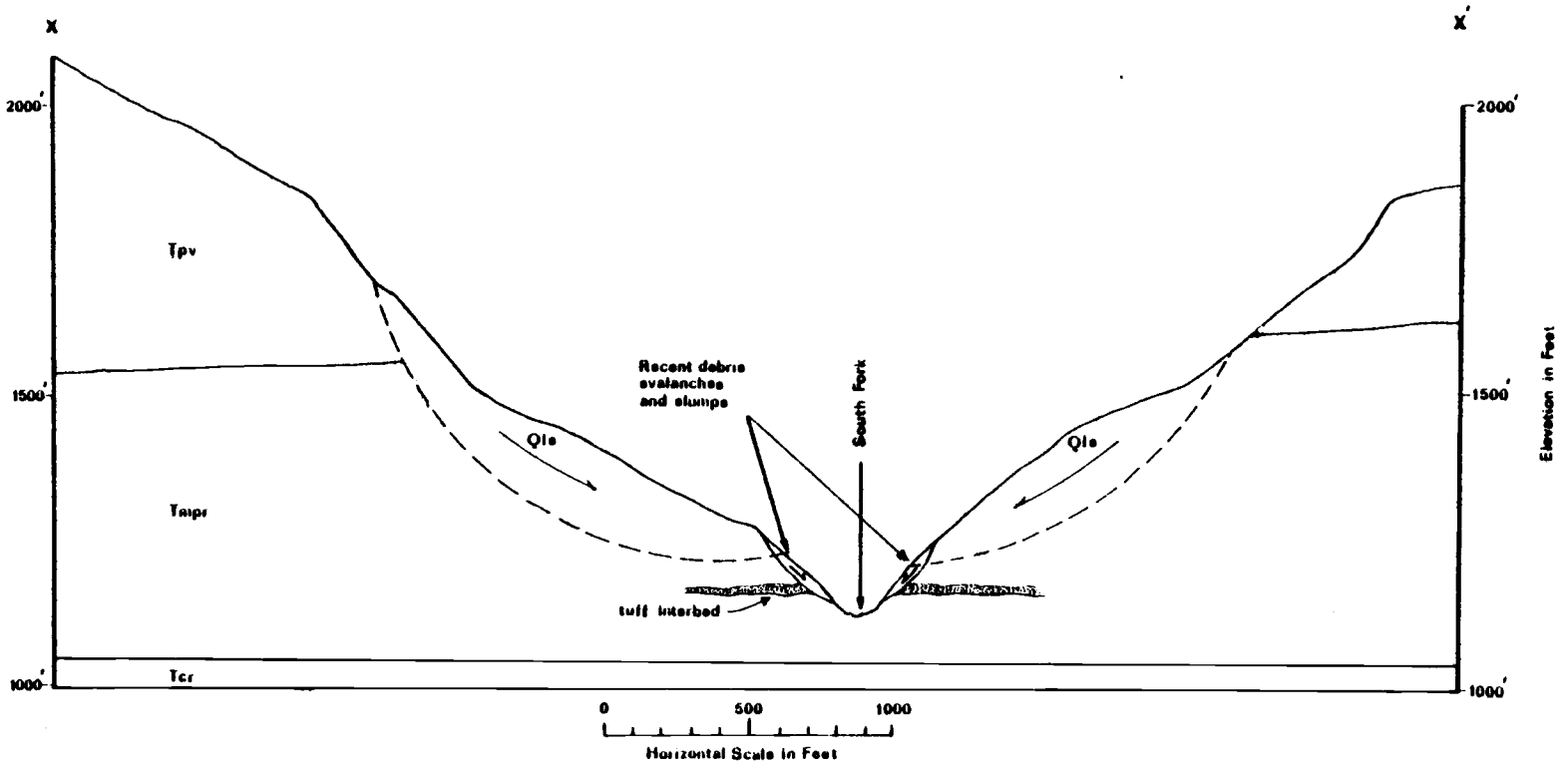

Figure 37. Generalized cross section of the South Fork of the Bull Run River. Location and legend shown on Plate 1. Vertical exaggeration = 2X horizontal.

at which backwasting by rotational failure in the pyroclastics began. This event may have been triggered catastrophically by a period of high runoff and stream bank erosion, possibly coinciding with Pleistocene glaciofluvial processes. Further downcutting in the pyroclastics may lead to remobilization of the initial, large, rotational failures by undercutting at the toe, where smaller mass movements, both slump-earthflow and debris avalanche, are common. The tendency toward remobilization is compounded by loading at the head of the large failures by rockfall-rockslide from the capping flow rock above. Stability of these slopes may be reached only after downcutting has proceeded through the pyroclastics and into the next flow unit (Tcr).

The South Fork, North Fork, and Bull Run rivers are in various stages of this geomorphic development, however, remobilization of the large complex-massive failures, in these areas, does not appear to be currently active, since mature forest vegetation is largely undisturbed on the failure sites. In the South Fork drainage, small to moderately large mass movements, predominantly debris avalanches, are numerous. The South Fork is the most active drainage in the watershed in terms of recent mass movement activity. Exposed in the heads of these recent failures are blocks of Quaternary landslide debris, whereas pyroclastics of undisturbed Rhododendron Formation are exposed in the toes (Figure 38). Groundwater flows freely

Figure 38. Scarp of a large debris avalanche in the South Fork drainage (mass movement no. 36). Note contact between weathered pyroclastics of the Rhododendron Fm. (buff) and overlying, blocky Quaternary landslide debris.

through the Quaternary landslide debris, but is not transmitted well through the underlying pyroclastics and thus tends to be channeled along the old failure surfaces of the complex-massive landslides. Where the old failure surfaces intersect the present hillslopes, saturation and failure of the soil mass occurs. Some of the recent failures have exposed red clay pods, similar to those located in the North Fork that were responsible for turbidity problems in 1972.

Another implication of the cap-rock situation lies in the development of flow rock colluvium over weathered pyroclastics. According to Taskey (1978), perched water tables often exist in colluvial soils developed above impermeable pyroclastics. The clay fraction of these colluvial soils consists of amorphous gel and halloysite, which maintain a high water content in the soil. These conditions commonly result in debris avalanche failure of colluvium overlying the pyroclastics.

Distribution

Creep is pervasively distributed throughout the watershed. Abnormally high rates of creep were noticed locally along many of the stream channels in the watershed. Areas undercut by debris torrent scouring along Log Creek show high creep rates. Quaternary landslide debris along S-10 north of Reservoir 2 is undergoing accelerated creep, as indicated by the tilting of telegraph poles.

Recent slump-earthflow is not common in the Bull Run Watershed, but does occur locally on mudstone of the Troutdale Formation, Quaternary landslide debris, and poorly indurated pyroclastics of the Rhododendron Formation, in the western part of the watershed. Two older slump-earthflows occurred on the Pliocene volcanic rock unit in the eastern part of the watershed, one of which is still partly active by earthflow. Many of the smaller slump-earthflows appear to be related to road construction and poor culvert location. Streamside slump-earthflows are rare.

Debris avalanches are relatively common in the Bull Run. Most debris avalanches are streamside events or are located on hillslopes near stream channels. Some debris avalanches occur within road rights-of-way; but few, other than very small soil slips, were found in clearcuts. A few debris avalanches were mapped around the still forested perimeter of clearcuts. The South Fork drainage contains the greatest abundance of debris avalanches, most of which are estimated to be 5-20 years old (Figure 39). These debris avalanches occur on Quaternary landslide debris and pyroclastics of the Rhododendron Formation. Debris torrents have triggered streamside debris avalanches in the North Fork (Figure 40), above Quaternary landslide debris, and in Log Creek, above flows of the Pliocene volcanic rock unit. Small debris avalanches, involving soil mantle failure over Columbia River Basalt Group bedrock, are common on steep slopes

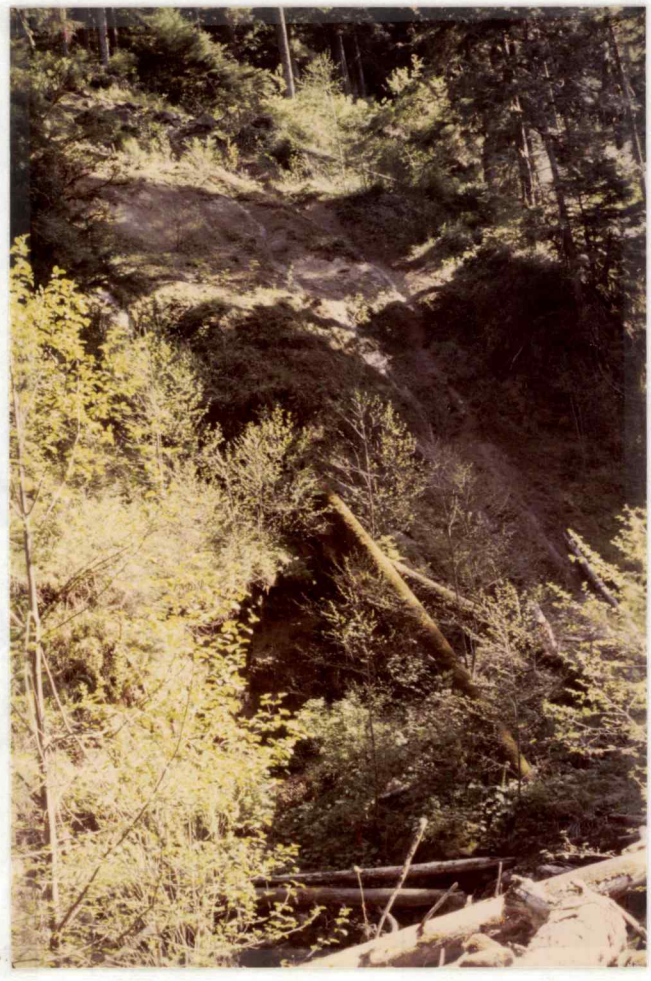

Figure 39. Debris avalanche in the South Fork drainage (mass movement no. 40). Failure surface is planar and consists of tuff and pyroclastic breccia of the Rhododendron Fm. Scarp consists of Quaternary landslide debris. Depositional mass at toe is revegetated with 15-20 ft alder suggesting an age of about 9 years for the failure. Distance from scarp to toe is 300 ft.

Figure 40. Streamside debris avalanche associated with North Fork debris torrent of January, 1972 (mass movement no. 6). Quaternary landslide debris is exposed in the failure surface Rip rap has been placed along the toe to retard further stream undercutting.

Figure 41. Debris torrent deposits in the upper North Fork drainage. Largest boulders are 8-10 feet in diameter. Present channel flows to the left of this deposit which defeated the pre-torrent channel.

in blazed Alder Creek, sections of the Bull Run River, and Falls Creek.

The pre-historic complex-massive landslides all occur within the Rhododendron Formation, accompanied by some undercutting of the capping Pliocene volcanic rock unit. The thickest deposits of debris (50-100 ft thick), resulting from these landslides, are located north of the Bull Run River from the access gate to Reservoir 2 and locally in the North Fork and South Fork drainages. Thinner Quaternary landslide deposits are located south of the Bull Run River near Reservoir 2, and locally on S-111 south of Reservoir 1 and in the Fir Creek drainage.

Rockfall-rockslide is widespread in the watershed. Rockfall road maintenance problems were noticed near the access gate, involving siltstone of the Troutdale Formation, near Falls Creek, involving pillow basalts, along S-10 near Bull Run Lake, involving platy andesites of the Pliocene volcanic rock unit, and at numerous sites, involving loosened boulders of Rhododendron Formation breccia. The confluence of Cedar Creek and South Fork is the site of abundant rockfall from Pliocene volcanic rock unit flows. Heavy fracturing of the Quaternary volcanic-intrusive complex at Thunder Rock has resulted in rockfall-rockslide along Thunder Creek; and brecciated basalt above the thrust fault in Blazed Alder Creek is also undergoing rockfall-rockslide.

Debris torrents have been documented for both North Fork and Log Creek. Heavy precipitation and snowmelt, during the week of January 16, 1972, in combination with temporary blockage and later failure of an ice dam at Boody Reservoir, resulted in a rapid release of floodwater down the North Fork drainage. The resulting debris torrent was capable of moving boulders ten feet in diameter (Figure 41), and scoured extensive sections of streambank, mostly in the area of Quaternary landslide deposits. Streamside debris avalanches resulted from bank undercutting in this area, and the sediment influx from these mass movements created a serious turbidity problem during the following weeks. Much of the debris entrained by the torrent was flushed through the entire length of the North Fork and deposited as a fan in Reservoir 1 (Figure 42). Most likely, more than one debris torrent event contributed to the fan deposits.

Log Creek has also been scoured by debris torrents. Ice damming followed by sudden dam failures at Blue Lake has probably been the cause for many flooding-scouring events in the Log Creek channel. Streambank erosion on the outside of stream meanders has exposed bare colluvial soil and has undercut valuable timber along most of the length of Log Creek. Several stages of debris torrent deposits have accumulated in old overflow channels and on the inside of stream meanders. The tops of old debris torrent deposits may be recognized by different ages of vegetative growth, which have been partly covered

Figure 42. Alluvial fan at the mouth of the North Fork, exposed by reservoir draw down. Debris torrent deposition has contributed heavily to the progradation of the fan.

by later deposits. Figure 43 contains a map and profiles of a section of Log Creek, which reveals evidence for at least two debris torrent events. The youngest debris has been deposited above the roots and around the base of 60 foot tall cedar, which had grown on an older deposit; and therefore the older deposit must be at least 100 years old.

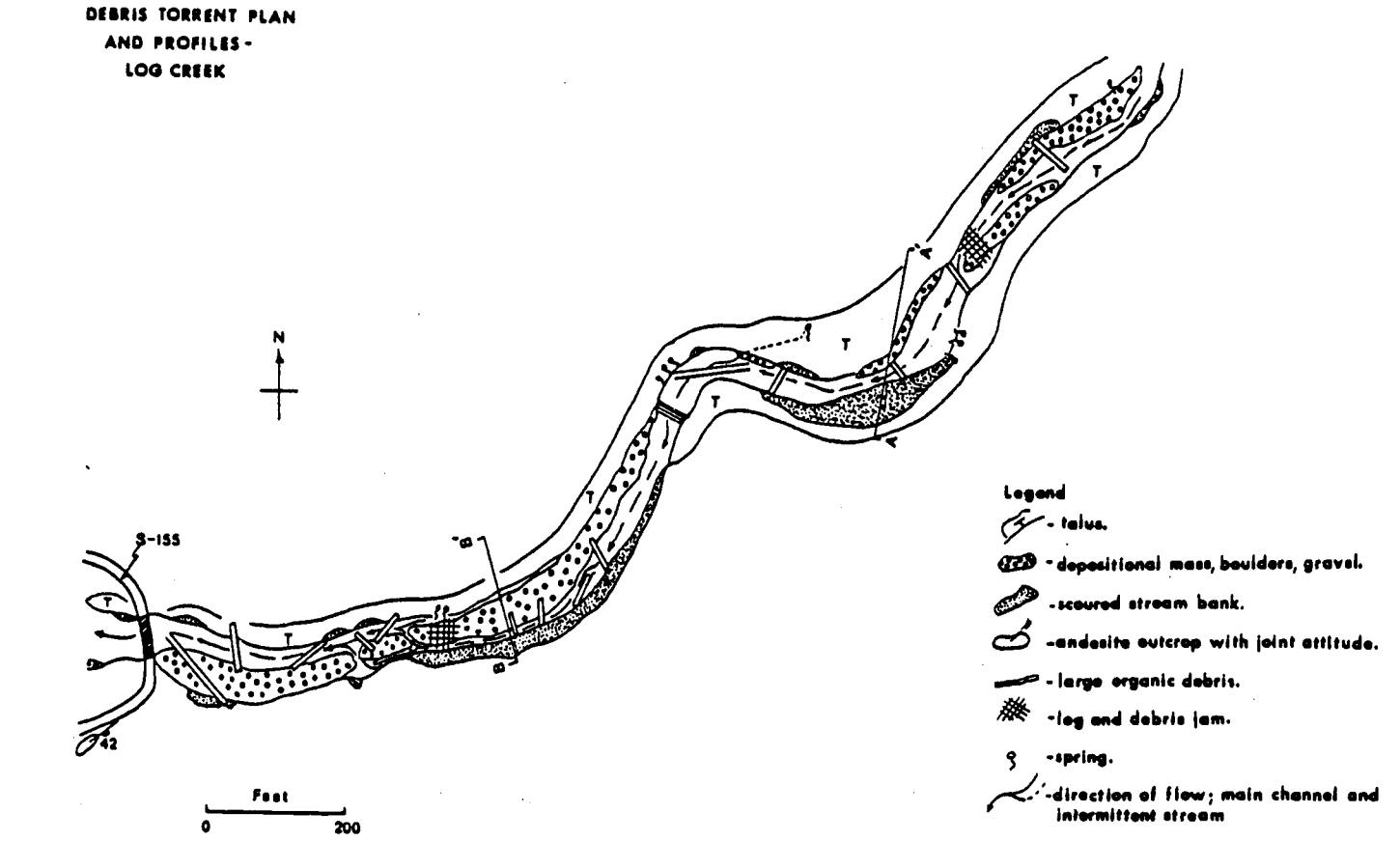

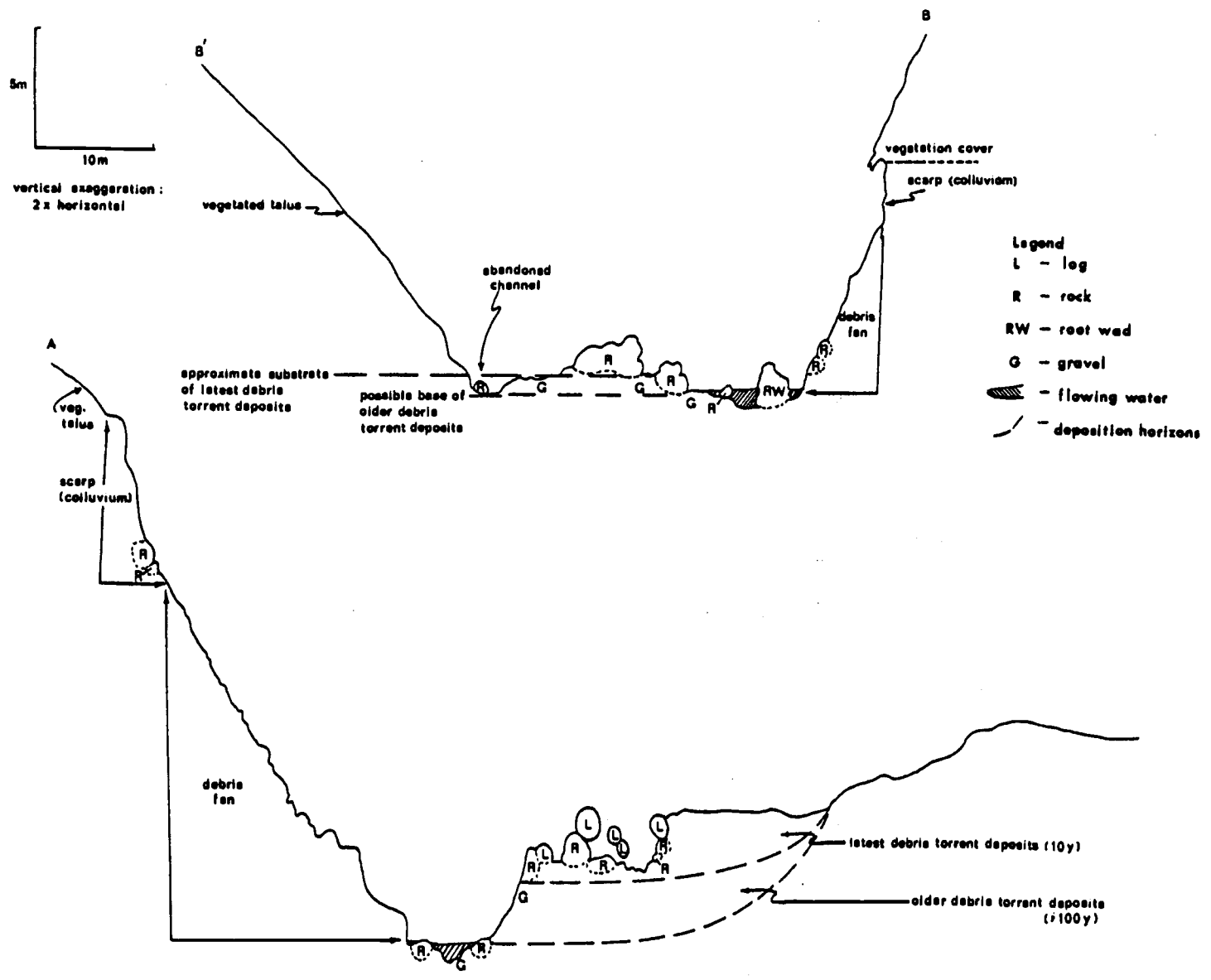

Figure 43. Plan and profiles of a section of Log Ck ., showing features of debris torrents. Note scour on the outside of stream meanders, deposition on the inside of stream meanders, and evidence for repeated debris torrent events.

MASS MOVEMENT HAZARD DETERMINATION

General Statement

The understanding gained from quantitative analyses of the relationship between mass movements and geologic factors can be used to develop a predictive model for mass movement occurrence. Each of the geologic factors analyzed is assigned a weighted value describing the significance of its correlation to mass movement occurrence. Various combinations of these weighted values describe geographic areas, which can be compiled on a base map to produce a hazard map. The hazard map delineates zones of high, moderate, and low hazard for each mass movement type considered.

Multiple Regression

Multiple regression is a type of multivariate analysis, which accounts for all possible correlations among a set of independent variables and a dependent variable, therefore the technique is applicable to weighting factors (independent variables). In addition, multiple regression programs may be written which will indicate the amount of multicollinearity (correlations among the independent variables). The basic requirement of a multiple regression analysis is that variables are measured on an interval or ratio scale and that the relationship among the variables is linear or additive. Significance tests

associated with multiple regression are based on four assumptions (Kim and Kahout, 1975):

1. The sample is drawn at random.
2. Each array of dependent variables for a given combination of independent variables is normally distributed.
3. The regression of dependent and independent variables is linear.
4. All the dependent variable arrays have the same variance.

A stepwise multiple regression analysis was used to define the relationship between two dependent variables (mass movement occurrence and volume of material moved by mass movements) and three independent variables (slope gradient, distance from the nearest geologic contact, and soil texture) for each mass movement type (Table 10). These independent variables were selected because they were likely to fulfill the linearity requirement and they were quantifiable over the entire study area. Mass movement occurrence was measured by the stability factor (Y) where Y = 0 at randomly selected stable sites and Y = 1 at mass movement sites, thus the stability factor is a dichotomous dependent variable, which does not strictly satisfy the normal distribution and linearity requirements of regression. However, dichotomous dependent variables may be used as approximations to continuous variables in regression (Hamilton, 1974). Volumes of individual mass movements (Y_2) were measured in the field. Slope gradients (X_1) for both mass movement sites and

stable sites were taken from the slope gradient map provided by Beaulieu (1974). Site specific slope gradients vary considerably from the generalized gradients shown on the map, and thus the slope gradient measurements used in the regression are approximations of actual site gradients. The regression, however, tests the correlation between the distribution of inventoried mass movements and the distribution of the steep slope gradient (high hazard) areas of Beaulieu (1974). The minimum distances from the site to the nearest geologic contact (X_2) were measured on Plates 1 and 3. In the case of large mass movements, X_2 measurements were taken from the geographic center of the mass movement, in map view. Soil texture (X_3) was measured from the soil maps and mapping unit descriptions provided by Howes (1979). Three categories were established to approximate continuous variations in the texture of sub-soil layers.

1. Coarse to moderately coarse-textured, including sands through fine sandy loams.
2. Medium-textured, including very fine sandy loams through silts.
3. Moderately fine to fine-textured, including sandy clays through clays.

Correlation coefficients for each independent variable are given by the Simple R value (Table 10) which ranges from 1 (complete correlation) to 0 (no correlation). The sign of the Simple R value

Table 10. Summary of multiple regression analysis of the relationship among geologic factors and mass movements

[Dependent variables: Y = stability factor (0 = random stable site, 1 = failure site), Y_2 = volume. Independent variables: X_1 = slope gradient, X_2 = distance between site and nearest geologic contact, X_3 = soil texture]

Dependent variable, slide type	Variable	Significance F to enter	Multiple R	R^2	Simple R	Significance overall F
Y, slump-earthflow	X_2	.000	.34583	.11960	-.34583	.000
	X_3	.019	.40252	.16202	+.25913	.000
	X_1	.312	.41608	.16981	+.17345	000
Y, Streamside slump-earthflow	X_1	.024	.22397	.05016	+.22397	.024
	X_2	.287	.24701	.06101	-.18127	.044
	X_3	.393	.26081	.06802	+.05937	.074
Y, Debris avalanche	X_2	.000	.35811	.12824	-.35811	.000
	X_3	.013	.41937	.17587	+.27710	.000
	X_1	.003	.48900	.23912	+.34154	.000
Y, Streamside debris avalanche	X_2	.000	.33795	.11421	-.33795	.000
	X_3	.100	.36704	.13472	+.18585	.000
	X_1	.475	.37224	.13856	+.15687	.001
Y, Rockfall-rockslide	X_1	.000	.34196	.11694	+.34196	.000
	X_2	.067	.38058	.14484	-.28925	.000
	X_3	.287	.39264	.15416	+.08041	.001
Y, Complex-massive	X_2	.017	.23235	.05399	-.23235	.017
	X_3	.033	.30859	.09523	+.23086	.006
	X_1	.358	.32051	.10273	+.12008	.011
Y_2, Slump-earthflow	X_3	.001	.74210	.55071	-.74210	.001
	X_2	.401	.75736	.57359	+.40236	.003
	X_1	.567	.76460	.58461	-.00317	.008
Y_2, Streamside slump-earthflow	X_1	.002	.98604	.97227	+.98604	.002
	X_3	.430	.99059	.98127	+.52880	.019
	X_2	.762	.99185	.98377	-.18409	.162
Y_2, Debris avalanche	X_1	.412	.21277	.04527	-.21277	.412
	X_2	.419	.30044	.09026	-.18282	.516
Y_2, Streamside debris avalanche	X_1	.351	.20393	.04159	+.20393	.351
	X_3	.423	.26947	.07261	+.20210	.471
	X_2	.791	.27588	.07611	-.11401	.672
Y_2, Complex-massive	X_2	.355	.32759	.10732	+.32759	.355
	X_1	.839	.33603	.11292	+.20801	.657

indicates whether the correlation between the dependent and independent variables is direct or inverse. Multiple R values are correlation coefficients for all variables entered in the regression at each step. R^2 values give the percent of variation in Y explained by the linear regression on X at each step. F to enter gives the significance of each variable, whereas F overall gives the significance of the regression for all variables, entered at each step.

When all mass movement types are considered together, mass movement occurrence (Y) is most highly correlated to the inverse of X_2, which is the first variable to enter the regression. That is mass movement occurrence is more likely as the distance between the site and a contact decreases. X_1 is the next most highly correlated variable, and as slope gradient increases the likelihood of mass movement increases. X_3 is weakly correlated and usually not significant in the analysis, but an increase in the likelihood of mass movement occurrence appears to vary directly with increasing clay content in the sub-soil layer.

When mass movement types are considered individually, the distance between the site and a geologic contact is most highly correlated to Y for debris avalanches and slump-earthflows, moderately correlated for streamside debris avalanches, and weakly correlated or rockfall-rockslide, complex-massive, and streamside slump-earthflow failures. A similar ranking of the correlation

between mass movements and distance to a contact by slide type, is evident in the chi-square test (Table 6). The complex-massive failures show weak correlations because they are so large that the centers of these mass movements may be far removed from a contact even though the initial failure may have been related to the presence of a contact, and the lack of a strong correlation here is misleading because of the measurement technique. Slope gradient is most highly correlated to Y for rockfall-rockslide and debris avalanche, moderately correlated for streamside slump-earthflow, and least correlated for slump-earthflow, streamside debris avalanche, and complex-massive failures (Table 10). This ranking, with the exception of the streamside events, is in rough agreement with the site specific data (Table 9). Streamside debris avalanches occur in narrow steep-gradient zones on either side of the stream channel; and these zones are too small to be represented accurately on the slope gradient map. X_3 appears to have little significance in the regression, probably because the mapping units of Howes (1979) could not be considered in their entirety in the regression, and it was necessary to extract one quantifiable variable (sub-soil texture) to characterize each map unit. However, the relative ranking, by slide type, of the strength of correlation between mass movement occurrence and clay content (soil texture), using Howes's data (Table 10), agrees identically with the ranking of average clay content by slide type using

the data in Table 1. Debris avalanche and slump-earthflow occurrence are more highly correlated to clay content than are streamside events.

When the volume of mass movements is used as a dependent variable (Y_2) the overall significance of correlation coefficients drops. Furthermore, there is no consistency in the sign of the correlation coefficient among different slide types. Many of these complications are the result of limited data and the consequently strong effect of very large mass movements on the correlations. In general though, X_1 is the most significantly correlated variable, so slope gradients appear to have an influence on the volume of mass movements as well as on their occurrence frequencies. Contact distance and soil texture do not appear to be significantly correlated to Y_2.

Multicollinearity can cause problems in a regression analysis. The SPSS regression program, however, computes a correlation matrix for the independent variables, which indicates the amount of multicollinearity. Intercorrelations among the independent variables in Table 10 is negligible for most combinations of independent variables. The only significant intercorrelation exists between slope gradient and distance to a contact (about -0.3 to -0.4), but this is probably not enough to seriously affect the regression. X_1-X_2 multicollinearity is a function of the simple geometry of flat-lying geologic units; on steep slopes map distances to contacts are minimized.

Resolution and Reliability of the Data

There are inherent problems in attempting to quantify largely qualitative factors such as bedrock type. Approximations to statistical parameters are necessary for qualitative variables which are not continuously measureable. Mass movement occurrence and bedrock outcrop are not randomly distributed and biases exist as to where data may be collected in the study area. In the Bull Run Watershed, additional complications result from very poor exposure, which inhibits accurate geologic mapping. Furthermore, the watershed is relatively stable with respect to mass movement occurrence frequency and a statistically meaningful number of samples is not readily obtainable. In addition, any relationship between geologic factors and mass movement type is a function of the classification system used, and a different classification system may bring out stronger correlations in the data.

In general then, data generated by this study are semi-quantitative. The results approximate the relative magnitudes of the relationships between geologic factors and mass movement occurrence that were heretofore considered intuitively. They provide the framework for a quantitative, predictive model of mass movement hazard determination in the Bull Run Watershed and similar terranes. Additional studies can be better controlled in more active areas providing a larger data base and may result in data that refine the

approximations presented here.

Hazard Weighting and the Hazard Map

In previous sections, soil and bedrock properties were analyzed qualitatively or by chi-square tests and multiple regression to determine their relationship to mass movement type and occurrence. The data suggest that different factors have different degrees of influence. Some tests are less meaningful or reliable than others because the correlations are less significant, the data sources are too general, or the number of cases is too small. Therefore it is necessary to rank the various tests in some order of reliability (Table 11) before using these data to weight the importance of geologic factors in controlling mass movement occurrence. Weighting of the factors must be partly subjective because different types of analyses were used and because it is not statistically valid to compare the results of chi-square tests with different degrees of freedom.

Using the data, considerations of their reliability, and geologic intuition, it is possible to list factors for which data exist over the entire watershed and to assign weighted values to each factor, which can be used to stratify mass movement hazard in the Bull Run (Table 12). These weighted hazard values vary for each slide type. Theoretical weights are estimations of the importance of each factor. Reliability factors were subtracted from the theoretical weights to

Table 11. Quality of the data for mass movement hazard determination

Factor	Relationship	Table	Strength		
			Good	Moderate	Poor
Clay content	mass movement occurrence	1	x		
Clay content	mass movement type	1			x
C and $\emptyset$	mass movement type	2			x
Clay mineralogy	mass movement occurrence	3	x		
Clay mineralogy	mass movement type	3		x	
Geologic unit	mass movement occurrence	4	x		
Geologic unit	mass movement volume	4	x		
Joint attitude	mass movement occurrence	5		x	
Contact zone	mass movement occurrence	6	x		
Springs and seeps	mass movement occurrence	6, 7	x		
Springs and seeps	mass movement type	8		x	
Slope gradient	mass movement type	9	x		
Slope gradient	mass movement occurrence	10		x	
Slope gradient	mass movement volume	10		x	
Contact	mass movement occurrence	10	x		
Contact	mass movement volume	10			x
Soil texture	mass movement occurrence	10			x
Soil texture	mass movement volume	10			x

Table 12. Mass movement hazard weights

[0 = least hazard weight, 5 = greatest hazard weight, DA = debris avalanche, SE = slump-earthflow, RR = rockfall-rockslide. Geologic unit abbreviations are the same as for Figure 3]

Factor	Theoretical weight			Reliability Factor	Stratification weight		
	DA	SE	RR		DA	SE	RR
Contact association	4	3	2	0	4	3	2
Joint attitudes	3	1	3	-1	2	0	2
Geologic unit	3	5	2	0	3	5	2
Slope gradient	5	3	4	-1	4	2	3
Soil texture	3	3	0	-2	1	1	0
Hydrology	5	4	1	0	5	4	1
				Total weighting points	19	15	10

Factor	Characteristics		Characteristic weighting points		
			DA	SE	RR
Contact association	within 200 ft of:	Tmpr-Tpv	4	3	2
		Tmpr-Qls	4	3	1
		Tcr-Tmpr	3	3	1
		Tcr-Qls	2	3	1
		Tmpr-Tpt	2	3	1
		Qls-Qtg	2	2	1
		Tpv-Tpt	2	2	1
		Tmpr-Qgl	1	2	1
		Tcr-Qgl	1	1	1
		Tcr-Qtg	1	1	2
		Tpv-Qls	2	1	2
		Tcr interflow	3	1	2
		Tpv interflow	2	1	2
		other	1	1	1
Joint attitudes		steeply, with slope	2	0	2
		other	0	0	0
Geologic unit		Qls	3	5	1
		Tmpr	2	5	1
		Tpt	1	4	2
		Tcr	3	2	2
		Tpv	2	2	2

Table 12. (Continued)

Factor	Characteristics	Characteristic weighting points DA	SE	RR
	Qvic	1	1	2
	Qtg	1	1	1
	others	0	0	0
Slope gradient (Beaulieu, 1974)	>50%	4	2	3
	26-50%	2	2	2
	11-25%	1	1	1
	0-10%	0	0	0
Soil texture (Howes, 1979)	mapping units: 15	1	1	0
	2	1	1	0
	340	1	1	0
	338	1	1	0
	339	1	1	0
	others	0	0	0
Hydrology	poorly drained, marshy	3	5	0
	wet, springs frequent	5	4	1
	dry, springs rare	0	0	0

Table 13. Hazard classes
[DA = debris avalanche, SE = slump-earthflow.
Total weighting points are in parentheses]

Hazard level	Hazard class DA	SE
High	I (12-19)	IV (12-15)
Moderate	II (6-11)	V (6-11)
Low	III (0-5)	VI (0-5)

take into account limitations of the accuracy of data source maps used for each factor. Geologic and hydrologic data were mapped in the field. Soil texture data were taken from the soil maps of Howes (1979). Slope gradients were taken from Beaulieu (1974). Stratification weights are the hazard values assigned to each factor, which are actually used in the hazard map compilation. Characteristic weighting points were assigned to the various characteristics of each factor, and their distributions were mapped on separate overlays. The maximum value of a characteristic weighting point is the value of the stratification weight for the respective factor and slide type. The minimum value of a weighting point is 0, indicating no relationship between a characteristic and mass movement occurrence.

Six overlays, one for each factor, were compiled and overlapping areas were summed for total weighting points for each mass movement type. Six classes of mass movement hazard were defined on the basis of these weighted areas (Table 13).

Slopes susceptible to high rockfall-rockslide hazard (8-10 total weighting points) were classified and mapped separately. The hazard map (Plate 3) is a synthesis of all factor overlays for both debris avalanches and slump-earthflows. It is intended for use in reconnaissance level management planning. More detailed study is recommended for project level planning.

DISCUSSION

Comparison of Results from Bull Run with Other Areas

Mass movement inventories have been conducted in other areas of the Pacific Northwest: Mapleton, Siuslaw National Forest, Oregon (Swanson and others, 1977; Ketcheson, 1978); H. J. Andrews Experimental Forest, Oregon (Swanson and Dyrness, 1975); Alder Creek, Willamette National Forest, Oregon (Morrison, 1975); Stequaleho Creek, Olympic Peninsula, Washington (Fiksdal, 1974); and selected drainages in the Coast Mountains, British Columbia (O'Loughlin, 1972). In forested areas of the Bull Run Watershed, debris avalanches are characterized by low occurrence frequency and moderate average volume with respect to documented occurrences elsewhere in the Pacific Northwest (Table 14). Total soil transfer rates in the Bull Run are lower than in any of the other areas listed. Therefore, the Bull Run Watershed is relatively stable with respect to debris avalanche occurrence in forested areas of the Pacific Northwest. Studies at other sites show that the frequency, and in some cases the average volume, of debris avalanches in clearcut sites are significantly higher than that of forested sites. The frequency increases are even greater in road right-of-way sites. In the Bull Run Watershed, however,

Table 14. Comparison of frequency, average volume and soil transfer rate of debris avalanches in forested areas in the Bull Run Watershed with other studies in the Pacific Northwest [see text for sources]

Site	Period of record (yr)	Frequency (events $km^{-2} yr^{-1}$)	Average volume (m^3)	Soil transfer rate ($m^3 km^{-2} yr^{-1}$)
Bull Run Watershed	40[1]	0.003	836	2.5
Mapleton				
Swanson and others	15	0.533	54	28
Ketcheson	15	0.432	25	11
H. J. Andrews	25	0.025	1,460	36
Alder Creek	25	0.023	1,990	45
Stequaleho Creek	84	0.015	4,660	72
Coast Mountains, B. C.	32	0.004	3,040	11

[1]Based on estimate of oldest event

hardly any debris avalanches occurred in clearcut sites, and very few occurred in road right-of-way sites.

Colman (1973) determined that 27.4 percent of the area studied in the Redwood Creek Basin, northern California is in slump-earthflow terrain. Swanston and Swanson (1976) reported that 25.6 percent of the area in the H. J. Andrews Experimental Forest, underlain by volcaniclastic bedrock, is in slump-earthflow terrain. Less than 1 percent of the slump-earthflow terrain is underlain by flow rock, even though 63 percent of the bedrock in the area is flow rock. Slump-earthflow terrain (slump-earthflow and complex-massive failure sites) in the Bull Run Watershed makes up 3.2 percent of the study area. Nearly all of this terrain is underlain by pyroclastics and epiclastics of the Rhododendron Formation, which make up only 6.6 percent of the study area. Thus, with respect to slump-earthflow mass movement distribution, the Bull Run Watershed is also more stable than some other documented areas in the Pacific Northwest.

Summary

1. The base of the stratigraphic section in the Bull Run Watershed consists of 900 feet of middle Miocene tholeiitic basalt flows of the Wanapum and Grande Ronde Basalt Formations of the Columbia River Basalt Group. These are unconformably

overlain by 600 feet of late Miocene to early Pliocene laharic breccia, tuff, lapilli tuff, and pyroclastic breccia of the Rhododendron Formation. The Rhododendron Formation was deposited in Miocene topographic lows and extends further to the east than previously mapped. The Rhododendron Formation is overlain in the west by an eastward-thinning wedge of fluvial siltstone, sandstone, and conglomerate of the Troutdale Formation. Greater than 2, 000 feet of Pliocene basaltic andesite and less abundant basalt and pyroclastics overlie all older units with local unconformity. Pliocene volcanic rocks are overlain, with local unconformity, by an erosional remnant of Quaternary hornblende andesite and equivalent pyroclastics. Quaternary basalt and andesite are present at Bull Run Lake. Most rocks are fresh and largely unaltered except for badly weathered pyroclastics of the Rhododendron Formation and siltstone of the Troutdale Formation.

2. Quaternary to Recent surficial deposits include thick landslide debris, extensive talus, and predominantly colluvial forest soils. Glacial outwash and moraine occur as scattered deposits but are not extensive. Glaciation generally did not extend below 2, 200 feet.

3. Bedding of all geologic units is nearly horizontal in the watershed. A gentle syncline and anticline trend N60E across the

eastern part of the area, and northwestward thrusting ruptured the northwest limb of the anticline (Vogt, 1979). Near vertical, northwest-trending faults and tectonic joints cut all geologic units and older structures. Cooling joints are randomly oriented regionally.

4. The distribution of mass movements, especially slump-earthflow, is strongly controlled by bedrock geology. The highest number of slump-earthflows per unit area occur on Quaternary landslide debris and the Rhododendron Formation. The density of debris avalanches in greatest on the Columbia River Basalt Group.

5. Complex-massive failures occurred in areas where pyroclastics of the Rhododendron Formation are intercalated between flow rock units. This stratigraphic juxtaposition of hard and soft rocks prevents the establishment of a stable slope profile and results in large slump-earthflow failure during drainage development. Debris avalanche commonly occurs along the contact of older landslide debris and the Rhododendron Formation in the North Fork and South Fork. These are the most active drainages in the watershed in terms of recent mass movements. Loading at the head of the complex-massive failures, by rockfall from the capping flow rock, and erosion at the toe, by smaller mass movements, may lead to large scale reactivations of these

failures, although undisturbed vegetation indicates that they have been stable for at least several hundred years.

6. Mass movement occurrence is preferentially distributed with respect to geologic contacts. Mass movements are most associated with the Tmpr-Tpv contact. Mass movement occurrence is also significantly associated with the Tmpr-Qls, Tcr-Tmpr, and Tcr-Qls contacts. The Tmpr-Tpv and Tcr-Tmpr contacts are most associated with the prehistoric complex-massive failures whereas the Tmpr-Qls and Tcr-Qls contacts are associated with recent reactivations of the older landslide deposits.

7. Springs and seeps are distributed preferentially with respect to geologic contacts in nearly the same way as mass movements, indicating a strong correlation between the two. Spring density is greatest on the Tmpr-Tpv, Tmpr-Qls, Tcr-Tmpr, and Tcr-Qls contacts. The presence of springs on a slope is associated more with debris avalanche occurrence than with other types of mass movement.

8. Clay contents of Bull Run soils are generally less than 15 percent. Clay content is higher in samples taken from failure sites than from stable sites. The Rhododendron Formation, Pliocene volcanic rock unit flow breccias, and Quaternary landslide debris weather to the most clay-rich soils.

9. Halloysite, generally in the hydrated state, is the most common clay mineral in Bull Run soils. Chloritic intergrades and smectites are also common. Kaolinite and mica are less abundant. Mass movement occurrence is favored by high smectite and possibly hydrated halloysite contents. Stable sites contain abundant chloritic intergrade and kaolinite. Clay mineral distribution varies with underlying bedrock. Flow rocks weather to soils with abundant chloritic intergrade and kaolinite, whereas soils overlying the Rhododendron Formation, Quaternary landslide debris, and flow breccias have high smectite and hydrated halloysite contents.

10. Jointing attitudes have only a minor effect on mass movement occurrence in the Bull Run Watershed. Mass movement occurrence is most likely where joints dip steeply with the slope and least likely where joints dip steeply into the slope, especially if the strike of the joints and slope are within 45° of one another.

11. Average slope gradients at mass movement sites in the watershed vary from 58 percent to 85 percent Slump-earthflows may occur on gentler slopes than debris avalanches.

12. Debris torrent events, resulting in extensive streambank erosion and debris avalanching, have occurred repeatedly on the North Fork and Log Creeks.

13. A stepwise multiple regression analysis indicates that the occurrence of mass movements is most strongly correlated to the inverse of the minimum distance between a site and the nearest geologic contact, moderately correlated to slope gradient, and weakly correlated to soil texture.

14. The relationship between geologic factors and mass movement occurrence in the Bull Run Watershed is quantifiable using chi-square tests and multiple regression analyses. Data generated by these tests can be used to weight geologic factors in terms of mass movement hazard levels. Stratification of the weighted values produces a predictive model in the form of a hazard map.

REFERENCES

Baldwin, E. M., 1964, Geology of Oregon: Univ. of Oregon Cooperative Bookstore, Eugene, Oregon, 165 p.

Barnes, F. F., and Butler, W., 1930, The structure and stratigraphy of the Columbia River Gorge and Cascade Mountains in the vicinity of Mount Hood: M.S. thesis, Univ. of Oregon, Eugene, Oregon, 73 p.

Beaulieu, J. D., 1974, Geologic hazards of the Bull Run Watershed, Multnomah and Clackamas Counties, Oregon: Oregon Dept. of Geology and Mineral Indus. Bull. 82, 77 p.

Beeson, M. H., Moran, M. R., Anderson, J. L., Timm, Susan, and Vogt, B. F., 1979, Stratigraphy and structure of the Columbia River Basalt Group in the Cascade Range, Oregon: Portland, Oregon, unpublished report to Oregon Dept. of Geol. and Mineral Indus, 87 p.

Blong, R. J., 1973, A numerical classification of selected landslides of the debris slide-avalanche-flow type: Eng. Geol., v. 7, p. 99-114.

Bouyoucos, G. J. 1962, Hydrometer method improved for making particle size analysis of soils: Agronomy Jour., v. 54, 464-468.

Burroughs, E. R., Chalfant, G. R., and Townsend, M. A., 1976, Slope stability in road construction: U.S. Dept. Agr. Bureau of Land Management, Portland, Oregon, 102 p.

Callaghan, Eugene, and Buddington, A. F., 1938, Metaliferous mineral deposits of the Cascade Range in Oregon: U.S. Geol. Survey Bull. 893, 141 p.

Colman, S. M., 1973, The history of mass movement processes in the Redwood Creek basin, Humboldt County, California: M.S. thesis, Pennsylvania State Univ., University Park, Pa., 151 p.

Dames and Moore, 1972a, Progress report, consultations and inspections, earth slide, North Fork of the Bull Run River: Portland, Oregon, unpublished report to City of Portland, 8 p.

Dames and Moore, 1972b, Progress report no. 2, consultations and inspections, earth slide, North Fork of the Bull Run River: Portland, Oregon, unpublished report to City of Portland, 4 p.

_____, 1973, Summary report, consultation and inspections, earth slide, North Fork Bull Run River: Portland, Oregon, unpublished report to City of Portland, 7 p.

Dyrness, C. T., 1967, Mass soil movements in the H. J. Andrews Experimental Forest: U.S. Dept. Agr. Forest Serv. Res. Paper PNW-42, 12 p.

Fiksdal, A. J., 1974, A landslide survey of the Stequaleho Creek watershed: Supplement to Final Report FRI-UW-7404, Fisheries Res. Institute, Univ. of Washington, Seattle, Wash., 8 p.

Geo-Recon, Inc., 1962, Report of geophysical investigation of Bull Run valley, City of Portland, Bull Run Dam no. 2: Portland, Oregon, unpublished report to City of Portland, Bureau of Waterworks, 2 p.

Hamilton, D. A., 1974, Event probabilities estimated by regression: U.S. Dept. Agr. Forest Serv. Res. Paper INT-152, 18 p.

Harper, H. E., 1946, Preliminary report on the geology of the Molalla quadrangle: M.S. thesis, Oregon State Univ., Corvallis, Oregon, 26 p.

Hodge, E. T., 1933, Age of Columbia River and lower Canyon [abs]: Geol. Soc. America Bull., v. 44, p. 156-157.

_____, 1938, Geology of the lower Columbia River: Geol. Soc. America Bull., v. 49, no. 6, p. 831-930.

Hoover, L., 1963, Geology of the Anlauf and Drain quadrangles, Douglas and Lane Counties, Oregon: U.S. Geol. Survey Bull. 1122-D.

Howes, Steve, 1979, Soil resource inventory: Portland, Oregon, Mount Hood National Forest, unpublished report, 312 p.

Ketcheson, G. L., 1978, Hydrologic factors and environmental impacts of mass soil movements in the Oregon Coast Range: M.S. thesis, Oregon State Univ., Corvallis, Oregon, 94 p.

Kim, J., and Kohout, F. J., 1975, Multiple regression analysis: subprogram regression, in Nie, N. H., ed., Statistical package for the Social Sciences, New York, McGraw-Hill, 675 p.

Loughnan, F. C., 1969, Chemical weathering of the silicate minerals: New York, Elsevier, 154 p.

McKee, Bates, 1972, Cascadia - The geologic evolution of the Pacific Northwest: New York, McGraw-Hill, 394 p.

McKee, E. H., Swanson, D. A., and Wright, T. L., 1977, Duration and volume of Columbia River Basalt volcanism, Washington, Oregon, and Idaho: Geol. Soc. of America Abstract with Programs, v. 9, no. 4, p. 463-464.

Merriam, J. C., 1901, A contribution to the geology of the John Day basin, Oregon: Univ. Calif. Dept. Geol. Sci. Bull., v. 2, p. 269-314.

Morrison, P. H., 1975, Ecological and geomorphological consequences of mass movements in the Alder Creek watershed and implications for forest land management: B.A. thesis, Univ. of Oregon, Eugene, Oregon, 102 p.

O'Loughlin, C. L., 1972, An investigation of the stability of the steepland forest soils in the Coast Mountains, southwest British Columbia: Ph.D. thesis, Univ. of British Columbia, Vancouver, B.C., 147 p.

Paeth, R. C., Harward, M. E., Knox, E. G., and Dyrness, C. T., 1971, Factors affecting mass movement of four soils in the western Cascades of Oregon: Soil Sci. Soc. America Proc., v. 35, p. 943-947.

Patterson, P. V., 1973, North Fork Bull Run River landslide - post construction geology report: Portland, Oregon, Mount Hood National Forest, Materials Engineering section, unpublished report, 32 p.

Peck, D. L., Griggs, A. B., Schlicker, H. G., Wells, F. G., and Dole, H. M., 1964, Geology of the central and northern parts of the western Cascades: U.S. Geol. Survey Prof. Paper 449, 56 p.

Piteau, D. R., and Peckover, F. Lionel, 1978, Engineering of rock slopes, in Schuster, R. L., and Krizek, R. J., Landslide analysis and control: National Academy of Sciences, Transportation Research Board, Special Report 176, 234 p.

Pope, R. S., and Anderson, M. W., 1960, Strength properties of clays derived from volcanic rocks: in Research Conference on Shear Strength of Cohesive Soils, Proc., Boulder, Colo., p. 315-340.

Ruff, L. L., 1957, Bull Run dam No. 2 - geology and foundations: Portland, Oregon, unpublished report to City of Portland, Bureau of Water Works, 11 p.

Russel, I. C., 1883, A geological reconnaissance in central Washington: U.S. Geol. Survey Bull. 108, 108 p.

Savarenski, F. P., 1935, Experimental construction of a landslide classification: Geolog. Razvedochnyi Instit(TSNICTRI), p. 29-37, in Russian - cited in Varnes, D. J., 1978, Landslide analysis and control: National Academy of Sciences, Transportation Research Board, Special Report 176.

Schlicker, H. G., 1961, Geological reconnaissance of Bull Run damsite No. 2: Portland, Oregon, unpublished report to City of Portland, Bureau of Water Works.

Shannon and Wilson, Inc., 1958a, Test embankment Bull Run dam No. 2: Portland, Oregon, unpublished report to City of Portland, 8 p.

_____, 1958b, Report of soil tests for the design of proposed Bull Run dam No. 2: Portland, Oregon, unpublished report to Stevens and Thompson, Inc., 10 p.

_____, 1961, Report on geology and engineering feasibility of increased storage at Bull Run Lake, Oregon: Portland, Oregon, unpublished report to City of Portland, 22 p.

_____, 1963, Design and performance memorandum, Bull Run Dam No. 2, Oregon: Portland, Oregon, unpublished report.

Shannon and Wilson, Inc., 1965, Preliminary site explorations and studies, Ditch Camp slide, Bull Run, Oregon: Portland, Oregon, unpublished report to Stevens and Thompson, Inc., 29 p.

_____, 1973, Geologic reconnaissance and preliminary engineering studies for a water tunnel - Bull Run dam No. 2 to Dodge Park area: Portland, Oregon, unpublished report to City of Portland, 15 p.

_____, 1978, Stilling pool excavation, Bull Run dam No. 2: Portland, Oregon, unpublished report to City of Portland, Bureau of Water Works, p. 1-34.

Sharpe, C. F. S., 1938, Landslides and related phenomena: New Jersey, Pageant, 125 p.

Skempton, A. W., 1953, Soil mechanics in relation to geology: Proc. Yorks. Geol. Soc., 28, p. 33-62.

Sowers, G. F., and Royster, D. L., 1978, Field investigation, in Schuster, R. L., and Krizek, R. J., eds., Landslide analysis and control: National Academy of Sciences, Transportation Research Board, Special Report 176, 234 p.

Stephens, F. R., 1964, Soil survey, Bull Run - Sandy area, Oregon: Portland, Oregon, Mount Hood National Forest Admin. Rpt., unpublished, 477 p.

Stevens and Thompson, Inc., 1957, Bull Run storage dam No. 2 and hydroelectric power facilities, Bull Run River: Portland, Oregon, unpublished report to City of Portland, 61 p.

_____, 1965, Report on water supply conduits through Ditch Camp slide area: Portland, Oregon, unpublished report to City of Portland, 9 p.

Stevens, Thompson, and Runyan, Inc., 1974, Hydrologic study North Fork Bull Run River: Portland, Oregon, unpublished report to City of Portland, 26 p.

Swanson, D. A., Wright, T. L., Hooper, P. R., and Bentley, R. D., 1979, Revisions in stratigraphic nomenclature of The Columbia River Basalt Group: U.S. Geol. Survey Bull. 1457-G, 59 p.

Swanson, F. J., and Dyrness, C. T., 1975, Impact of clearcutting and road construction on soil erosion by landslides in the western Cascade Range, Oregon: Geology, v. 3, p. 393-396.

_____, and James, M. E., 1975, Geology and morphology of the H. J. Andrews Experimental Forest, western Cascades, Oregon: U.S. Dept. Agr. Forest Serv. Res. Paper PNW-188, 14 p.

_____, and Lienkaemper, G. W., 1978, Physical consequences of large organic debris in Pacific Northwest streams: U.S. Dept. Agr. Forest Serv. Gen. Tech. Rep. PNW-69, 12 p.

_____, Swanson, M. M., and Woods, C., 1977. Inventory of mass erosion in the Mapleton Ranger District, Siuslaw National Forest: unpublished report to Siuslaw National Forest, 41 p.

_____, and Swanston, D.N., 1977, Complex mass-movement terrains in the western Cascade Range, Oregon: Geol. Soc. America Reviews in Engineering Geology, v. 3, p. 113-124.

Swanston, D. N., 1969, Mass wasting in coastal Alaska: U.S. Dept. Agr. Forest Serv. Res. Paper PNW-83, 15 p.

_____, and Swanson, F. J., 1976, Timber harvesting, mass erosion and steepland forest geomorphology in the Pacific Northwest, in Coates, D. R., ed., Geomorphology and engineering: Stroudsburg, Pa., Dowden, Hutchinson, and Ross, Inc., p. 199-221.

Taskey, R. D., 1978, Relationships of clay mineralogy to landscape stability in western Oregon: Ph.D. thesis, Oregon State Univ., Corvallis, Oregon, 122 p.

Terzaghi, Karl, and Peck, R. B., 1967, Soil mechanics in engineering practice: New York, John Wiley, 729 p.

Thayer, T. P., 1936, Structure of the North Santiam River section of the Cascade Mountains in Oregon: Jour. Geology, v. 44, no. 6, 701-716.

_____, 1939, Geology of the Salem Hills and North Santiam River basin, Oregon: Oregon Dept. of Geol. and Mineral Indus. Bull. 15, 40 p.

Treasher, R. C., 1942, Geologic history of the Portland area: Oregon Dept. of Geol. and Mineral Indus. Short Paper 7, 17 p.

Trimble, D. E., 1957, Geology of the Portland quadrangle, Oregon-Washington: U.S. Geol. Survey Geol. Quad. Map GQ 104.

_____, 1963, Geology of Portland, Oregon and adjacent areas: U.S. Geol. Survey Bull. 1119, 119 p.

Varnes, D. J., 1978, Landslide types and processes, in Schuster, R. L., and Krizek, R. J., eds., Landslide analysis and control: National Academy of Sciences, Transportation Research Board, Special Report 176, 234 p.

Vogt, B. F., 1979, Columbia River Basalt Group stratigraphy and structure in the Bull Run Watershed, western Cascades, northern Oregon [abs., presented at Oregon Academy of Sciences, 37th, Gresham, Oregon]: in Proc. Oregon Academy of Sciences, v. 15, p. 51.

Vokes, H. E., Snavely, P. D., and Myers, D. A., 1951, Geology of the Southern and Southwestern border areas of the Willamette Valley, Oregon: U.S. Geol. Survey Map OM-110.

Waters, H. C., 1961, Stratigraphic and lithologic variations in the Columbia River Basalt: Am. Jour. Sci., v. 259, no. 8, p. 583-611.

Watkins, N. D., and Bakshi, A. K., 1974. Magnetostratigraphy and oroclinal folding of Columbia River, Steens, and Owyhee basalts in Oregon, Washington, and Idaho: Am. Jour. Sci., v. 274, p. 148-189.

Wells, F. G., and Waters, A. C., 1935, Basaltic rocks in the Umpqua Formation: Geol. Soc. America, v. 46, no. 6, p. 961-972.

_____, 1956, Geology of the Medford Quadrangle, Oregon - California: U.S. Geol. Survey Geol. Quad. Map GQ 89.

Williams, I. A., 1920. Some features of the geologic history of Bull Run Lake: Oregon Bureau of Mines and Geology, unpublished report on file with City of Portland, Bureau of Water Works, 32 p.

Wilson, S. D., 1970, Observational data on ground movements related to slope instability: Jour. Soil Mechanics and Found. Div., Am. Soc. Civil Engineers Proc., v. 96, p. 1521-1544.

Wise, W. S., 1969, Geology and petrology of the Mount Hood area - a study of High Cascade volcanism: Geol. Soc. America Bull., v. 80, no. 6, p. 969-1006.

Zaruba, Q., and Mencl, V., 1969, Landslides and their control: New York, Elsevier, 205 p.

APPENDICES

APPENDIX I

Mass Movement Inventory

Listed below are descriptions of individual mass movements mapped in the Bull Run Watershed. Location of each mass movement is shown on Plate 3. The following abbreviations are used: mass movement types; SE = slump-earthflow, SSE = streamside slump-earthflow, DA = debris avalanche, SDA = streamside debris avalanche, RR = rockfall-rockslide, CM = complex-massive. Clay minerals present in scarp samples; M = mica, K = kaolinite, C = chloritic intergrade, D = dehydrated halloysite, H = hydrated halloysite, S = smectite. Abbreviations of geologic units are the same as in Figure 3.

APPENDIX I. MASS MOVEMENT INVENTORY

Location	Type	Bedrock	Area (ft^2)	Volume (yd^3)	Slope (%)	Aspect	% Clay	Clay minerals	Approx. age (y)	Comments
1	DA	Tcr	4,800	700	90	NE	18.8	C, K	3	sedimentary interbed present
2	SE	Tmpr	240	35	75	NE	--	--	5+	covered by glacial outwash
3	SDA	Tcr	500	35	100+	N	--	--	2	
4	SE	Tcr	900	100	75	NE	--	--	3-4	
5	SSE	Qls	12,000	3,100	75	SE	--	--	7+	west slide of Dames and Moore (1972)
6	SDA	Qls	15,000	2,780	80	E	--	--	7	middle slide of Dames and Moore (1972)
7	SDA	Qls	6,250	925	75	W	--	--	7	red clay present
8	SDA	Qls	15,000	2,200	90	SE	6.6	H, C (minor)	7	upper slide of Dames and Moore (1972)
9	SDA	Qls	4,250	315	100	E	--	--	7	assoc. w/debris torrent
10	DA	Qls	160	12	75	W	--	--	2	reactivation of no. 7
11	RR	Qtg	--	--	100+	SE	--	--	active	
12	SE	Qls	150	30	35	S	--	--	3-5	failure in cutbank
13	SE	Qls	150	30	35	S	13.8	H, D, C (minor)	3-5	failure in cutbank
14	SSE	Qls	450	70	50	N	--	--	active	red clay present
15	SE	Tmpr	375	55	80	SE	14.8	C, D, M (minor)	1	assoc. w/blowdown - culvert loc.
16	SDA	Tpv	11,250	2,000	100	NW	6.8	C, H or M	5	assoc. w/debris torrent
17	DA	Tcr	450	35	85	SW	--	--	2	clearcut above scarp
18	SDA	Tcr	750	140	60	NW	--	--	2	
19	SSE	Tpv	--	--	60	E	--	--	active	talus creep-earthflow
20	RR	Tcr	7,500	3,300	90	NE	--	--	10+	pillow basalt in scarp
21	RR	Tpv flow bx.	--	--	100+	NW	--	--	active	
22	SDA	Tmpr	3,000	555	60	NW	--	--	5-10	loc. on overflow channel
23	SE	Tmpr	13,500	6,250	65	S	--	--	200+	
24	SDA	Tpv flow bx.	700	80	90	W	--	--	2-5	
25	SDA	Tcr-Tmpr	100	7	60	SW	--	--	2-3	Tmpr clay layer in scarp
26	SDA	Tpv flow bx.	3,600	530	100	SW	6.8	H, C (minor)	5-6	glaciofluvial deposit in scarp
27	SE	Tcr-Tmpr-Tpv	6,400	1,900	100	S	10.8	H, C	15	transitional w/DA
28	DA	Tcr	400	30	65	S	5.8	C, D	5-10	earthflow above scarp
29	DA	Tcr	225	17	100	S	--	--	--	
30	SE	Tmpr	3,750	970	90	NW	26.8, 8.8, 10.8	H, S	5-6	poor culvert loc.
31	SDA	Tpv	50,000	14,800	80	NW	9.8, 5.8	C, D, H (minor)	200+	transitional w/RR
32	DA	Tpv tuff	900	65	90	W	9.8, 35.8	H, S	4-5	
33	SSE	Tmpr	200	20	55	NW	7.8	S, K or D	2-3	
34	SE	Tcr-Qls	2,800	620	80	W	8.8	H	2-15	failure to cutbank

APPENDIX I. (Continued)

Location	Type	Bedrock	Area (ft^2)	Volume (yd^3)	Slope (%)	Aspect	% Clay	Clay minerals	Approx. age (y)	Comments
35	DA	Tmpr-Qls	20,000	3,700	65	S	14.8, 15.8	H, S	3-5	red clay present
36	DA	Tmpr-Qls	20,625	5,730	60	NW	--	--	4-5	transitional w/SE
37	RR	Tpv	--	--	100+	NW	--	--	--	
38	SDA	Tmpr-Qls	4,000	890	65	NW	--	--	8-10	
39	SDA	Tmpr-Qls	4,225	470	100	SE	17.8	S, D	4-5	
40	DA	Tmpr-Qls	60,000	13,300	85	N	17.8, 10.6, 14.6	D, H, S (minor)	9-10	transitional w/SE
41	DA	Tmpr-Qls	6,000	1,100	85	S	--	--	5-6	transitional w/SE
42	RR	Qvlc	600	90	70	W	10.6	C, K (minor)	2-3	transitional w/DA
43	RR	Qvlc	--	--	50+	E	--	--	--	
44	SDA	Qvlc	240	25	70	W	--	--	2	transitional w/RR
45	SSE	Tmpr	1,250	280	55	N	4.6	C	4-5	
46	SE	Tcr	1,000	75	80	W	--	--	--	earthflow, potential slump
47	DA	Tcr	600	45	100+	E	--	--	2-3	
48	SDA	Tcr	2,100	230	80	N	--	--	--	progressing upslope
49	SE	Tmpr-Qls	--	--	65	S	--	--	15-25	
50	SDA	Tcr	6,875	764	100	S	11.6	H, S	7-10	
51	SDA	Tcr	120	5	75	E	--	--	2-5	possibly assoc. w/blowdown
52	SDA	Tcr	100	4	100+	E	--	--	2-5	failure in cutbank
53	SDA	Tcr	300	17	100	S	--	--	5	failure in road fill
54	SDA	Tcr	750	110	75	NE	--	--	8	
55	DA	Tcr	1,200	265	100	SW	--	--	9	near thrust fault
56	SE	Tmpr	1,800	335	90	SE	--	--	10-15	
57	SE	Tmpr-Qls	52,500	17,500	35	S	--	--	15	
58	DA	Tmpr-Tpt-Qls	40,950	6,070	100+	SE	11.6	C, D	9-13	failure after clearcut
59	SE	Tpv	600,000	450,000	60	S	--	--	200+	
60	SDA	Tmpr-Qls	600	45	100	SE	--	--	10-12	
61	DA	Tcr	5,850	650	85	W	7.6	S	12-15	failure in cutbank
62	SE	Tpv	216,000+	925,000+	26	NE	7.6	--	100+	head still active
63	SDA	Tcr	500	45	100	NW	--	--	5	
64	DA	Tcr	1,800	400	100+	NW	--	--	15-50	possibly due to dam construction
65	DA	Tcr	1,800	350	100+	NW	--	--	15-50	possibly due to dam construction
66	DA	Tcr	1,500	110	100+	NW	--	--	15-50	possibly due to dam construction
67	RR	Tcr	--	--	75	S	--	--	active	assoc. w/thrust fault
68	RR	Tpv	--	--	60	NE	--	--	active	
69	RR	Tcr	--	--	100+	SE	--	--	active	
70	RR	Tcr	--	--	100+	S	--	--	active	
71	RR	Tcr	--	--	65	W	--	--	active	

APPENDIX I. (Continued)

Location	Type	Bedrock	Area (ft^2)	Volume (yd^3)	Slope (%)	Aspect	% Clay	Clay minerals	Approx. age (y)	Comments
72	RR	Tpv	--	--	35	NW	--	--	active	flow bx. present
73	RR	Tmpr	--	--	30	S	--	--	active	
74	SE	Tpt-Qls	20,000	5,185	60	SE	--	--	20+	Little Sandy R. slide (Shannon and Wilson, 1965)
75	CM	Tmpr-Tpv	--	15×10^6	30-60	SE	11.8	H,S	500+	probably pleistocene
76	CM	Tmpr-Tpt-Tpv	--	148×10^6	30-60	SE	--	--	500+	probably pleistocene
77	CM	Tmpr-Tpv	--	35×10^6	0-60	NW	--	--	500+	probably pleistocene
78	CM	Tmpr-Tpv	--	10×10^6	50+	S	--	--	500+	probably pleistocene
79	CM	Tmpr-Tpv	--	15×10^6	50+	N	--	--	500+	probably pleistocene
80	CM	Tmpr-Tpv	--	5×10^6	40-60	SW	--	--	500+	probably pleistocene
81	CM	Tmpr-Tpv	--	6×10^6	30-60	NW	--	--	500+	probably pleistocene
82	CM	Tmpr-Tpv	--	45×10^6	0-60	SE	--	--	500+	probably pleistocene
83	CM	Tmpr-Tpv	--	2×10^6	25-40	SE	--	--	500+	probably pleistocene
84	CM	Tmpr-Tpv	--	1×10^6	25-40	NE	--	--	500+	probably pleistocene
85	SSE	Tcr-Qls	3,850	570	55	N	--	--	7	
86	SE	Qls	8,100	4,500	75	E	8.6	C, K (minor)	active	failure in roadfill

APPENDIX II

XRD Patterns

Illustrated below are typical XRD patterns of the clay fraction of soils sampled from slump- earthflow, debris avalanche, and stable sites in the Bull Run Watershed. Treatments are: 1 = K-saturated, 105°C; 2 = K-saturated, 54% RH; 3 = K-saturated, 300°C; 4 = K-saturated, 500°C; 5 = Mg-saturated, 54% RH; 6 = Mg-saturated, glycerol solvated; 7 = Mg-saturated, ethylene glycol solvated

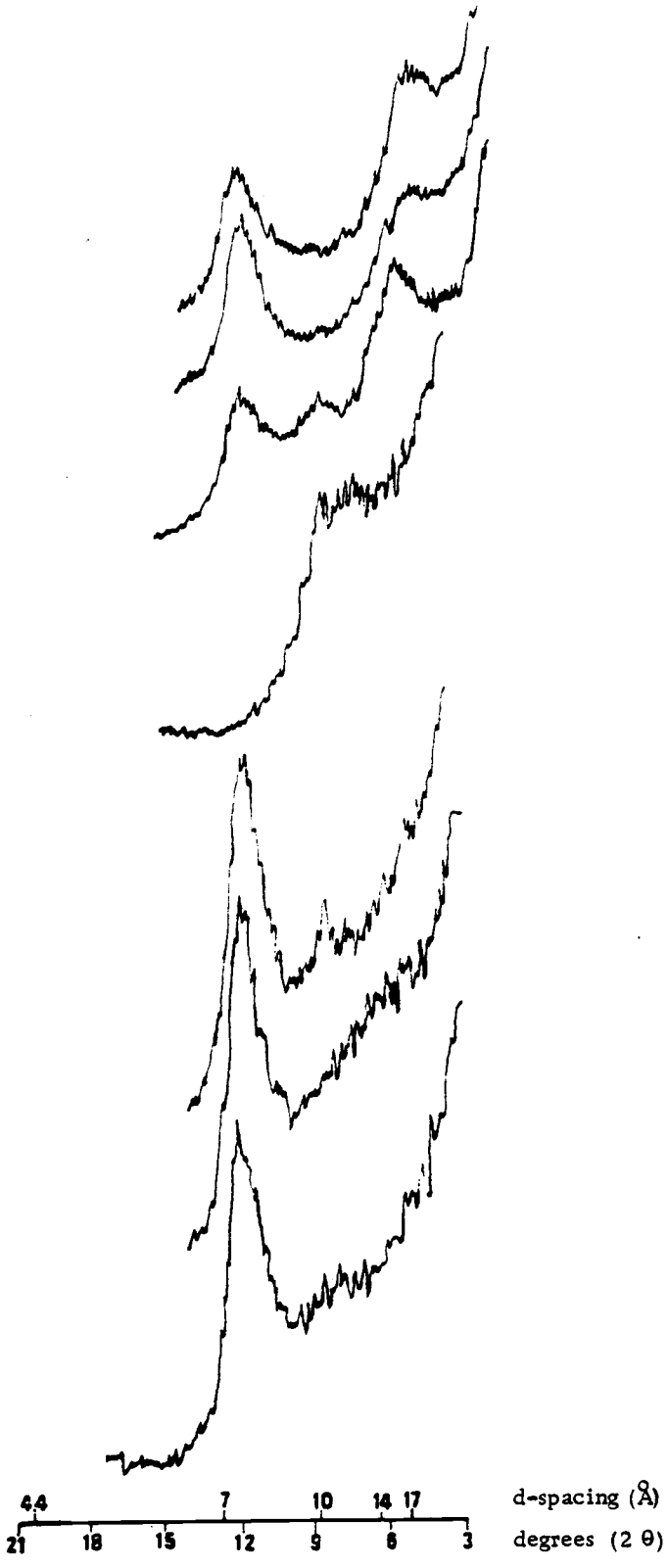

Typical XRD pattern of slump-earthflow sites.
Cu K α source, 35 kv, 25 ma.

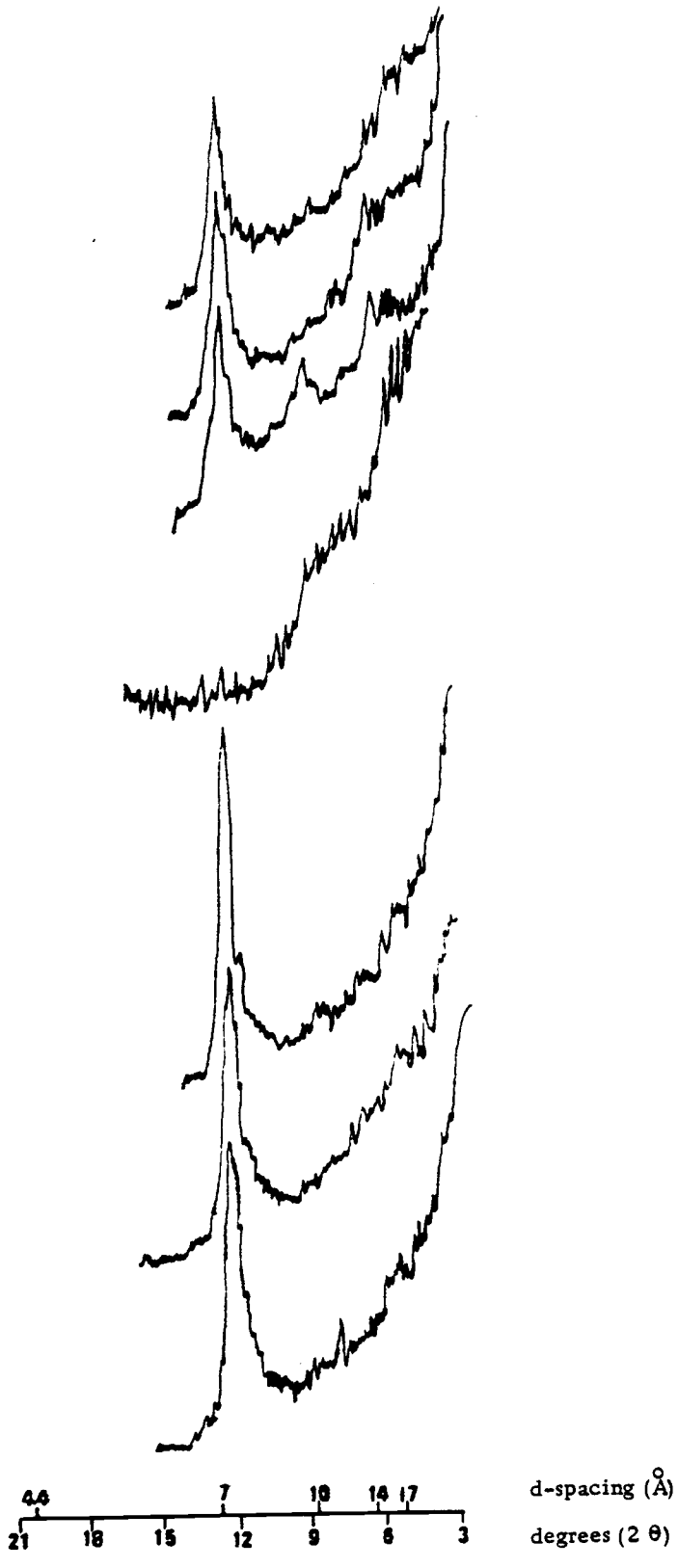

Typical XRD pattern of debris avalanche sites. Cu K α source, 35 kv, 25 ma.

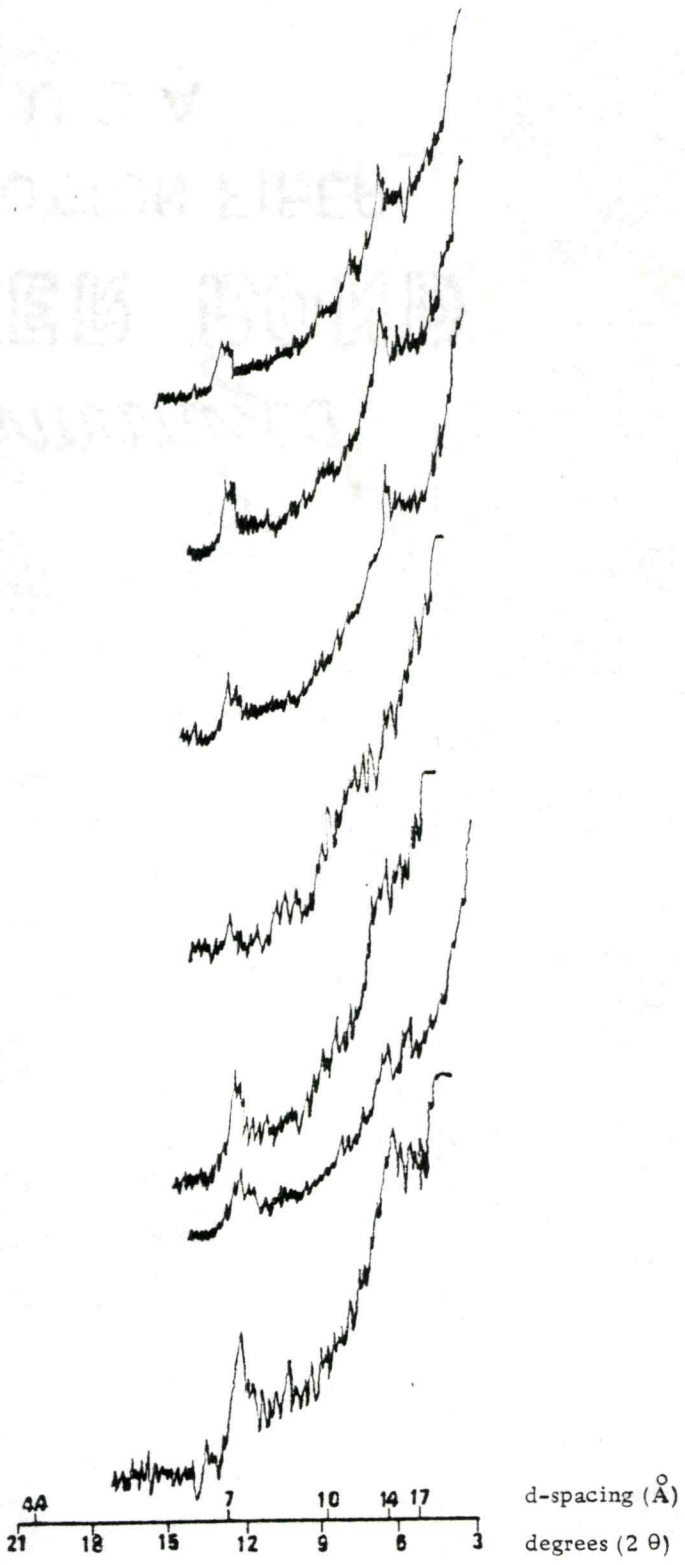

Typical XRD pattern of stable sites.
Cu K α source, 35 kv, 25 ma.